April 2010

Drive-Line Generator Dynamometer Design

David Bernard Boudreau
Worcester Polytechnic Institute

Molli Anne Malcolmson
Worcester Polytechnic Institute

Follow this and additional works at: https://digitalcommons.wpi.edu/mqp-all

Drive-Line Generator Dynamometer Design

A Major Qualifying Project Report
Submitted to the Faculty of
WORCESTER POLYTECHNIC INSTITUTE
In partial fulfillment of the requirements for the
Degree of Bachelor of Science
Submitted by:

David Boudreau
Molli Malcolmson

Date: April 28, 2010

Approved:
Eben Cobb, Advisor

Abstract

The goal of this project was to design a dynamometer to test a driveline generator. Dynamometer component designs were created, analyzed and iterated until all function requirements were met. All components were designed with safety factors greater than two except the shaft, which had a safety factor or 1.282 in the keyways. Using Solidworks, each component was modeled and Finite Element Analysis was completed. Upon satisfactory completion of the design, component drawings were made for future manufacturing.

Acknowledgement

The project team would like to thank the following people for all of their time and guidance in the completion of this project:

Professor Eben Cobb

Professor Robert Norton

Mr. Torbjorn Bergstrom

Mr. Neil Whitehouse

Mr. Thomas Kenney

Mr. Michael Phenauf

Mr. Dominic Spano

Mr. Barry Joseph

Authorship

<u>David Boudreau:</u>

- Analysis- shaft

- Writing-

    o Design Concepts and Solutions

    o Detailed Design:

        ▪ Shaft

        ▪ Prime Mover & Prime Mover Support

        ▪ Base Structure

        ▪ Test cell Layout

    o Conclusion

    o Recommendations

    o References

    o Appendices

- Models and Drawings

<u>Molli Malcolmson:</u>

- Analysis- Finite Element Analysis on all components

- Writing-

    o Abstract

    o Acknowledgements

    o Introduction

- Background

- Project Objectives

- Detailed Design:

  - Bearings and Bearing Support

  - Torque Meter and Torque Meter Support

  - Stator Support Structure

  - Couplings

  - Adapters

- Conclusion

- Recommendations

- References

- Appendices

- Models and Drawings

Table of Contents

List of Figures

List of Tables

List of Equations

Introduction

In today's world, more efficient methods for producing power are constantly being sought out. Machines such as generators are continually being researched and studied as companies look for ways to advance their product. As new technology is established, methods for testing new ideas and theories are always required. Therefore, production of test equipment is often required.

This project entailed the design of a dynamometer, which will be used to test a permanent magnet generator. This generator has been designed by DRS Power Technology, Inc. (DRS-PTI) in Fitchburg, Massachusetts. This project proved to be an ideal exercise in mechanical engineering as it encompassed numerous facets of the design process and required its participants to think critically to solve many and varying engineering hurdles. Students were expected to not only design, analyze and optimize the structures needed to test the generator, but were also expected to investigate and recommend the items such as prime movers and certain types of data acquisition equipment as well.

Completion of this project was of high importance for DRS-PTI. The generator that they will be testing is different from most products that they have developed and tested in the past. The design of this generator does not include a shaft, as it is expected to be used as part of the drive train in high torque vehicles. However, this unique design posed a challenge for DRS as they did not have a means of testing this product. Therefore, it was necessary to design a test stand as unique as the generator itself.

In order to complete the task of designing this test stand, the project group began by establishing design parameters through communication with DRS-PTI and reviewing the statement of work supplied by the company. Initial designs were then created, compared, and iterated until a single design that fulfilled the statement of work and other design goals. Solid models were then generated using Solidworks 2009. These models were then used to create drawings for fabricated or machined

parts. The purpose of this report is to document the design choices that were made, and to offer recommendations for further improvements on this project.

Background

DRS Power Technology, Inc.

DRS Power Technology, Inc. is one branch of DRS Technologies, A Finmeccanica Company. DRS Technologies is a multibillion dollar defense systems company. Based out of Parsippany, New Jersey, DRS Technologies has been characterized as "one of the fastest growing defense companies in the world" ("Corporate information," 2008). They are involved in many different areas of defense systems, ranging from optics, night and thermal vision systems to tactical computing and intelligence systems. DRS Technologies also provides telecommunication and logistics devices along with power and controls systems. Not only does DRS engineer and manufacture these types of products, but they are also involved in the training and support services for all branches of the military.

DRS Power Technology, Inc. (PTI) plays an important and significant role in DRS Technologies support to the military. Located in Fitchburg and Hudson Massachusetts, PTI has a hand in both military and commercial power systems. A leader in turbine development and systems engineering, PTI is a major contributor to today's steam and gas turbine market, specializing not only in the design and manufacturing of new steam and gas turbine units, but in the refurbishment of older units as well. PTI is unique in that it is rooted in the General Electric legacy of steam and gas turbine design, but is constantly working with or on cutting edge technology to improve and advance their products (Awiszus, 2010).

PTI also plays a principle role in developing and manufacturing high power permanent magnet machines. Having developed a wide range of permanent magnet machines, PTI's equipment is often

used in areas such as navy auxiliary supply, military vehicles, renewable and wind energy, the commercial marine industry and the oil and gas industry. PTI is also currently becoming more and more involved in the electric drive industry as well (Awiszus, 2010).

Permanent Magnet, Drive-line Generators

Permanent Magnet machines are becoming more and more popular in both military and commercial applications. This is due to their versatility, compact size and power output capability. Permanent Magnet generators work by creating an electromagnetic field (EMF) within stator winding usually made of copper or some other type of conductive material. The EMF is generated by placing magnets, commonly made of samarium cobalt or neodymium iron boron, on a rotor. The rotor sits within a stator housing, which also contains the stator windings. As the rotor-magnet assembly spins, a magnetic flux is generated which induces an EMF. The change that is seen in this magnetic flux is proportional to the EMF that is generated (Hill & Mountain, 2002).

PTI is currently developing a new line of drive-line generators. These drive-line generators are permanent magnet generators that are positioned on the drive shaft between the engine and transmission of an automotive vehicle. This type of generator is unique in that it does not include any type of shaft as part of the generator design. Until the generator is placed on the shaft, the rotor is free floating within the stator housing. This is an important fact that must be taken into account when manufacturing, shipping, and installing the generator. The concentricity of the rotor and stator housings are critical to proper function of the generator. This is also something that needs to be considered when designing any type of dynamometer for testing this system ("Corporate information," 2008).

Project Objectives

Goal

As previously stated, PTI is currently developing a new family of permanent magnet, drive-line generators. The generators are not only unique to themselves, but are also unique to PTI, as they do not have any other type of permanent magnet machine like these. Because of this, PTI does not currently have any type of dynamometer that would be able to test these generators. It was the task of this project team to design a dynamometer that would be capable of doing so. Upon completion of the dynamometer design, a full analytical report, including all calculations, along with Solidworks models, drawings for manufacturing and a bill of materials was delivered to PTI.

Task Specifications

The following task specifications were given as minimum requirements that the dynamometer must meet:

1. The dynamometer must be able to provide a generator speed range of 100-5000RPM.

2. The dynamometer must be able to withstand an input torque range of 5-750ft-lb.

3. The dynamometer must be capable of testing different sized generators ranging from twenty-one inches in diameter to twenty-seven inches in diameter.

4. The dynamometer must be capable of mounting generators with different interfaces as seen in the drawings provided by PTI.

Design Concepts

Several design concepts were developed over the course of this project. They can be organized

into categories relating to generator interface concepts, rotor support concepts, and data acquisition

concepts.

The first concept discussed was whether the dynamometer should be specialized to test only

the specific generators identified in the statement of work, or to make the test stand adaptable and able

to handle other generators that may be developed in the future. This concept was closely related to the

various shaft concepts being discussed at the time. Initially, two main types of shafts were discussed

(Figure 1). The first was a fitted shaft, designed to interface with a specific generator, and the second

was a shaft with an adapter. Later in the design processes, a third option, a shaft fitted specifically for a

smaller generator, but designed to be able to carry the loads of the larger of the prospective generators

and be adapted to interface with other adapters, was iterated.
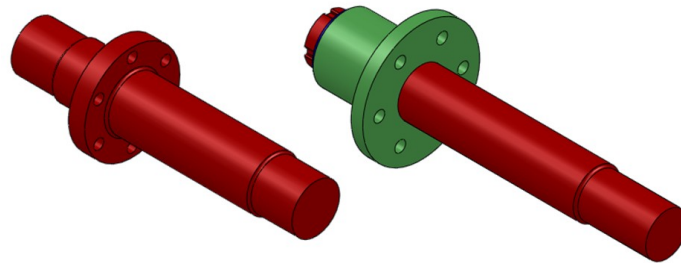
Figure 1: First Two Shaft Concepts

In addition to the basic shaft itself, the way in which the shaft would be supported became an

especially important aspect of the overall design. Two main concepts were investigated in order to find

the best solution for this problem. One concept consisted of a simply supported shaft, where a bearing

is located on each end and the rotor would be positioned in the middle. Although this design was

simple and rugged and experienced low deflections, it would present difficulties when trying to

interchange generators being tested. A second concept was a shaft which cantilevered the rotor out beyond the bearing mounts. This concept was very adaptable, but would be less rugged than its counterpart. Early iterations of both simply supported and cantilever design concepts are depicted in Figure 2.
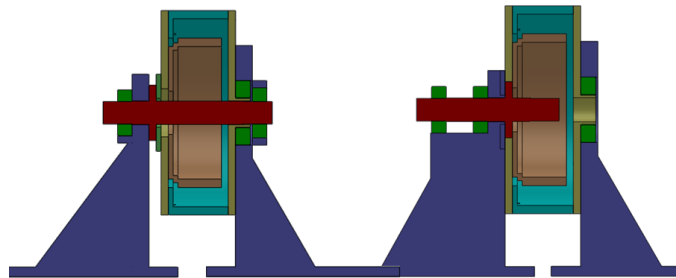
Design concepts relating to data collection were more varied than the shaft or the support structure. A number of methods for measuring the torque were then analyzed. The first concept involved using the generator as a motor to drive a motor/generator that has a known torque constant and measure the output of that generator to determine torque and angular velocity output of the test generator. A related concept was to use a motor with a known torque constant and drive the generator, measuring the input to the motor and the output of the generator. Another concept was to use a prime mover to drive the generator and to measure the reaction torque on the stator itself with a torque flange or strain gages. Figure 3 is a diagram of a torque flange. The last concept focused on measuring the torque in the shaft through use of a torque cage. This concept was later simplified with the replacement of the torque cage with a torque meter.
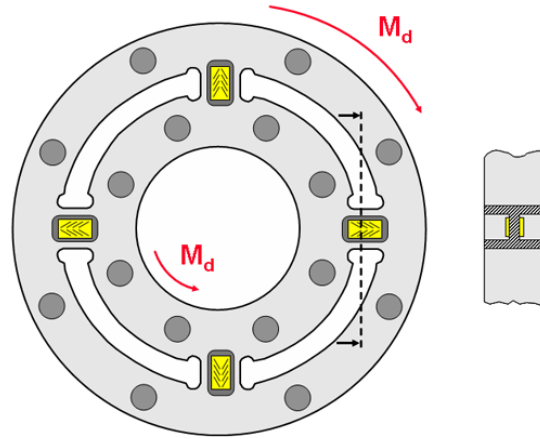
Figure 3: Torque Flange

Design Selection

The final design concept was selected through analysis of the advantages and disadvantages of each of the various design concepts. Competing or overlapping design concepts were grouped together in tables to facilitate selection. These design concepts were discussed at a design review with PTI.

The primary design decision focused around whether to design a dynamometer tailored for a specific generator or to make an adaptable system. Table 1 lays out the advantages and disadvantages of the primary design decision. The final design was a hybrid of the two concepts. The dynamometer was designed specifically to interface directly with the small generator, but could still perform tests on larger generators by using adapter plates for the rotor and stator interfaces.

	Single Generator	Multiple Generator
Advantages	• Inexpensive • Tighter tolerances	• One dynamometer can test multiple generator prototypes with minor adjustments
Disadvantages	• Need a different dynamometer for future generator prototypes	• Expensive • Larger tolerances

Table 1: Single Generator vs Multiple Generator

The secondary design decision was whether to use a fitted shaft or to use a shaft with an adapter. The advantages and disadvantages of this decision were organized into Table 2, taking into account that the advantages and disadvantages would change based on the primary design decision. Once again, the final design was a combination of the fitted shaft and the adapter. The shaft was designed to interface directly with the small generator, but has the option of using an adapter plate to interface with other generators.

Table 2: Fitted Shaft vs Shaft with Adapter

	Single Generator	Multiple Generator
Fitted Shaft	Advantages: • High durability • Low stress concentration factors	Advantages: • High durability • Low stress concentration factors
	Disadvantages: • Milled from large stock material	Disadvantages: • Milled from large stock material • Requires a different shaft for each generator • Expensive • Long assembly for cantilever
Adapter	Advantages: • Can be machined at WPI • Inexpensive	Advantages: • Can be machined at WPI • Shorter fabrication per generator • Inexpensive
	Disadvantages: • High stress concentration factors • May cause locating issues	Disadvantages: • High stress concentration factors • May cause locating issues

The tertiary design decision was whether to use a simply supported or a cantilever support configuration for the shaft. This decision was particularly hard to make and a design matrix was used to simplify the process. Figure 4 shows that a simply supported shaft was more appropriate for a single generator specific design, but a cantilever shaft was more desirable for use with an adaptable design that supports various size and configurations of generators. Since an adaptable strategy was selected for the primary design decision, the cantilever support configuration was determined to be the optimal choice.

	Weight		Support for One Generator			Support for Different Generators	
			Simply Supported	Cantilever		Simply Supported	Cantilever
Safety Factor of 2 (150 ft-lb Torque)	10		9	8		9	8
Safety Factor of 2 (750 ft-lb Torque)	7		X	X		9	8
Deflection	5		7	5		7	6
Ease of first time assembly/disassembly	5		7	5		7	7
Ease of operational assbly/disassbly	7		X	X		4	8
Accommodate variations in size of generator being tested	6		X	X		7	9
Accommodate variations in mass of generator being tested	6		X	X		9	8
Cost	6		9	8		7	7
Weighted Total			214	178		389	401

Figure 4: Simply Supported vs Cantilever Design Matrix

The final basic design decision to be made was the method of data acquisition. After much discussion at the design review, it was determined that the torque flange, the leading concept at the time, would be hard to calibrate and harder to implement. It was also determined that the simplest and most reliable data acquisition method was to measure the stresses in the shaft. The concept of using a torque cage was abandoned because it would be difficult to construct, but a similar concept, the use of a torque meter between the prime mover and shaft, was selected.

Detailed Design

Shaft

The primary component of the dynamometer is the shaft. The shaft supports the rotor and provides it with an input torque and angular velocity. It was designed to support a rotor weighing up to 250 lbs cantilevered from one end with its center of mass 3.12 inches from the end of the shaft. Furthermore, the shaft was designed to accommodate both the smallest and the largest generators, meaning that it would need to have a small interface with the rotor, yet be strong enough to transmit the 750 ft-lb torque required by the task specifications.

The shaft, depicted in Figure 5, is cantilevered using two bearing seats and has a large bolt flange on one end. This geometry necessitated that the shaft have steps that increase in diameter from one end to the other in order to easily assemble the bearings to the shaft. The shaft has a total of 6 steps: the keyway section, the first bearing seat, the middle span, the second bearing seat, the shoulder that bounds the second bearing seat, and the bolt flange. The three keyways on one end of the shaft allow it to interface with the torque meter – shaft coupling. The other end of the shaft has a flange with a six hole bolt circle used to fasten the rotor to the end of the shaft. Two dowel pin holes are machined into the flange; one will have a pin to be used for locating.
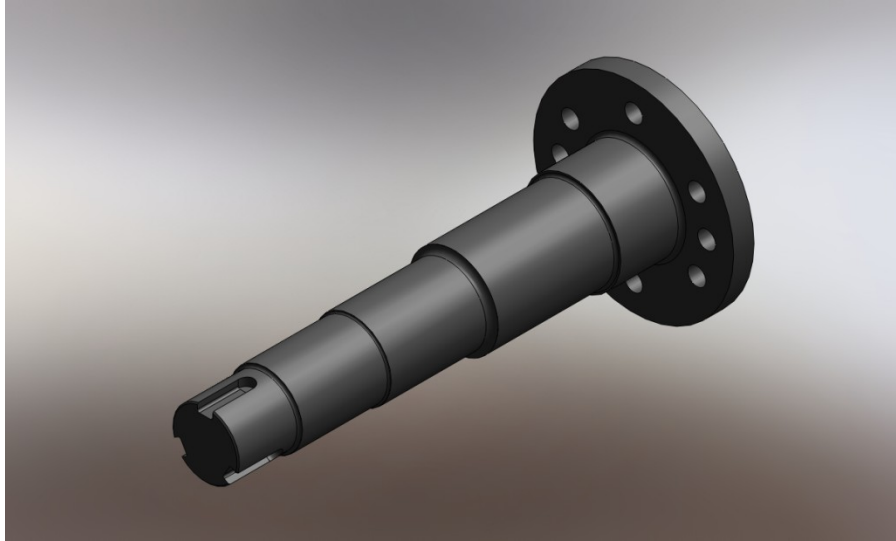
Figure 5: Final Design of Shaft

The shaft was designed for radial symmetry in order to prevent vibration due to imbalances. The shaft was designed with three equally spaced keyways to help maintain balance. The dowel pin holes give the shaft bilateral symmetry. In order to allow for balancing after fabrication, sacrificial material was added to a segment at each end of the shaft, as seen in Figure 6. The segment that constitutes the first bearing seat was elongated by 5/8 inches to create the sacrificial material on the first balance plane. The segment between the second bearing seat and the flange contains the sacrificial material on the second balance plane. If an imbalance is discovered, some of this material can be removed in order to rebalance the shaft.
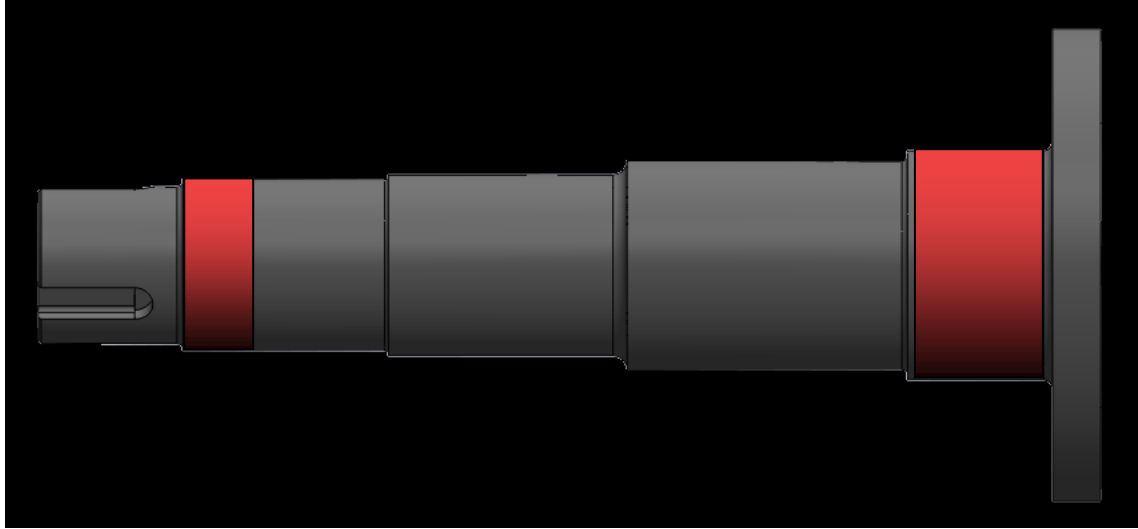
The first step in analyzing the shaft was to calculate the reaction forces that would be experienced at each bearing. The reaction forces at each bearing are calculated by summing the moments about the center of the other bearing and solving for the unknown reaction force with the assumption that the system is static and all moments sum to zero. The moment applied by the weight of each segment is calculated as shown in Equation 1, then inserted into Equation 2 and 3 and solved for the reaction force. In Equation 2, the moments applied by segments 1, 2, 3, and 4 are negative because they are applying a positive moment on the shaft and the moments applied by segments 5 and 6 and the Rotor are positive because they are applying a negative moment on the shaft, all which need to be opposed by the reaction force at Bearing A, the first bearing. In Equation 3, the moments applied by segments 1 and 2 are negative because they are applying a positive moment on the shaft and the moments applied by segments 3, 4, 5, and 6 and the Rotor are positive because they are applying a negative moment on the shaft, all which need to be opposed by the reaction force at Bearing B, the second bearing. Note that both F_A and F_B are magnitudes; F_A acts in the $-Y$ direction and F_B acts in the $+Y$ direction. F_A and F_B are measured in lb_f. These calculations and the following calculations were

completed using program Mathcad, which would continuously update itself as input information changed. This document can be found in Appendix A of this report.

Equation 1: Moment Calculation for a Segment "i" of the Shaft

$$M_i = w_i \times \left(x_{bearing} - x_i\right)$$

Equation 2: Reaction Force at Bearing A

$$F_A = \frac{-M_1 - M_2 - M_3 - M_4 + M_5 + M_6 + M_{rotor}}{x_B - x_A} = 312.06 \; lb_f$$

Equation 3: Reaction Force at Bearing B

$$F_A = \frac{-M_1 - M_2 + M_3 + M_4 + M_5 + M_6 + M_{rotor}}{x_B - x_A} = 573.97 \; lb_f$$

Where:

M_i = Moment applied by segment i

w_i = Weight of segment i

$x_{bearing}$ = location of center of bearing about which moments are being calculated

x_i = location of center of segment i

Next, singularity function describing the load, shear, and moments experienced at any point along the length of the shaft were generated. These singularity functions represent the loads on a beam as functions that are valid, through logical operations, over the entire continuum of beam length (Norton, 2010). The weight of each section as well as the reaction forces of the bearings are modeled as distributed loads rather than point loads to increase the accuracy of this analysis. The weight of the

rotor was modeled as a point load since the material properties and dimensions of the rotor would be different for each prototype generator.

The singularity functions for the Shear and Moment were then plotted from the beginning of the shaft to the point load that is used to model the center of mass of the rotor. Figure 7 shows the plot of the shear over the length of the shaft and Figure 8 shows the Moment plot. The shear experienced at the center of mass of the rotor is calculated as $-2.842E10^{-14}$ lb_f and the moment at the same point is $-2.236E10^{-12}$ in-lb_f. These values should be equal to zero, but these discrepancies are extremely small and likely caused by rounding in MathCAD. The largest magnitude of the shear plot is experienced at the beginning of the second bearing, at x=6.721 inches, where it is -317.02. The largest magnitude for the moment plot is $-1.215E10^{3}$ in-lb_f and occurs at the same location.
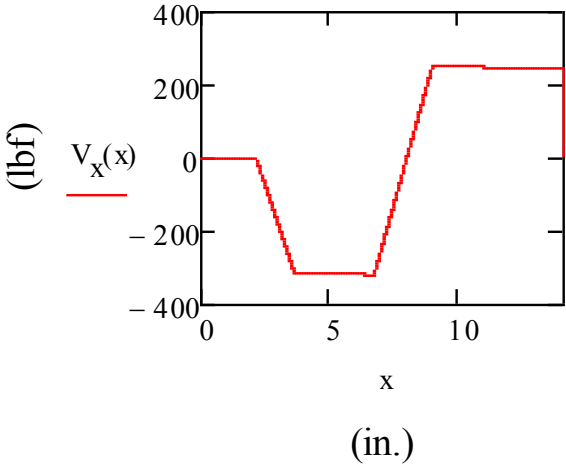
Figure 7: Plot of Shear Over the Length of the Shaft
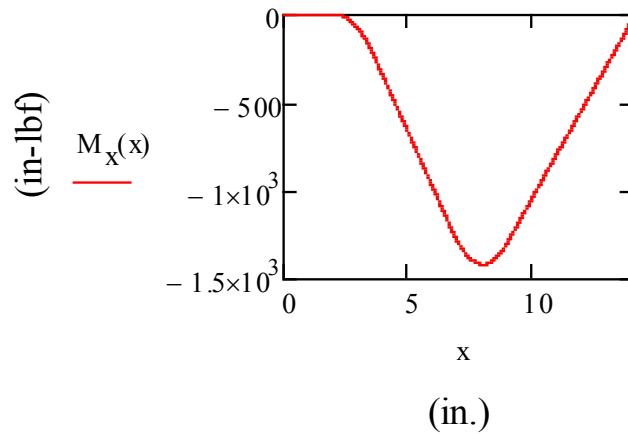
Figure 8: Plot of Moment Over the Length of the Shaft

Stress concentrations experienced at various points along the length of the shaft were then calculated. The Neuber's Constant ($\sqrt{a}$) of the shaft was defined as a function of ultimate tensile strength so that it would update whenever the material properties of the shaft were changed. This function was created using linear interpolation of Table 6-6 in Norton, 2010. The Neuber's Constant in torsion is calculated similarly to in bending, but as if the ultimate tensile strength was 20 kpsi higher. The notch sensitivity for bending and torsion, $q_{bending}$ and $q_{torsion}$ respectively, were defined as a function of position along the length of the shaft by using equation 6.12 in (Norton, 2010). The K_t for bending and torsion were calculated for shoulder fillets and for keyways as described in Pilkey, 2008. Using these equations, the stress concentration factor for bending and torsion were calculated in Equations 5 and 6. Since a safety factor greater than one is desirable, the maximum stress should never exceed the yield strength of the shaft material. This fact means that the mean stress fatigue-concentration factor, K_{fm} and K_{fsm}, should be equal to the K_f and K_{fs} respectively as shown in Equations 7 and 8.

$$K_f(x) := 1 + q_{bending}(x) \cdot \left(K_{t\_bending}(x) - 1\right)$$

$$K_{fs}(x) := 1 + q_{torsion}(x) \cdot \left(K_{t\_torsion}(x) - 1\right)$$

$$K_{fm}(x) := K_f(x)$$

$$K_{fsm}(x) := K_{fs}(x)$$

The stress concentration factors are highest in the keyways, with a K_f of 2.707, and a K_{fs} of 2.928. The keyway ends a distance at least 0.2 times the width of the keyway from the edge of the first shoulder fillet to prevent the stress concentration factor of the keyway from increasing in response to proximity to another notch. The transition from one step to the next includes a shoulder fillet, which has a stress concentration factor based on the diameter of the steps on both sides of it and the notch radius of the fillet. The main stress concentration factors are summarized in Table 3.

Table 3: Stress Concentration Factors

Location	K_f (Bending)	K_{fs} (Shear)
Keyway Channel	2.707	2.928
End of Keyway	2.707	2.696
1st Shoulder Fillet (segment 1 to 2)	1.827	1.444
2nd Shoulder Fillet (segment 2 to 3)	1.918	1.502
3rd Shoulder Fillet (segment 3 to 4)	1.696	1.361
4th Shoulder Fillet (segment 4 to 5)	2.024	1.552
5th Shoulder Fillet (segment 5 to 6)	2.325	2.009

The shaft was modeled as being in alternating bending, but steady torsion, as the shaft will be rotating at a steady angular velocity for extended periods of time and will only experience a changing torque when it is being sped up or slowed down. With this in mind, the alternating and mean von Mises Stresses along two lines on the outer fibers of the shaft were calculated. One line is on the top edge, furthest from the neutral axis, where the maximum bending stresses are experienced. For this line, the highest mean Von Mises stress was 5.418×10^4 psi, and occurred at the keyway. The highest alternating Von Mises stress was 2.665×10^3 psi, which occurred at the shoulder fillet between the middle span and the second bearing seat. This is depicted in Figure 9. The other line is on the side edge, at the neutral axis, where the shear and torsion stresses add together. For this line, the highest mean Von Mises stress was 5.418×10^4 psi, and occurred at the keyway. The highest alternating Von Mises stress was 665.072 psi, which occurred at the shoulder fillet between the first bearing seat and the middle span. This is depicted in Figure 10.
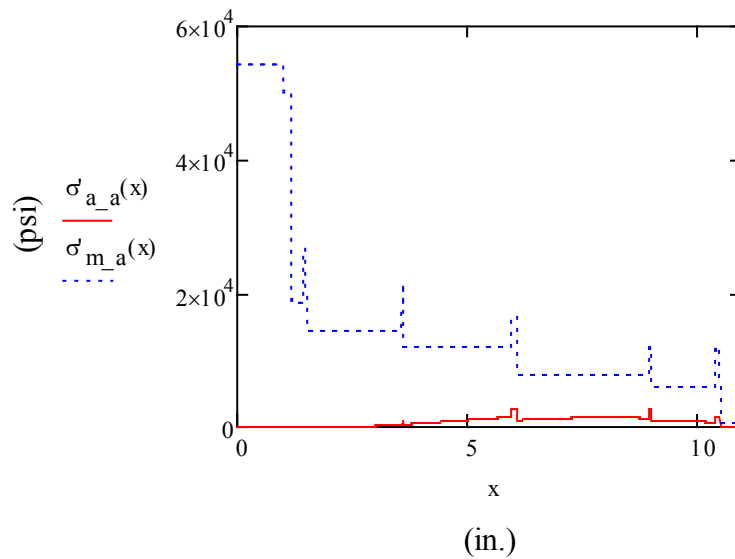
Figure 9: Plot of Alternating and Mean Von Mises Stresses Along a Line at the Top Outer Fibers
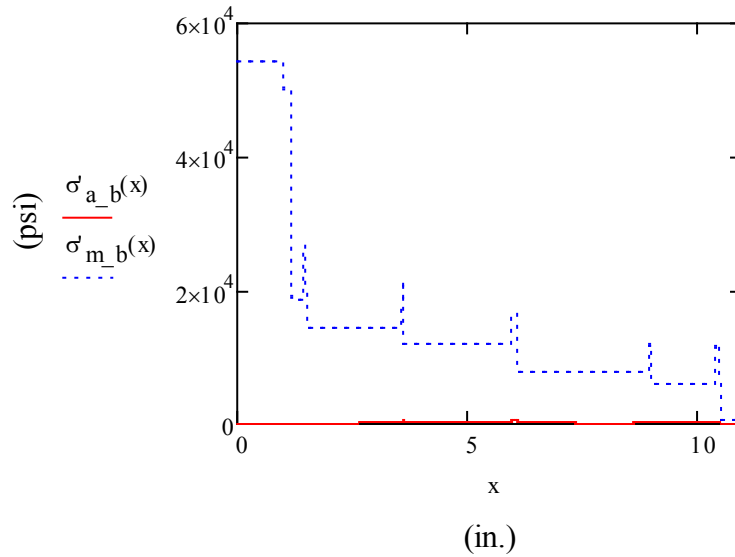
Figure 10: Plot of Alternating and Mean Von Mises Stresses Along a Line at the Side Outer Fibers

Upon completing the stress concentration analysis, the corrected fatigue strength of the shaft was then calculated. Several assumptions were made in determining the corrected fatigue strength of the shaft. No axial loads would be applied to the shaft, only bending loads since one bearing would be free to move along its axis to allow for thermal expansion. This is discussed in more detail in the bearing support structure section. The operating temperature for normal duty would be less than 450 C. The shaft would be between 0.3 and 10 inches in diameter, meaning that the size factor would be calculated using Equation 9. The shaft would be fabricated with a lathe, resulting in a machined surface finish, meaning that the surface factor would be calculated as per Equation 10. A reliability factor of 99% was selected. Each of these factors ware used to calculate the corrected fatigue strength, S_f, with Equation 11 (Norton, 2010).

Equation 8: Size Effect Correction Factor

$$C_{size}(x) = 0.869 \times d_o(x)^{-0.097}$$

$$C_{surf} = 2.7 \times \left(\frac{S_{ut}}{1000}\right)^{-0.265} = 0.768$$

Equation 10: Corrected Fatigue Strength Calculation

$$S_f(x) = S_{e'} \times C_{load} \times C_{temp} \times C_{reliab} \times C_{size} \times C_{surf}$$

Analysis for the infinite life safety factor along the two lines previously discussed was calculated next. A case 4 load scenario was used to calculate the safety factor of the shaft because both the mean and alternating stresses may increase over the operational lifetime of the part (Norton, 2010). Case 4 loading is also the most conservative loading option available for calculation of safety factor for the shaft. With case 4 loading, safety factor is calculated using the shortest path from the "Z" point on the modified-Goodman diagram to the "S" point on the bounds of the diagram.
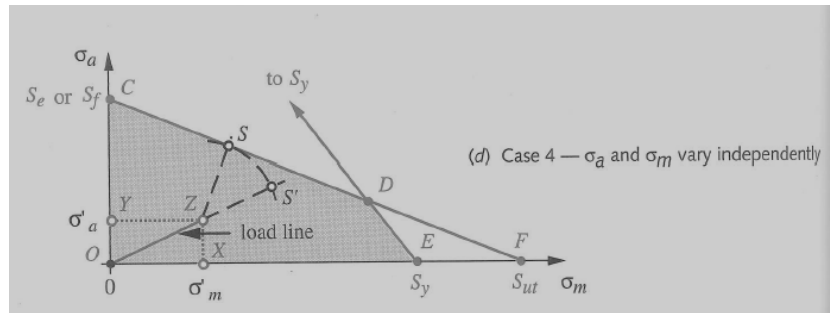
Figure 11- Case 4 Modified-Goodman Diagram

 The minimum safety factor for both lines is 1.282, which occurs at the keyway. Figure 12 shows that the shaft maintains a safety factor higher than two after the transition to the second segment. Figure 13, a detail view of the first four segments of the shaft, shows that both the keyway and the first shoulder fillet reduce the safety factor to below 2. In addition, the differences between the line along the top fibers, line a, and the line along the side fibers, line b, are visible in Figure 13. It can be observed

that the Von Mises stresses are noticeably lower along the side of the shaft than the top for each of the

steps after the second.
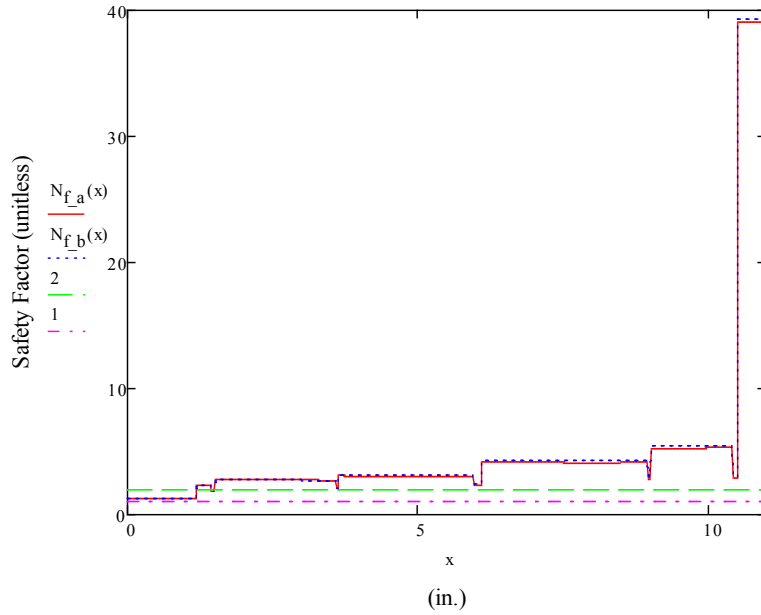
Figure 12: Graph of Safety Factor for Shaft
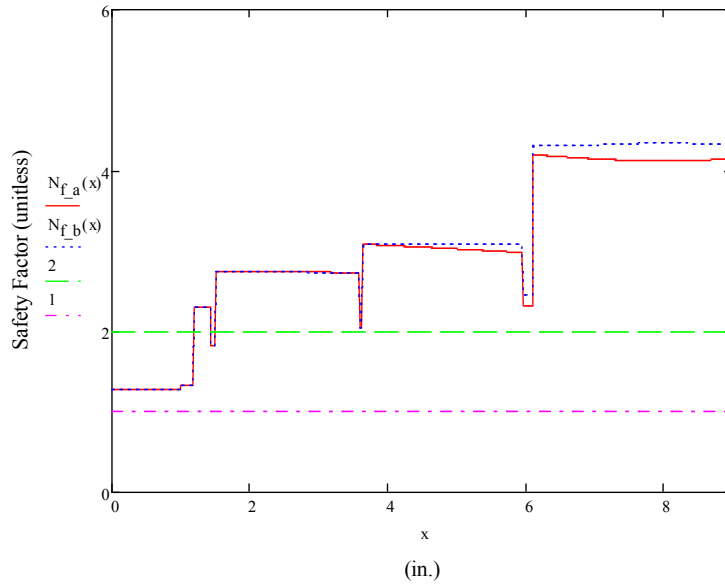
Figure 13: Graph of Safety Factor for Shaft - Detail View of First Four Steps

Next, the deflection of the shaft was analyzed. First, torsional deflection is calculated using the

modulus of rigidity, G, and the second polar moment of area about the z-axis through the centroid of

the shaft. Since the cross-sectional area of the shaft varies from segment to segment, the torsional

deflection was calculated piecewise and added together, as demonstrated in Equation 12. The torsional

deflection in the final shaft at maximum operational torque is calculated to be 6.349×10^{-3} radians, or

0.364 degrees.

<div align="center">Equation 11: Torsional Deflection of Shaft</div>

$$\theta_{deflection} := \frac{T_{max}}{G_{shaft}}\left(\frac{x_1}{J_1} + \frac{x_2 - x_1}{J_2} + \frac{x_3 - x_2}{J_3} + \frac{x_4 - x_3}{J_4} + \frac{x_5 - x_4}{J_5} + \frac{x_6 - x_5}{J_6}\right) = 6.349\times10^{-3}\cdot rad$$

The bending deflection was then calculated using the singularity functions developed earlier.

Angular deflection, $\theta_x(x)$, of the shaft is the first integral of the moment singularity function and

deflection, $y_x(x)$, is the second integral of moment. The equation for each is slightly different than the

standard progression of singularity functions, as they involve division by the moment of inertia, I, and

the elastic modulus, E. This analysis resulted in a shaft angular deflection of -6.34×10^{-4} radian (-0.036

degree) and an end deflection of -1.873×10^{-3} inches.

The appropriate keyway dimensions were then solved for. Peterson's Stress Concentration

Factors (Pilkey, 2008) uses key seat dimensions determined by ratios based on the outer diameter of the

shaft. It is unlikely that a key as specific as one determined through a ratio would be commercially

available. The Machinery's Handbook 28th edition (Oberg, 2008) was referenced to determine the

standard key size, based on the outside diameter of the shaft. ANSI Standard keyway for a 1.5 inch shaft

is 3/8 (0.375) in. key width and 3/16 (0.188) in. key depth. In use, it is likely that all three keyways will

share the load, but at the moment the torque is applied, only one key will be in mesh and it will have to

deflect before any other keys can mesh and carry load. This means, that each individual key has to be able to survive carrying the full 750 ft-lbs of torque delivered to the shaft without shearing or undergoing plastic deformation. Using the key material's yield strength, the minimum length necessary to avoid shear or bearing failure can be calculated.

Finally, vibration analysis on the shaft was completed. The vibration analysis was calculated using the Rayleigh-Ritz method for bending deflections (Thomson, 1988). The shaft was modeled as a simply supported "pinned-pinned" beam, with the mode shape from Equation 13. The mode shape and the mass of each segment are used to calculate the mass components of the matrix. The Young's Modulus, area moment of inertia, and the second integral of the mode shape are used to calculate the spring constant components of the matrix. The matrix is then populated as depicted in Equation 14. Next, the determinant of the matrix is found to be the characteristic equation of the system, which is then solved to determine the natural frequency of the system. The natural frequency of the final shaft design was found to be 6.079×10^3 RPM.

Equation 12: Mode Shape for Pinned-Pinned Beam

$$\sin\left(\frac{i * \pi * x}{L}\right)$$

Equation 13: Rayleigh-Ritz Matrix of Differential Equations

$$\begin{bmatrix} \left(k_{11} - \omega^2 \cdot m_{11}\right) & \left(k_{12} - \omega^2 \cdot m_{12}\right) \\ \left(k_{21} - \omega^2 \cdot m_{21}\right) & \left(k_{22} - \omega^2 \cdot m_{22}\right) \end{bmatrix}$$

After the analysis on the shaft was completed, different geometries were tested to determine their advantages and disadvantages. A rough geometry for the shaft was determined, bearings with

appropriate diameters were selected, and the geometry was adjusted slightly to fight the bearings. The

shoulder fillets abutting the bearing seats had to be decreased in radius to ensure that they would not

prevent the bearing from sitting properly. In addition, it was determined that the bearings needed to be

doubled up to keep them in proper precision, so the bearing seats on the shaft had to be elongated.

The larger bearing seat only needed to be extended to 2.904 inches and the smaller bearing seat needed

to be extended to 2.125 inches to accommodate the double bearings as well as 0.625 inches of sacrificial

material for balancing.

In addition to the length of the steps, the keyway was adjusted so that it would fit a standard

sized 3/8 inch square key. McMaster-Carr was selected as a source for key stock. Most of the key stock

was relatively weak and would require extending the keyway. However, McMaster-Carr carries high

carbon square keys. These keys are constructed out of annealed AISI 1095 steel. The annealed keys

would be too weak to carry a 750 ft-lb torque, but they would be soft enough to cut to length. After any

cutting or machining is performed, they would need to be heat treated. For purposes of analysis, a

treatment of normalization at 900 C followed by air cooling resulted in a high enough yield strength that

a 1 inch key would be able to avoid plastic deformation at 750 ft-lbs of torque with a safety factor of

1.559 in shear and 1.351 in bearing failure.

Originally, the shaft was going to be constructed from AISI 4340 steel so that it could survive 750

ft-lbs of torque without being so thick that it would interfere with the bolt circle. However, the surface

hardness of AISI 4340 is too high to be machined with standard machine tools. If it were to be turned in

the WPI machine shop, special tools would have to be purchased.

It was determined that a new material would be necessary. The new material would have to

have a high Young's Modulus to prevent large deflections, a high yield and ultimate tensile strength in

order to survive the torque required of it, a "knee" in the fatigue strength graph so that it would have an

infinite fatigue life, and have a low enough surface hardness that it could be turned without the need for special tools. When selecting a new material the team chose to use the catalog of Ryerson, a steel vendor, because PTI has purchased stock from them in the past and been satisfied.

Several steels were selected out of the Ryerson catalog and used in the analysis. Most were discarded immediately, but the AISI 1144 had mechanical properties that would survive the 750 ft-lbs of torque the shaft would be required to carry, and a hardness low enough to allow for machining with regular machine tools. In particular, 1144 steel has a yield strength of a minimum of 100 kpsi, a minimum ultimate tensile strength of 115 kpsi, and a hardness of 238 on the Brinell scale ("Estimated Mechanical Properties of Steel," n.d.).

When the design of the shaft was completed, it was modeled in Solidworks, as shown in Figure 14.
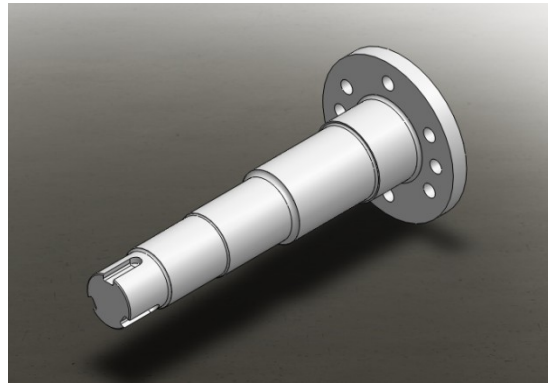
Figure 14: Solid Model of Shaft

This model was then used in Solidworks Simulation to complete a Finite Element Analysis on the structure. A material definition for AISI 1144 Steel was created in Solidworks to be used in the completion of the FEA, which resulted in a minimum factor of safety of approximately 90 under bending forces (Figure 15). These analyses were performed to support the longhand calculations.
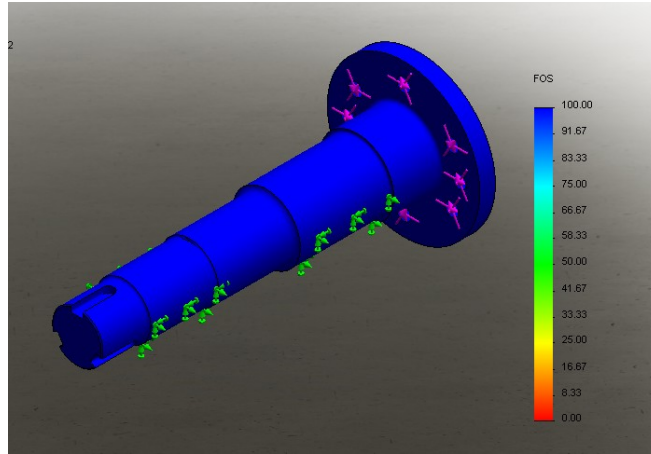
Figure 15: Shaft Factor of Safety Results

The von Mises stresses and displacement were then studied. The results, displayed in Figures 16 and 17 respectively, show that the maximum stress this component would need to withstand would be approximately 795 psi. The maximum displacement the component would be expected to withstand is approximately .008 of an inch.
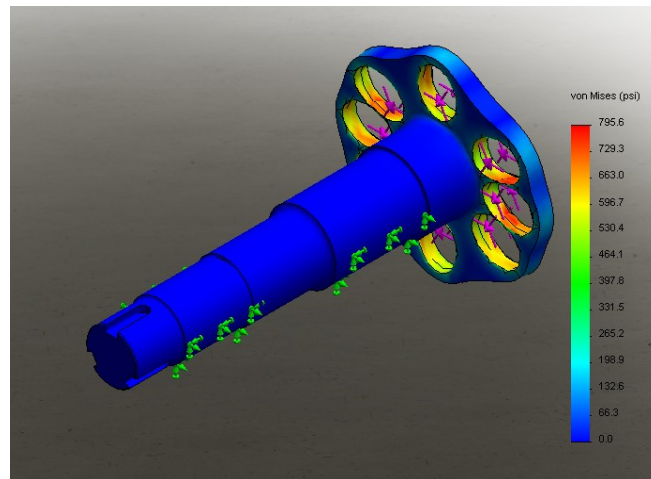
Figure 16: Shaft von Mises Stress Calculation Results
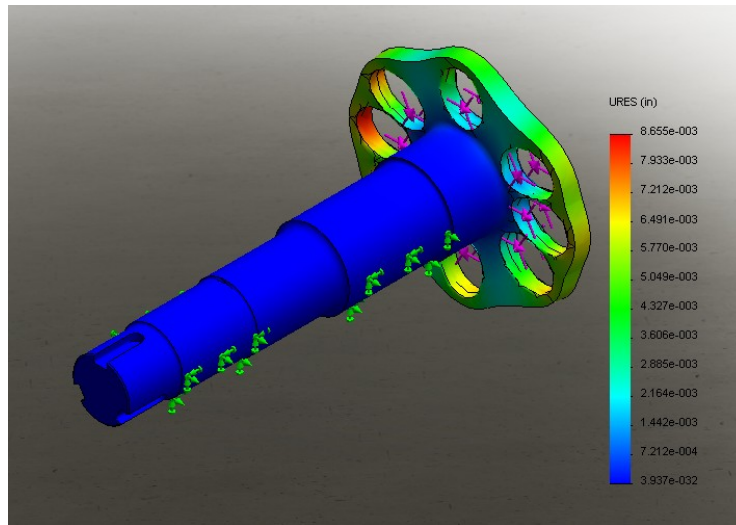
Figure 17: Shaft Displacement Calculation Results

Bearings and Bearing Support Structure

Bearings

In order to properly support the shaft, proper bearings had to be selected. Although there are many bearing companies that would be able to provide appropriate bearings, Timken was the company that the team chose to work with. Timken was selected because PTI has a known successful history of working Timken.

Initially, roller bearings were investigated as the type of bearing to be used to support the shaft. The Light 7200WN Series was originally chosen. After reading about the bearings however, there were some questions on whether this was the right choice. Although these bearings are rated to withstand 5200lbs under static loading and 9200lbs under dynamic loading, the bearings required special care and repositioning or alignment when installing just one bearing. Timken strongly suggested that these bearing be used in pairs. Because there were going to be two locations that required bearing support, this meant that four bearings would have to be ordered ("Light 7200wn series," 2003).

In order to try to avoid ordering four bearings, Timken was contacted and the guidance of an engineer with the company was sought. Once the application was understood, it was established that a DN Factor calculation needed to be completed. This was done using equation one below.

$$BB \times RPM$$

Where:

BB is the bearing bore measured in millimeters

RPM is the rotational speed of the shaft

The solution of which is unitless

It was established that the result of this calculation would determine the type of bearing that could be used for this specific application. If the result was less than 250,000, then a radial bearing could be used. If the result was greater than 250,000, but less than 750,000, then a precision bearing was recommended.

Because the shaft needed to be supported in two locations with two different size outer diameters, two calculations were completed. Table four shows the input data and the results of the calculation.

Table 4- DN Factor Calculation Data and Results

Bearing Bore (mm)	Rotational Speed (RPM)	Calculated DN Factor
45	5000	225000
55	5000	275000

These bearing bore diameters were chosen because they were equal to that of the shaft. A rotational speed of 5000RPM was chosen to be sure that the bearings, like the shaft, could withstand the high rotational speed that could be expected during testing. The calculations resulted in DN Factors of 225,000 and 275,000. Both solutions were close to the 250,000 limited that was established by Timken, with one of the solutions surpassing this bench mark. Therefore, precision bearings were selected. The results were then presented to Timken for further guidance on the right precision bearing for this application. A 3mm300WI Series bearing was recommended. This bearing would not only be able to withstand the expected high rotational speeds, but it is also rated for minimum static loads of up to 8500 lbs and minimum dynamic loadings of up to 14,600 lbs. These bearings were therefore selected and recommended to PTI of use with this dynamometer ("Medium 2mm300wi series," 2003).

Bearing Support Structure

Once the bearings were selected, it was then necessary to design a support structure that would not only locate them on the center line of the dynamometer, but would also hold the bearing centers concentric with each other. Initially, two separate bearing supports were designed and modeled. It was quickly established however, that due to such a short shaft length, that there would not be enough room to have two separate bearing supports. The two structures were quickly consolidated into one structure (Figure 18).
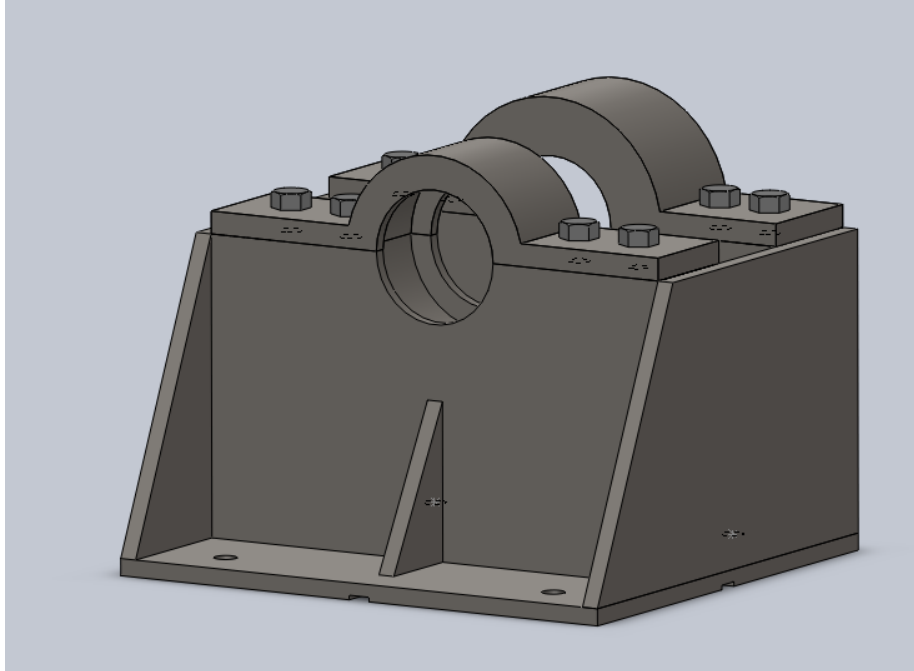
Figure 18- Final Design of the Bearing Support Structure

When looking at Figure 19 it is important to notice that the second bearing support plate is designed so that the bearing in only fixed in the axial direction on one side. This was done so in order to allow for any thermal expansion that the shaft might experience. Although the calculations (Appendix B) showed that the shaft would see a thermal expansion of about 0.0075 inches with a temperature change of 100°F, it was thought best to leave this side of the bearing support open to allow for that possible thermal expansion rather then put unwanted stress on both the bearings and the support structure.
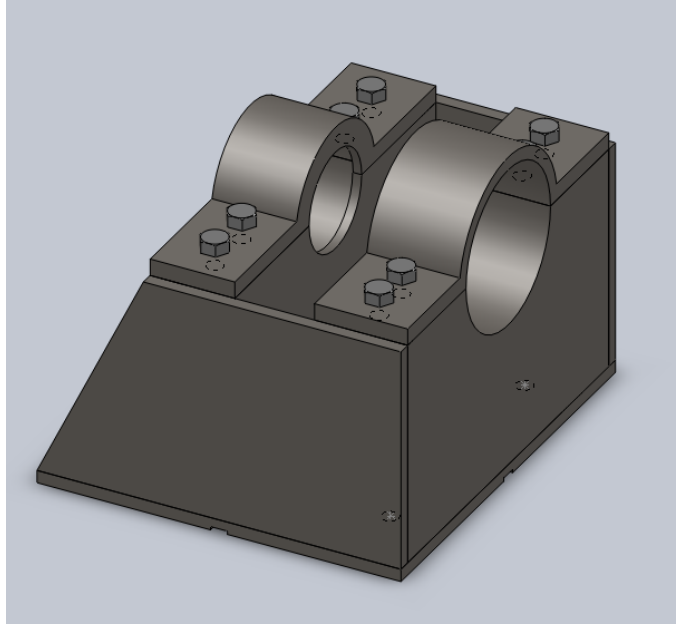
Figure 19- Bearing Support Structure Second Support Plate View

Next, a material was selected for this component. A36 Structural Steel was selected, as it has a yield strength of 36ksi and a tensile strength if about 60ksi. Finite Element Analysis was then completed on this component using Solidworks Simulation. The component was "fixed" at the bolt holes and the calculated reaction loads of 350 lbs and 610 lbs were applied at the bearing seats to simulate what the component would experience during testing. The model was then meshed, and the analysis was run. The results showed that the average safety factor for this structure was around 100 with drops down to about 65 at the corners where the side plates met the bearing seat plates (Figure 20).
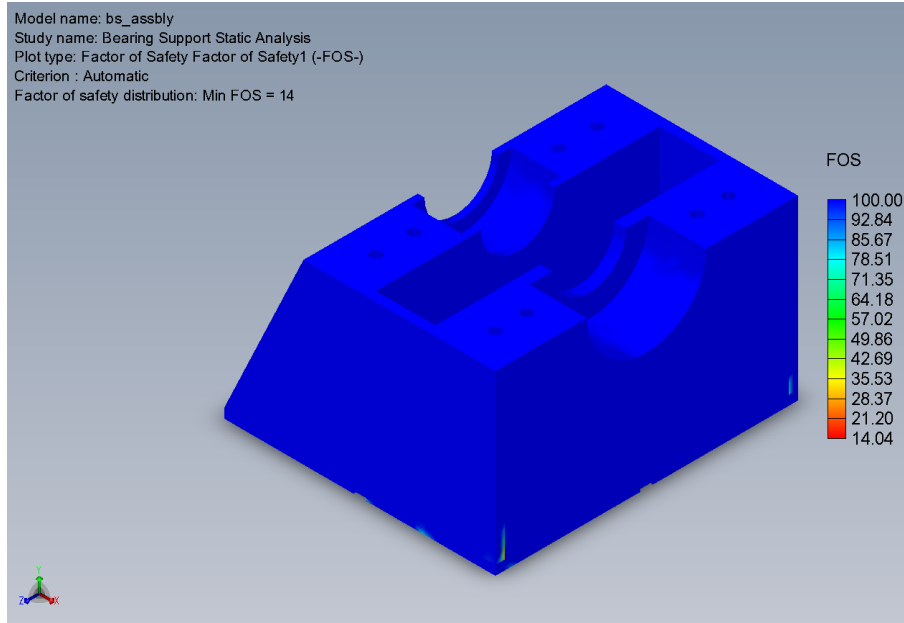
Figure 20- Bearing Support Structure FEA Factor of Safety Results

The average von Misses stress for the bearing support structure was approximately zero for

most of the support structure. The stresses did rise to about 2600 psi in areas around the corner where

the side plates met the bearing support plates (Figure 21). Even these higher stresses were not a

concern however as the yield strength of the material is more than ten times the maximum stress this

component is ever expected to experience.
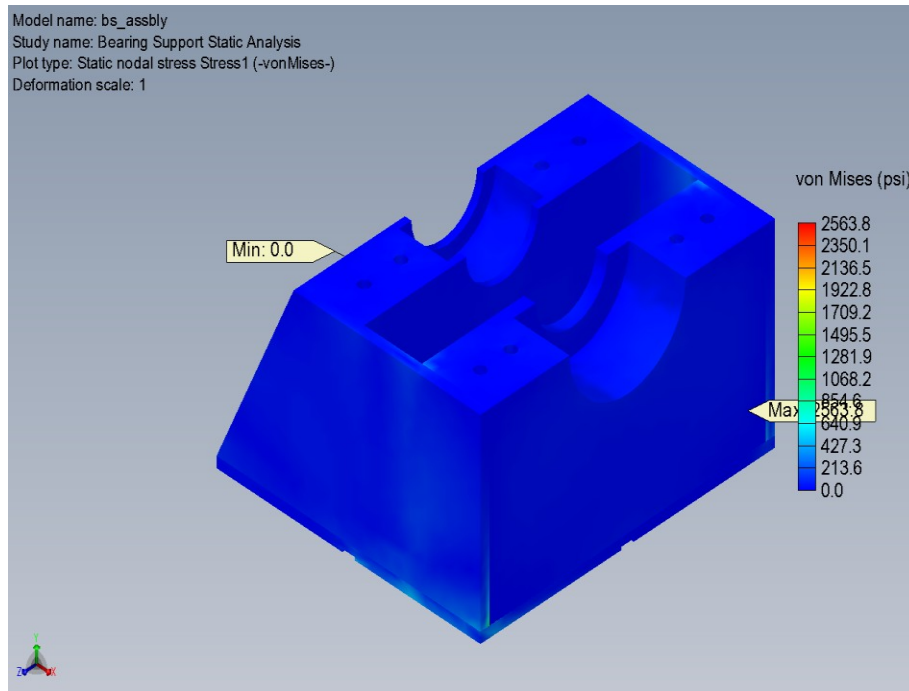
Figure 21- Bearing Support Structure FEA Calculated von Misses stresses

Finally, the displacement that this component was expected to experience was studied. As seen in Figure 22, the displacement that bearing support structure will experience varies. It is important to notice that the maximum displacement however, is less than one ten thousandth of an inch (it is actually calculated to be 8.722E-5 inches). This final calculation solidified this design for the bearing support structure as the final design.

Model name: bs_assbly
Study name: Bearing Support Static Analysis
Plot type: Static displacement Displacement1 (-Res disp-)
Deformation scale: 1

URES (in)

8.722e-005
7.995e-005
7.268e-005
6.541e-005
5.814e-005
5.088e-005
4.361e-005
3.634e-005
2.907e-005
2.180e-005
1.454e-005
7.268e-006
0.000e+000
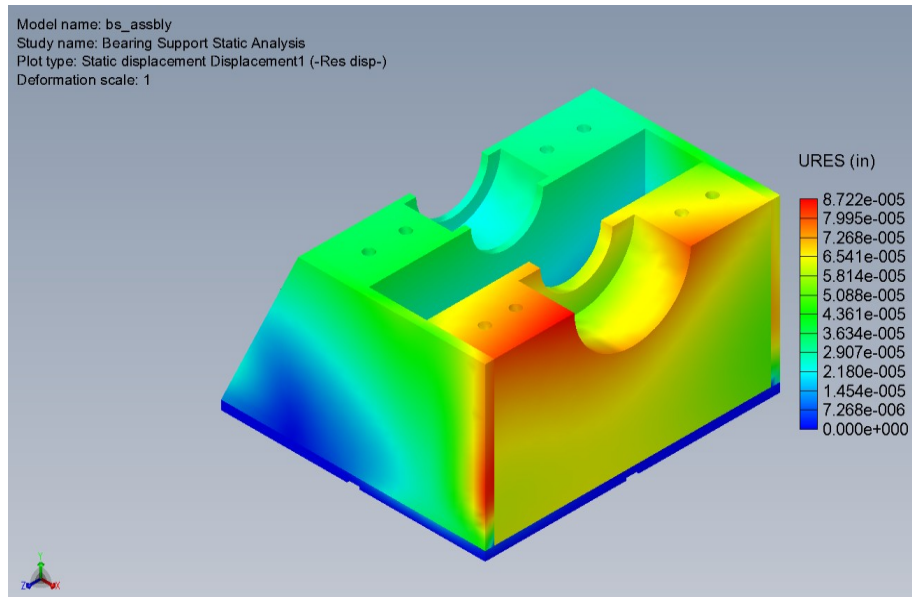
Figure 22- Bearing Support Structure FEA Displacement Results

Torque Meter and Torque Meter Support

Torque Meter

As part of the task specifications, the dynamometer needed to be able to withstand an input torque range of 5-750 ft-lbs of torque. It was also established that the dynamometer would also have to be able to provide some type of torque data measurement. Two main forms of torque measurement were then investigated, torque flanges and torque meters. After discussions with PTI, it was established that a torque meter would best fit the application at hand, and that a torque meter that could measure torque for the small generator would be acceptable (up to 150ft-lbs of torque). With this information in mind, a torque meter produced by Omega Engineering, the TQ501-2K was selected (Figure 23).

Figure 23- Omega TQ501-2K Torque Meter

This torque meter has the ability to measure up to 2000 in-lbs (166.67 ft-lbs) of torque. Another benefit of selecting this torque meter, is that is comes from a family of torque meters, all with similar designs, only varying in dimensions. Torque meters in this family have the capability of measuring up to 10,000 in-lbs (833.33 ft-lbs) of torque. This capability would be necessary when testing the largest generator, which is capable of handling up to 750 ft-lbs of torque.

Torque Meter Support

After selecting a prime mover for recommendation, a support structure needed to be designed. There were two main requirements that this toque meter support needed to meet. First, it needed to be able to support any and all forces that would be placed on it. Second, it needed to locate the torque meter on the centerline of the dynamometer.

The first requirement was met be designing a fixture that mocked the shape on an I-beam. This shape was determined to be ideal because of the strength I-beams are commonly known to have. The second requirement was met first by determining the height of the centerline from the ground. The base plate and top plate thicknesses were then both determined to be 3/8 of an inch. With this information, the correct height of the side plates was then calculated to be 4.13 inches.

Once the design was complete, it was modeled in Solidworks (Figure 24).
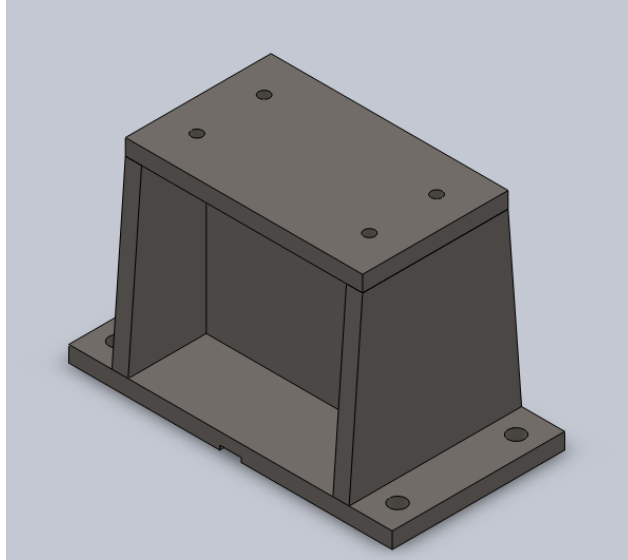
Figure 24- Solid Model of Torque Meter Support Structure

This model was then used in Solidworks Simulation to complete a Finite Element Analysis on the

structure. A material of A36 Steel was chosen to be used in the completion of the FEA, which resulted in

a minimum factor of safety of 91 (Figure 25).
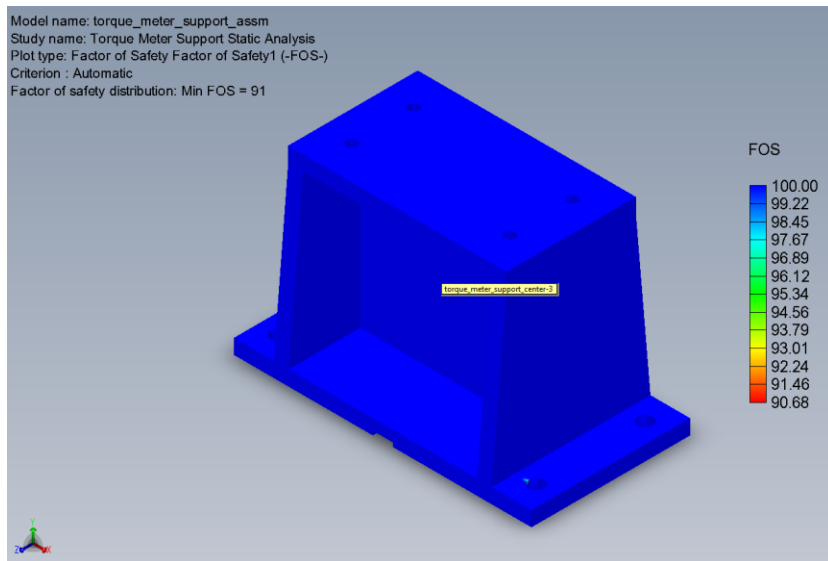
Figure 25-Torque Meter Support Factor of Safety Results

The von Mises stresses and displacement were then studied. The results (given in Figures 26 and 27 below) show that the maximum stress this component would need to withstand would be approximately 397psi. The maximum displacement the component would be expected to withstand would be much less than one ten thousandth of an inch.
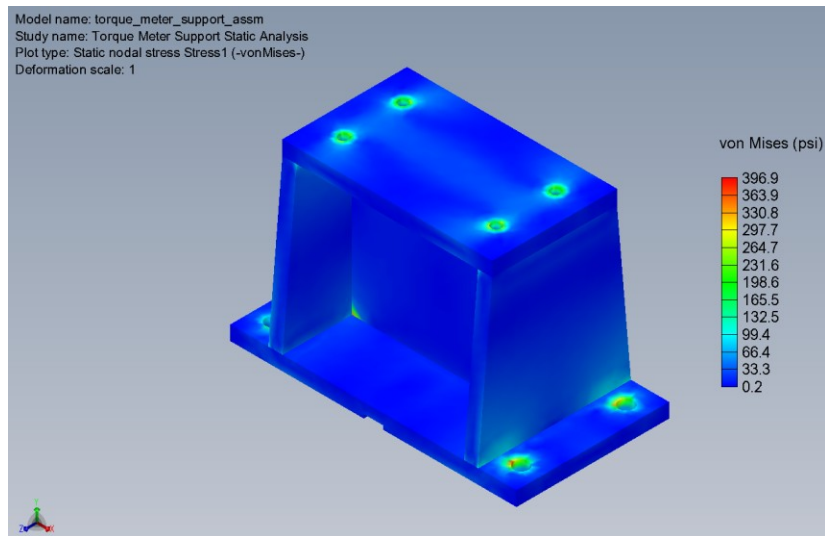
Figure 26-Torque Meter Support von Mises Stress Calculation Results
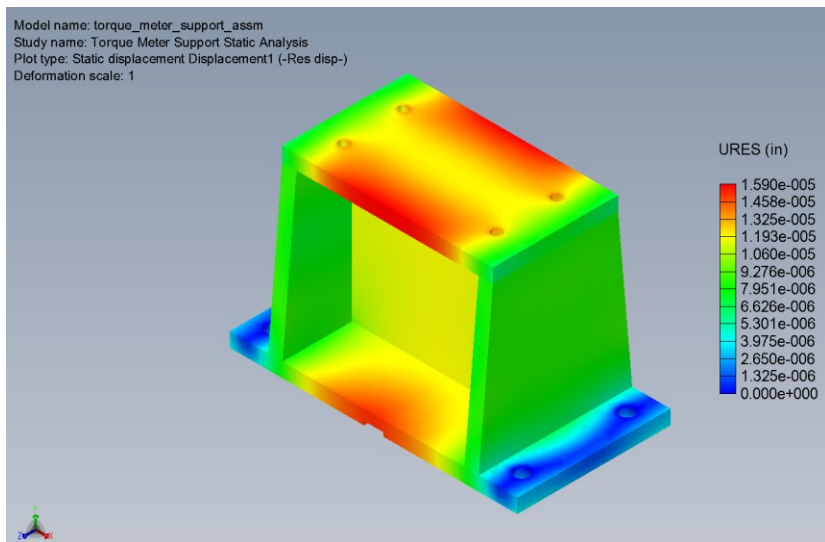
Figure 27- Torque Meter Support Displacement Calculation Results

Prime Mover and Prime Mover Support

Prime Mover

As part of the task specifications, the dynamometer needed to be able to apply a torque range of 5-750 ft-lbs to the rotor. This task seems straightforward, but 750 ft-lbs is a large amount of torque to produce, especially with a maximum operational speed of 5000 RPM. After discussion with PTI, it was determined that PowerTec would be a good starting point to begin researching prime movers. Despite their selection, there was no motor that could produce 750 ft-lbs over the full 5000 RPM operational range.
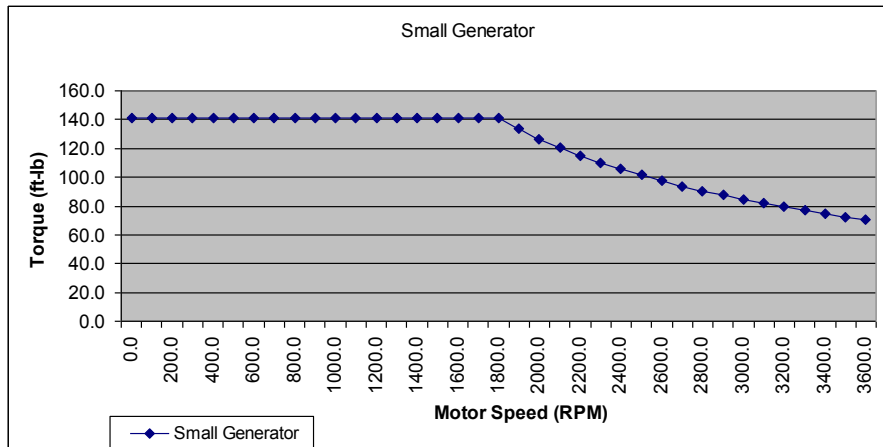
Figure 28: Small Generator Torque Curve

PTI provided the project group with an expected torque curve for the small generator, Figure 28.
The E218E2, pictured in Figure 29, is the only motor in the E21X line that can match or exceed the
torque curve for the small generator test. The gray portion of the E218E2 torque curve, depicted in
Figure 30, is the continuous duty curve, meaning the motor can operate within that curve continually.
The Blue curve is the intermittent duty curve, which covers the full capabilities of the motor, but is not
recommended for long-term use. As can be seen, when comparing Figure 28 to Figure 30, the E218E2
can produce 135 ft-lbs of torque at 3600 rpm, and its torque increases as the angular velocity decreases,
ensuring that at any speed, it can provide enough torque to match the small generator's torque curve.
PowerTec does manufacture larger motors capable of providing the input torque for the small
generator, but they are likely more expensive.

E218E2 MOTOR

2D WINDING CONNECTION

Reference Points		
T_{PK}	660	
T_{CS}	190	
T_{CR}	135	
W_R	3,600	
I_{CS}	142.0	
I_{CR}	100.0	
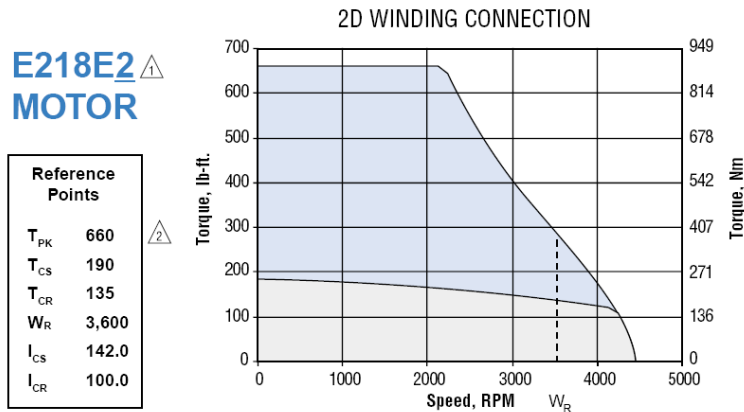
Figure 30: PowerTec E218E2 – DPBV Torque Curve

A different motor, the E32BE2, whose torque curve is pictured in Figure 31, was found to be able, with some gearing, to reproduce the medium and large generator's torque curve, but PTI chose not to pursue it in favor of using a motor made in-house.

E32BE2 MOTOR

2D WINDING CONNECTION

Reference Points		
T_{PK}	2050	
T_{CS}	1090	
T_{CR}	943	
W_R	1750	
I_{CS}	408	
I_{CR}	357	
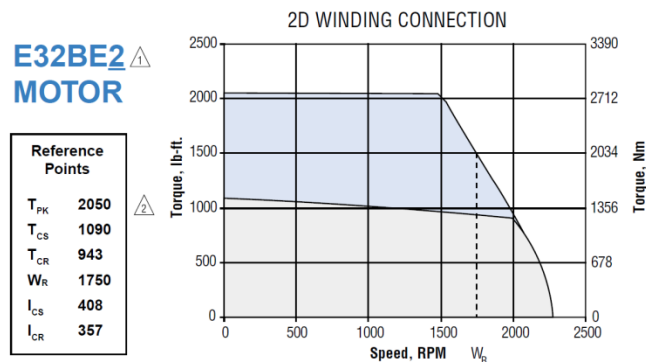
⚠ See model number code, page 46.
⚠ This is also the demagnetization limit. User should apply appropriate safety margins in its use.

Figure 31: PowerTec E32BE2-DPBV

Prime Mover Support

After selecting a prime mover for recommendation, a support structure needed to be designed. There were two main requirements that this prime mover support needed to meet. First, it needed to

be able to support any and all forces that would be place on it. Second, it needed to locate the prime mover on the centerline of the dynamometer.
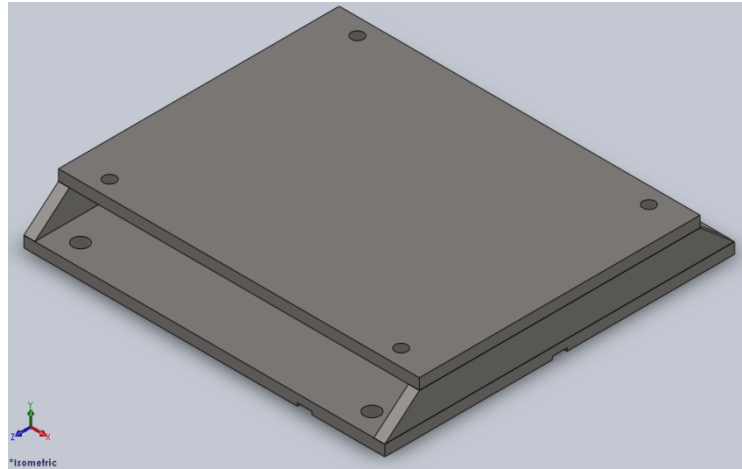
A preliminary design, pictured in Figure 32, was constructed out of several plates, much like the other support structures, though the forces it would experience were much higher than any of the other support structures and a more rigid system was needed. The first requirement was met by designing a fixture that was, in essence, a solid block of material with holes for bolts. The second requirement was met first by determining the height of the centerline from the base support. The centerline is supposed to be 7 inches above the base support structure. The drawings of the E218E2 dimensioned the centerline as being 5.250 inches from the bottom surface of the motor's bolting flange. The difference between needed and actual centerline leaves a gap of 1.75 inches that needs to be filled with the prime mover support structure.

The final support structure design was a solid plate with threaded holes for 3/8 inch heavy hex head bolts that allow the prime mover to be secured to the support structure, and a set of four countersunk free fit holes for half inch bolts that secure the support structure to the base support

structure. The prime mover support structure was increased in width to allow for wrenches to freely

access the bolts that fasten it to the base support.

Once the design was complete, it was modeled in Solidworks (Figure 33).
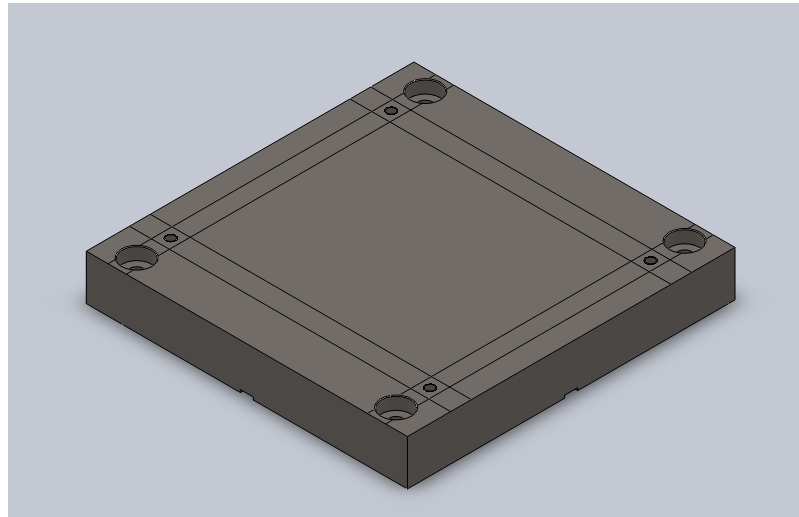
This model was then used in Solidworks Simulation to complete a Finite Element Analysis on the

structure. A material of A36 Steel was chosen to be used in the completion of the FEA, which resulted in

a minimum factor of safety of 10.04, which occurred in the bolt holes (Figure 34).
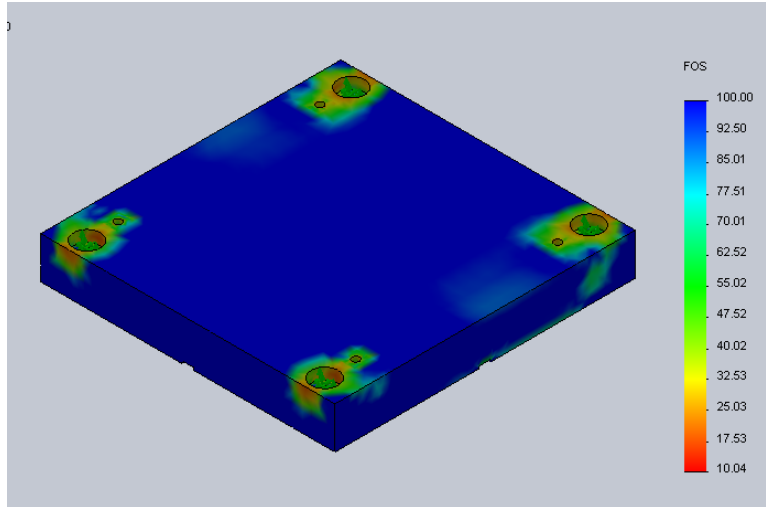
Figure 34: Prime Mover Support Factor of Safety Results

The von Mises stresses and displacement were then studied, shown in Figures 35 and 36 respectively. The results show that the maximum stress this component would need to withstand would be approximately 3600 psi. The maximum displacement the component would be expected to withstand would be much less than one thousandth of an inch.
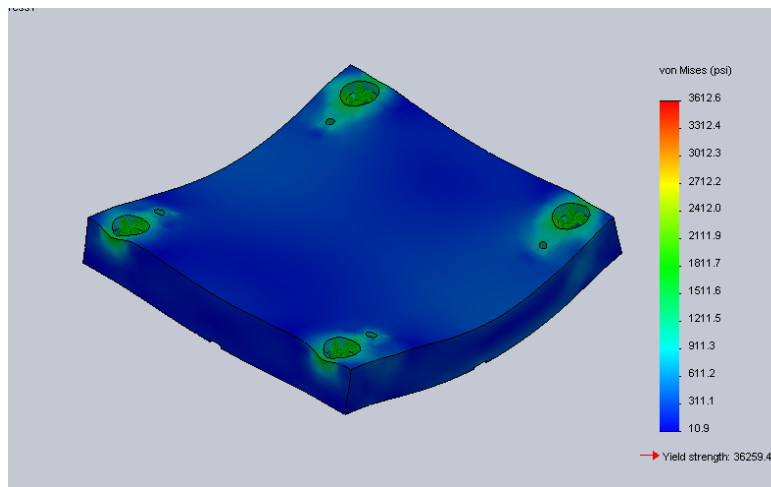
Figure 35: Prime Mover Support von Mises Stress Calculation Results
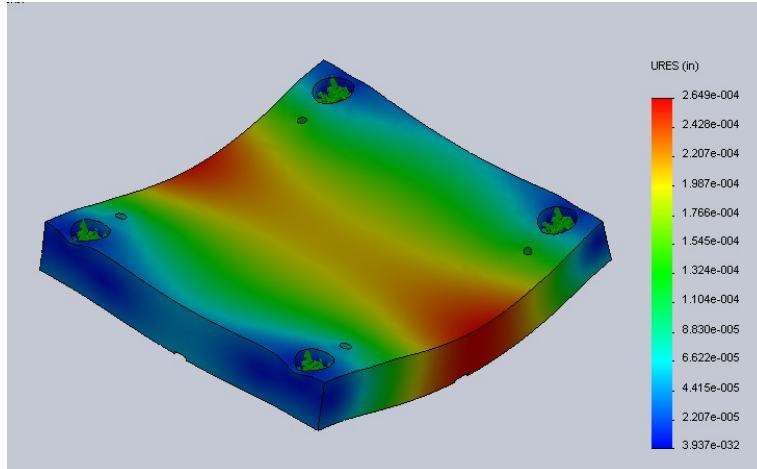
Stator Support Structure

The design of the generator itself requires that both the rotor and stator housing be supported.

Although the shaft was designed to support the rotor, it is not capable of supporting the stator housing

as well. To accomplish this, a separate support structure needed to be designed.

Two design iterations were established for the stator support structure. The first iteration was in

the form of a T with support ribs on both sides of the center vertical plate (Figure 37).
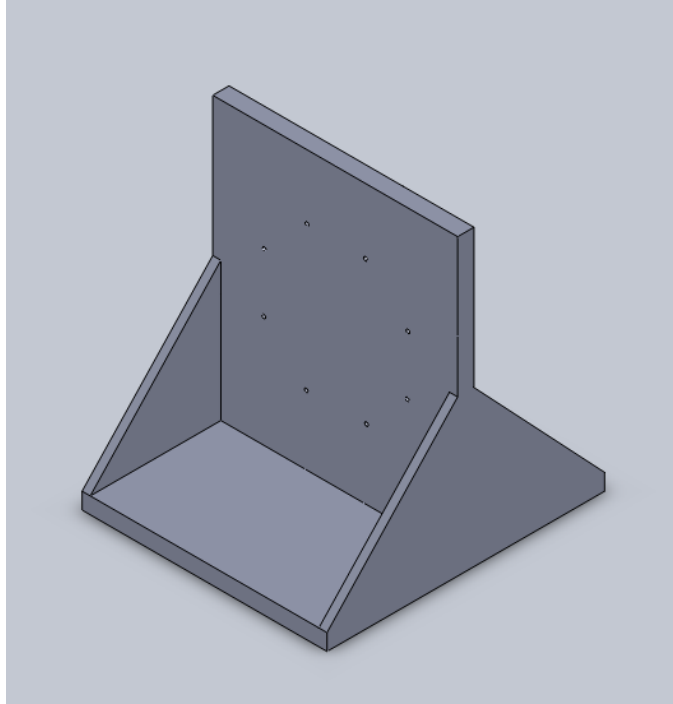
Figure 37- Initial Stator Support Design Iteration

Although this design would have supported the stator housing without any difficulties, it was established that this design would minimize the accessibility of the shaft-rotor assembly, which would be necessary to have in order to make adjustments during testing.

A second design iteration was then created, which positioned the support ribs on the outside of the center vertical plate, parallel to the bolting face (Figure 38).
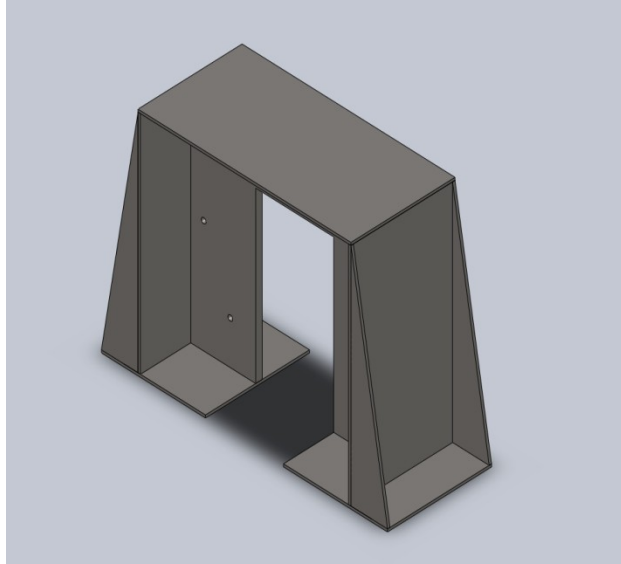
Figure 38- Second Stator Support Design Iteration

This design allowed for much more accessibility to the shaft-rotor assembly, while providing the same amount of structural support.

Once the design was finalized and modeled, Solidworks Simulation was used to complete a Finite Element Analysis of the support structure. A material of A36 Steel was initially chosen to complete the FEA. The FEA resulted in a minimum factor of safety of 100 (Figure 39).
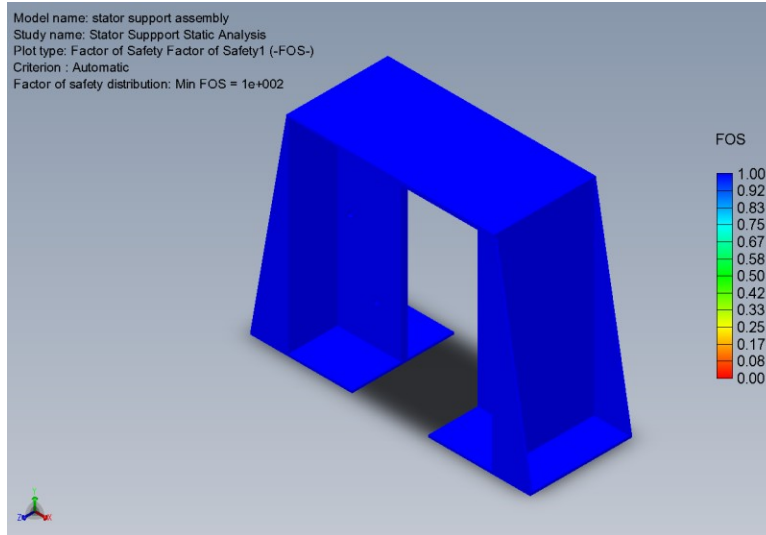
Figure 39- Stator Support Factor of Safety Results

Next, the von Mises stresses and the displacement were studied. The results (given in Figures 40 and 41 below) showed that the maximum stress this structure would experience is approximately 350psi and that the maximum deflection would be less than one ten thousandth of an inch.
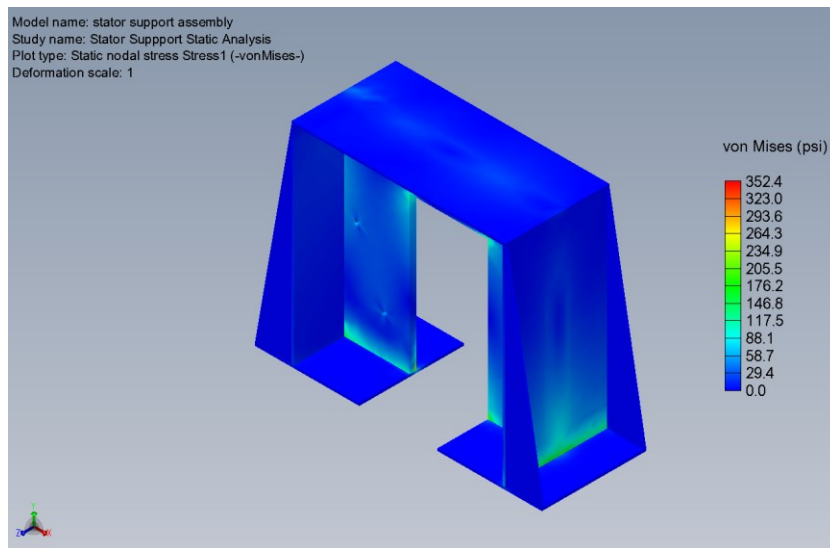
Figure 40- Stator Support von Mises Stress Results

Model name: stator support assembly
Study name: Stator Suppport Static Analysis
Plot type: Static displacement Displacement1 (-Res disp-)
Deformation scale: 1

URES (m)

5.168e-006
4.737e-006
4.306e-006
3.876e-006
3.445e-006
3.015e-006
2.584e-006
2.153e-006
1.723e-006
1.292e-006
8.613e-007
4.306e-007
0.000e+000

Figure 41- Stator Support Displacement Results

Base Support Structure

The purpose of the base support is to support the various subsystem structures used in the dynamometer. The base support is a large rigid support structure that raises the effective "ground level" for most of the components much closer to the centerline, as can be seen in Figure 42. The ideal height of the base support was determined to be 9 inches because it reduced the height of the subsystem supports, improving rigidity and precision of the individual supports bolted onto it. The centerline for the entire system is located 16 inches from the test cell floor. A higher centerline would likely result in larger side to side deflections in the support structures.

The base support structure is designed with a protrusion on the top surface that assists in locating the individual support structures that are bolted on top of it. The protrusion is 0.1 inches tall and follows the centerline of the base support, branching underneath each of the individual supports to locate them both on the X and Y axis. A complimenting channel is also milled into the bottom surface of each support structure. Bolt holes in the base support structure are free fit to ensure that the bolts themselves do not interfere when locating the supports.
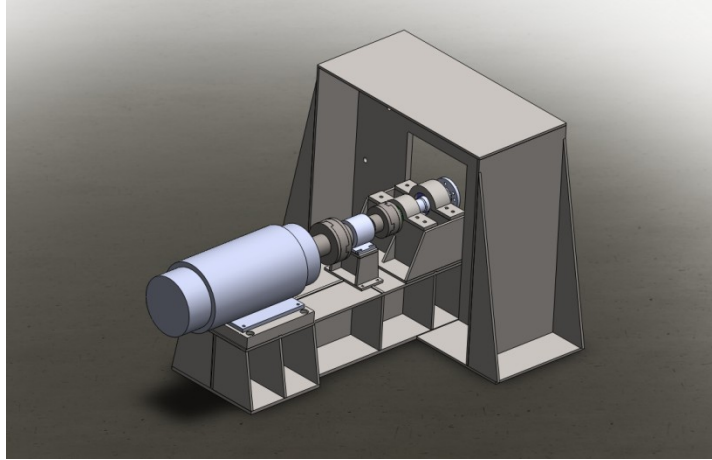
Figure 42: Base Support Structure Design in Full Assembly Supporting Prime Mover, Bearing, and Torque Meter Supports

Two design iterations were established for the base support structure. The first iteration, shown in Figure 43, is very similar to the final design, though with fewer support ribs and a thinner top and bottom plate.
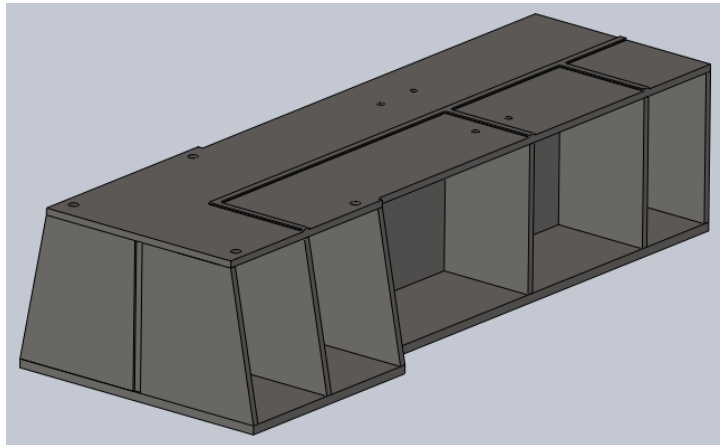
Figure 43: Initial Base Support Structure Design Iteration

Although this design appeared as though it would have supported the prime mover and its associated support structure without any difficulties, it was established that this design did not have enough structural rigidity to prevent unwanted deflections.

A second design iteration was then created, which added four new support ribs under the prime mover support structure, two new support ribs under the bearing support structure, and increased the thickness of the top and bottom plates, as shown in Figure 44. The height of the center rib, the short ribs, and long ribs were adjusted to accommodate the thicker top and bottom plates without moving the centerline.
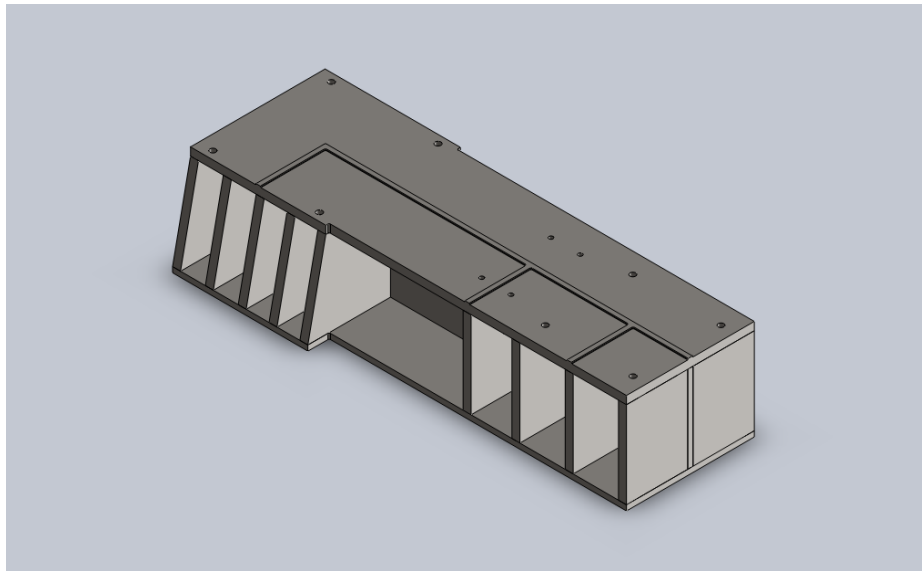
Figure 44: Second Base Support Structure Design Iteration

This design improved the rigidity of the base support and reduced deflections at all of the locations where subsystem supports are bolted in place without changing the envelope that the base support occupies.

Once the design was finalized and modeled, Solidworks Simulation was used to complete a Finite Element Analysis of the support structure. A material of A36 Steel was initially chosen to complete the FEA. The FEA resulted in a minimum factor of safety of 7.2 (Figure 45).
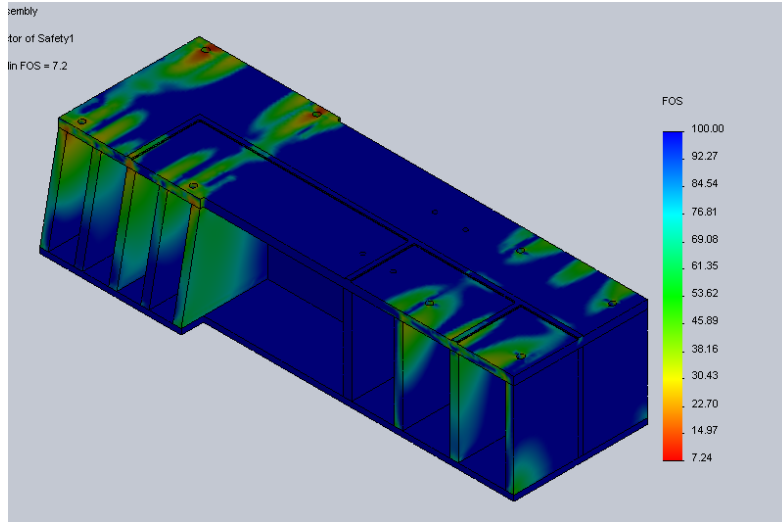
Figure 45: Base Support Structure Factor of Safety Results

Next, the von Mises stresses and the displacement were studied, shown in Figures 46 and 47 respectively. The results showed that the maximum stress this structure would experience is approximately 5000 psi and that the maximum deflection would be less than one thousandth of an inch.

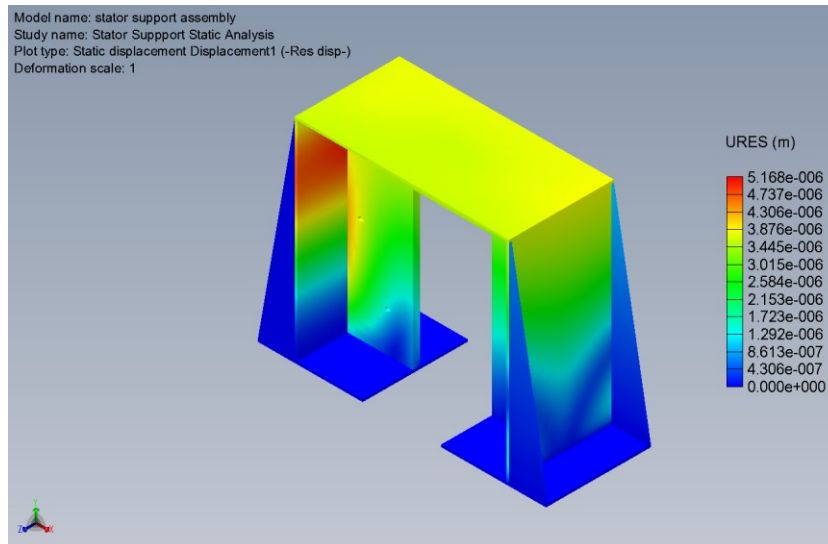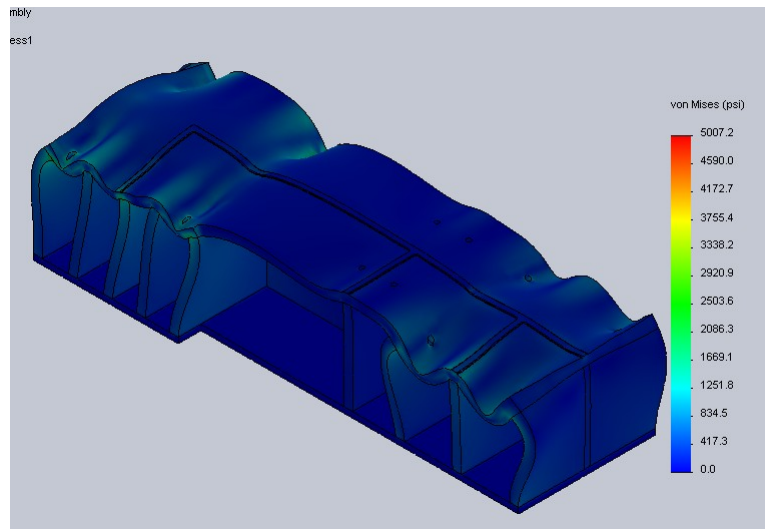Figure 46: Base Support Structure von Mises Stress Results
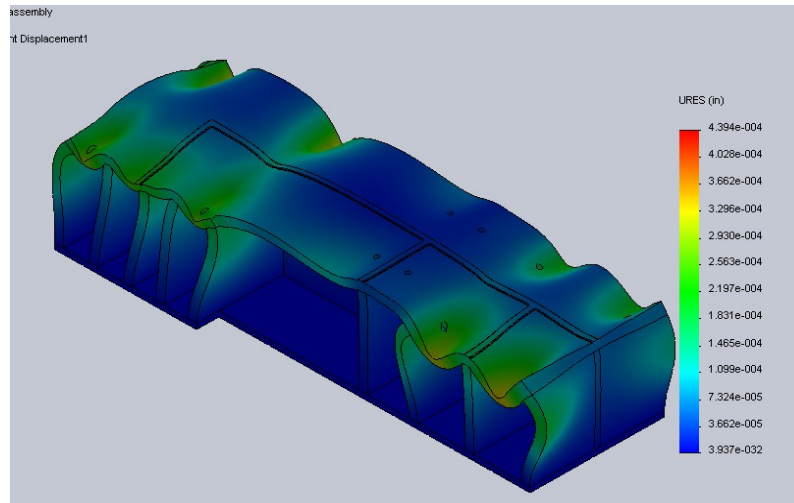
Figure 47: Base Support Structure Displacement Results

Couplings

It was necessary to establish some type of connector for the interface between the prime mover

and torque meter shafts and between the torque meter and generator shafts, because the generator

would not directly be run by a prime mover with the current design. The type of connector commonly

used is a coupling. For this application, off-the-shelf couplings were originally investigated and sought

out. This would save time from design work, but would also allow a tested and proven product to be

used. Unfortunately, the shaft sizes and designs of the components used in this dynamometer did not

allow for off-the-shelf couplings to be used. Reasons for this depended specifically upon the shafts that

were mated.

Prime Mover to Torque Meter Coupling

The only issue with finding a coupling for the prime mover to torque meter interface was the

dramatic difference in shaft diameters. In this case, the recommended prime mover for testing the small

generator had an approximately two inch diameter shaft. This shaft needed to be mated with an

approximate one inch torque meter shaft. Finding a coupling off-the-shelf that met such requirements

was unsuccessful. Therefore, a coupling meeting these requirements was designed. The design itself

went through two iterations. Originally, the coupling was designed as three separate pieces, a piece that would mate to the prime mover shaft; a piece that would mate to the torque meter shaft, and a center plate that would be used to connect the two pieces. The coupling was designed so that all three pieces bolted together (Figure 48).
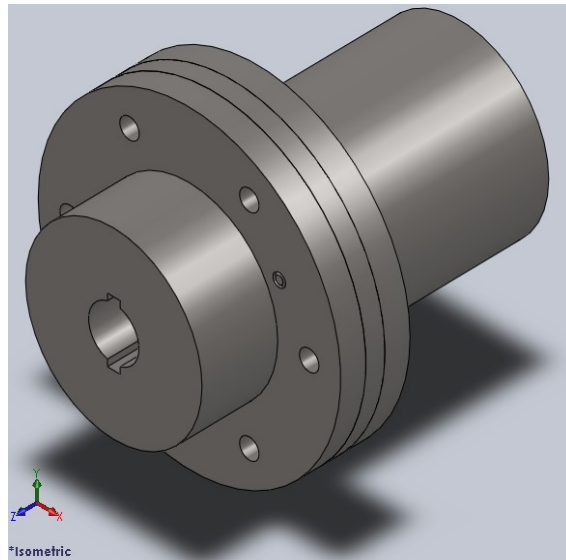
Figure 48- Original Prime Mover to Torque Meter Design

Although this design met the basic requirements of connecting the two shafts and allowing rotation of the shafts, there was concern with alignment allowance of the shafts. The keyways in the coupling would allow for axial misalignment, but not for radial misalignment. Although no radial misalignment was expected during testing, it was thought best that the design of the couplings allowed for some anyway. In order to allow for radial misalignment, a new coupling based on the Oldham coupling design was created (Figure 49). This design would allow for both axial and radial misalignment.
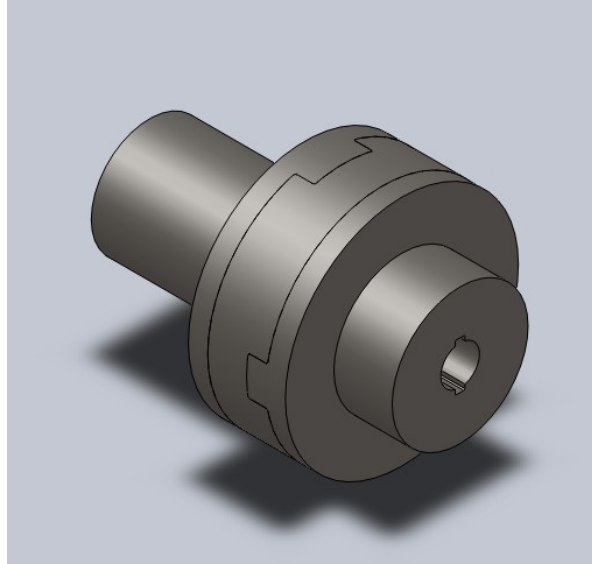
Figure 49- Prime Mover to Torque Meter Oldham Coupling Design

Once the design was complete, the model generated was used in Solidworks Simulation to complete a Finite Element Analysis on the coupling. A material of A36 steel was initially chosen to run the FEA. This FEA resulted in a minimum safety factor of 4.75 as seen in Figure 50 below.
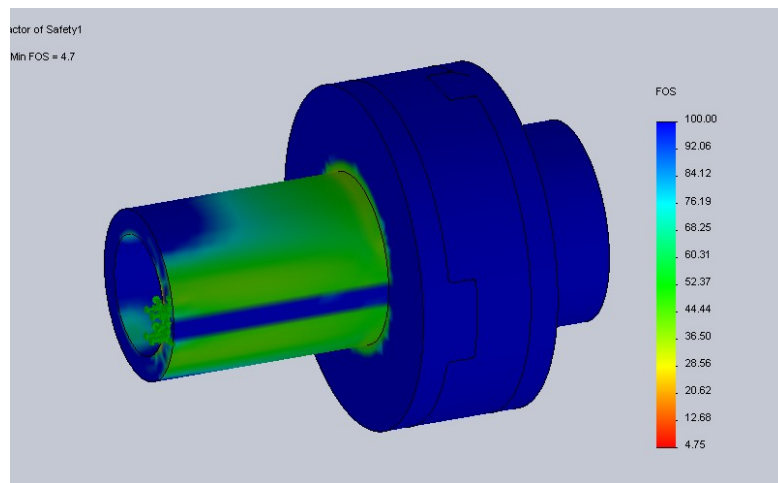
Figure 50- Prime Mover to Torque Meter Oldham Coupling FEA Factor of Safety Results

Next, the von Mises stresses and displacement results were studied. The results (given in Figures 51 and 52 below) showed that maximum stress experienced by this coupling would be approximately 6700 psi and that maximum displacement would be less than one ten thousandth of an inch.
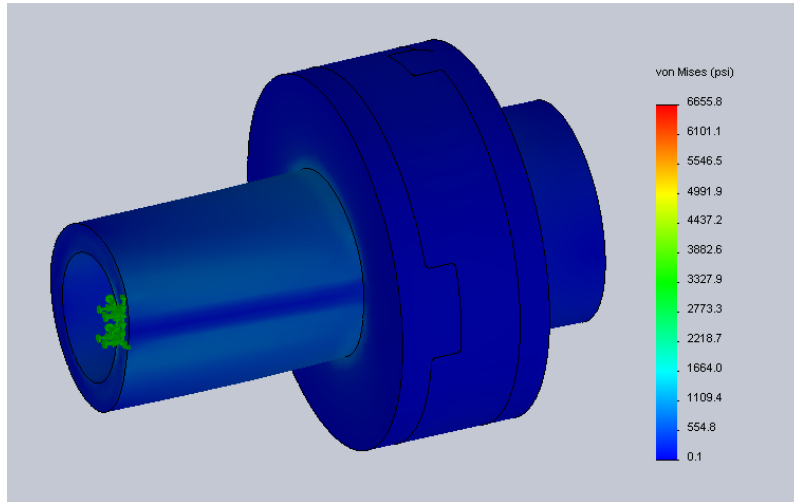
Figure 51- Prime Mover to Torque Meter Oldham Coupling von Mises Stress Results
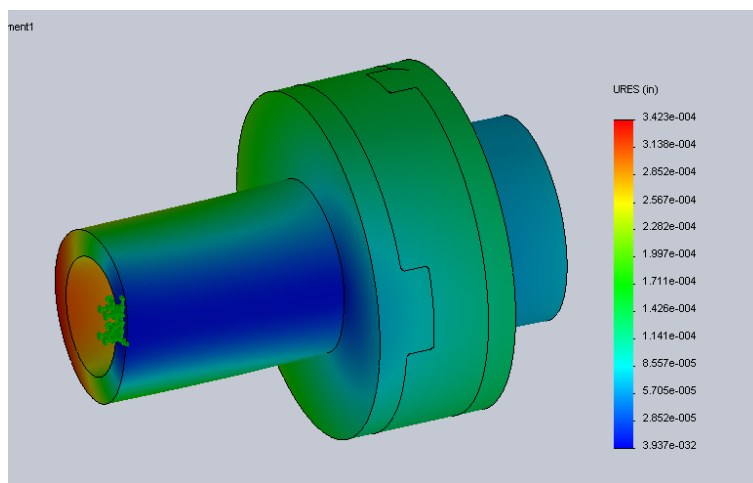
Figure 52- Prime Mover to Torque Meter Oldham Coupling Displacement Results

Torque Meter to Shaft Coupling

The torque meter to shaft coupling also need to be custom designed. While with this design the

change in shaft diameter was not very large (1 inch to 1.62 inches), the coupling piece mating with the

shaft would have to be unique, as the shaft was designed with three keyways. It was established

through research, that finding a coupling that met this criteria would not be possible.

As with the prime mover to torque meter coupling, this coupling when through two design

iterations. The initial design was the same as the first design for the prime mover to torque meter

coupling, with the only difference being the diameters of the mating parts (Figure 53).
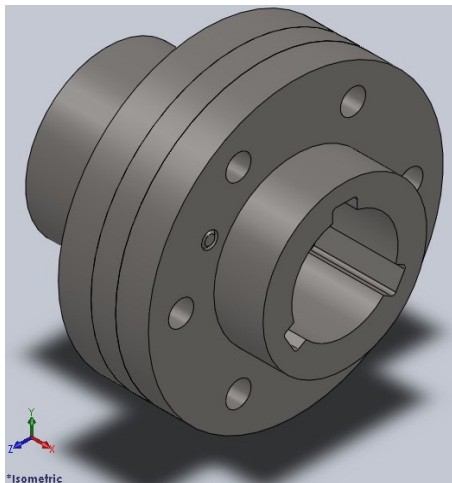
Figure 53- Initial Torque Meter to Shaft Coupling Design

This design also presented concerns that no radial misalignment would be allowed. In order to

overcome this concern, the Oldham coupling design was again applied in the second design iteration

(Figure 54).
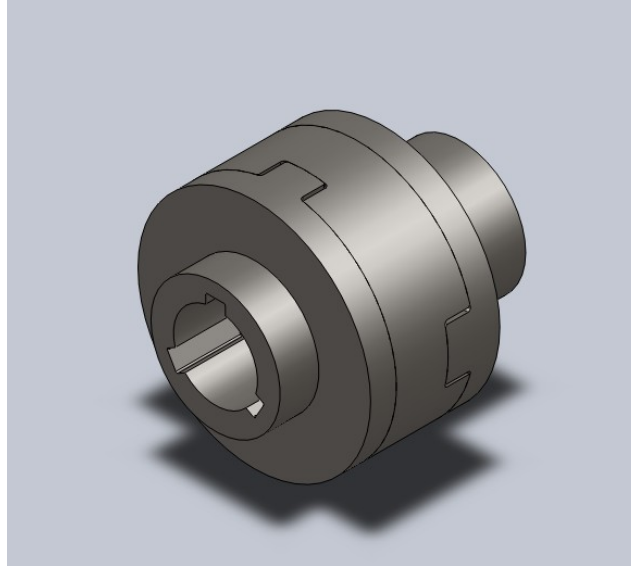
Figure 54- Torque Meter to Shaft Oldham Coupling Design

Again, Finite Element Analysis was completed on the coupling using A36 Steel. The FEA resulted

in a minimum factor of safety of 3.38 (Figure 55).
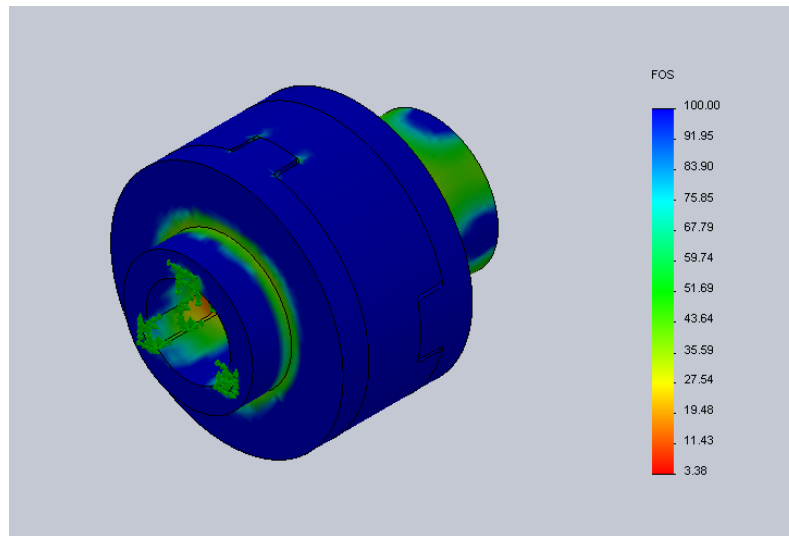
Figure 55- Torque Meter to Shaft Oldham Coupling Factor of Safety Results

The von Mises stress and displacement were then studied. The FEA (given in Figures 56 and 57) showed

that the maximum stress this coupling was expected to withstand was approximately 10725 psi. The

maximum displacement the coupling would be expected to experience is also less than one ten

thousandth of an inch. These results were satisfactory and therefore these designs were accepted as

final designs.
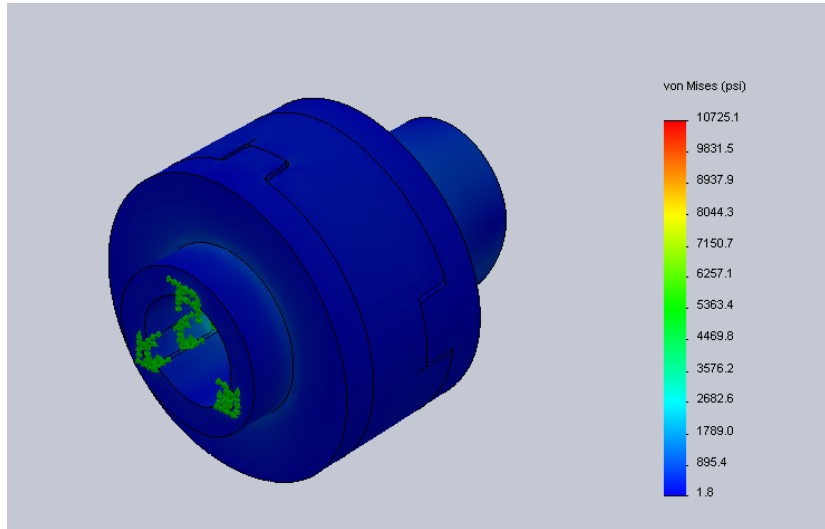
Figure 56- Torque Meter to Shaft Oldham Coupling von Mises Stress Results
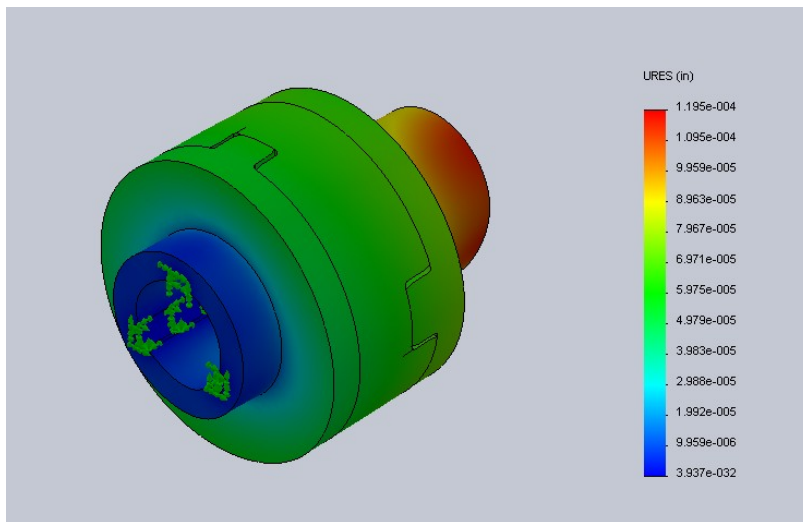
Figure 57- Torque Meter to Shaft Oldham Coupling Displacement Results

Test Cell Layout

The dynamometer assembly will be affixed to the platform of a test cell. The test cell room is

186 inches long by 144 inches wide, and is represented by the larger of the two platforms in the

assembly in Figure 58. The platform itself is 120.5 inches long by 120 inches wide and is represented in

the diagram by a large protrusion from the platform that represents the test cell room. The

dynamometer assembly can be affixed directly to the platform or it could be placed on a taller platform

atop the base platform if the assembly is too short to be used ergonomically. Each of the support

structures in the assembly are quite heavy and will likely need a crane or some other method of assisted

lifting to move them into place. The base support weighs 260 lbs and the stator support weighs 340 lbs.
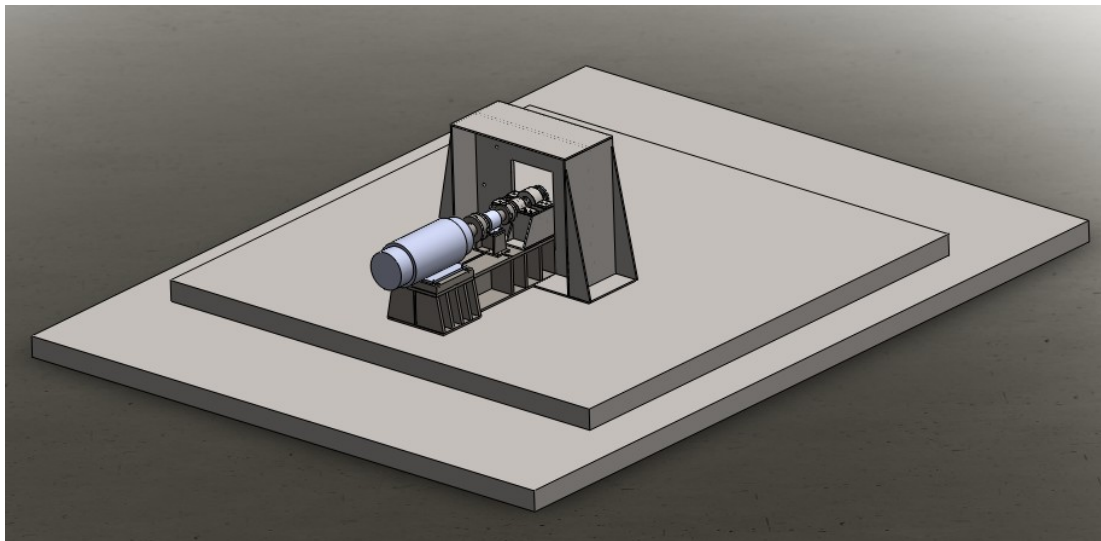
Figure 58: Test Cell Layout

The assembly is arranged in the following way. The base support is affixed to the platform. The

bearing support is placed on the front end of the base support and bolted into place. A protrusion on

the base support locates the bearing support to prevent misalignment. The torque meter support is

bolted in place at the next branch of the locating protrusion and the prime mover support is bolted into

place at the last branch. The shaft and bearings are installed in the bearing support and the prime

mover is bolted onto the top of its support. The holes in the bolting flange of the prime mover are slightly larger than the bolts that go through them, which may allow some angular and axial misalignment. These bolts can be loosened and the prime mover may be able to be adjusted slightly. The couplings are installed on the prime mover, shaft, and torque meter. Next, the torque meter would be installed on top of its supports. Since the couplings are based on the Oldham design, they can be slid into place from the side, allowing the torque meter to be installed after the two heavier components to either side of it. The Stator support is positioned as it appears in Figure 58, straddling the base support. The generator is then attached to the dynamometer, with the rotor bolted to the shaft and the stator housing bolted to the stator support structure.

Adapters

As previously mentioned, this dynamometer will be used to test a family of generators or all different sizes and capabilities. Therefore, it is necessary that the dynamometer can adapt to the different generator interfaces. Originally, iterations involving multiple shafts and support structures were looked into. These ideas were turned down because they would require assembling and taking apart parts of the dynamometer every time a new generator would be tested. After some careful thought, it was decided that the best solution would be to design the dynamometer components that would interface with the generator to be able to support the largest size generator. It would then be recommended that PTI design adapter plates to connect the shaft to the different rotors as the bolt patterns will most likely be different. Adapter plates would also be needed to attach the generator stator housing to the stator support structure, as the bolt patterns will most likely be different as well.

Conclusion

This project successfully developed a dynamometer to be used by DRS Power Technologies, Inc. in Fitchburg, MA. Analysis on all of the components has been completed, and Finite Element Analysis

using Solidworks Simulation was completed as a verification and comparison to the hand calculations that were done using Mathcad. Solid models for each component were made using Solidworks, and part drawings and assemblies drawings were made from these models. The current dynamometer design meets all of the specified requirements for testing the smaller generator described by PTI. The dynamometer is designed however, to be easily adapted for the testing of larger generators.

Recommendations

This project entailed designing and analyzing the many components that make up this dynamometer. Although hand calculations, which were completed using Mathcad, supported the Finite Element Analysis done using Solidworks Simulation, it is recommended that the Finite Element Analysis of the shaft and the couplings be reviewed as Solidworks Simulation did present some difficulties for the project team when performing certain analyses. It is also recommended that the torsional vibration analysis be reviewed. The project team would also recommend that material selection of the shaft be reviewed in order to find a possibly less expensive solution.

It is important to note that the base structure may need to be changed to accommodate a different prime mover for testing. Another important note is that the recommended torque meter in this report comes from a family of torque meters. Within this torque meter family is a torque meter that can read torques up to 10,000 in-lbs. This size torque meter would be needed in order to test generators with input torques up to 750ft-lbs. If a larger torque meter is selected, the torque meter support structure will have to be changed in order to accommodate this different size torque meter.

Currently, there is no suggested method for attaching either the base structure or the stator support structure to the floor of the test cell. It is recommended that engineering establish the best method for attaching this to the floor of the test cell. It is also recommend that the method of attaching

the stator support structure to the floor be adjustable to allow the stator support structure to be moved towards or away from the base structure.

Finally, the project group recommends that the manufacturing of the support structures be revisited. Currently, each piece of each assembly is cut and machined from A36 Steel. The pieces are then aligned and welded together. This presents concerns of both warping during welding, and lack of concentricity where it may be required. In order to avoid these issues, it is recommended that the assemblies pieces be cut and welded together, which would be as called for in a fabrication drawing. It is then recommended that the assemblies undergo a final machining that would add any of the necessary features. This would be called out on a machining drawing.

References

Awiszus, G. (2010). *Drs Power Technology, Inc, A Finmeccanica Company*.

Callister, W.D. (2007). *Material science and engineering: an introduction*. York, PA: John Wiley & Sons,

      Inc..

Corporate information. (2008). Retrieved from http://www.drs.com/CorporateInfo/index.aspx

Estimated Mechanical Properties of Steel. (n.d.). Retrieved April 25, 2010, from

      http://www.ryerson.com/stocklist/n-%252F376.sta-2312.html

Hill, J.E., & Mountain, S.J. (2002). Control of a variable speed, fault-tolerant permanent magnet

      generator. *Power Electronics, Machines and Drives, 2002. International Conference on , 487*.

      Retrieved from

      http://ieeexplore.ieee.org/stamp/stamp.jsp?tp=&arnumber=1031742&isnumber=22154

Light 7200wn series. (2003). *Timken Service Catalog*, 48.

Medium 2mm300wi series 3mm300wi. (2003). *Timken Sevice Catalog*, 83-87.

Norton, R.L. (2010). *Machine design: an intergrated approach*. Boston: Prentice Hall.

Oberg, E., Jones, F. D., Horton, H. L., & Ryffell, H. H. (2008). *Machinery's Handbook* (28th ed.,). Industrial

      Press. Retrieved April 25, 2010, from Pilkey, W. D., & Pilkey, D. F. (2008). *Peterson's Stress*

      Concentration Factors (3rd ed.). John Wiley & Sons. Retrieved April 25, 2010, from

      http://knovel.com/web/portal/browse/display?_EXT_KNOVEL_DISPLAY_bookid=2436&VerticalI

      D=0

Pilkey, W. D., & Pilkey, D. F. (2008). *Peterson's Stress Concentration Factors* (3rd ed.). John Wiley & Sons.

      Retrieved April 25, 2010, from

http://knovel.com/web/portal/browse/display?_EXT_KNOVEL_DISPLAY_bookid=2436&VerticalI D=0

Steffen, J.R. (2009). *Analysis of machine elements: using solidworks simulation 2009*. Mission, KS: SDC Pulications.

Thomson, W. T. (1988). *Theory of Vibration with Applications* (3rd ed., pp. 304-306). Englewood Cliffs, NJ: Prentice Hall.

Appendix A- Shaft Mathcad Analysis

F_a

W_{rotor}

r_1 r_2 r_3 r_4 r_5

d_1

d_2 W_{shaft} d_3 d_4

d_5 d_6

x_1

x_2

x_3

x_4

x_5

x_6

F_b

L
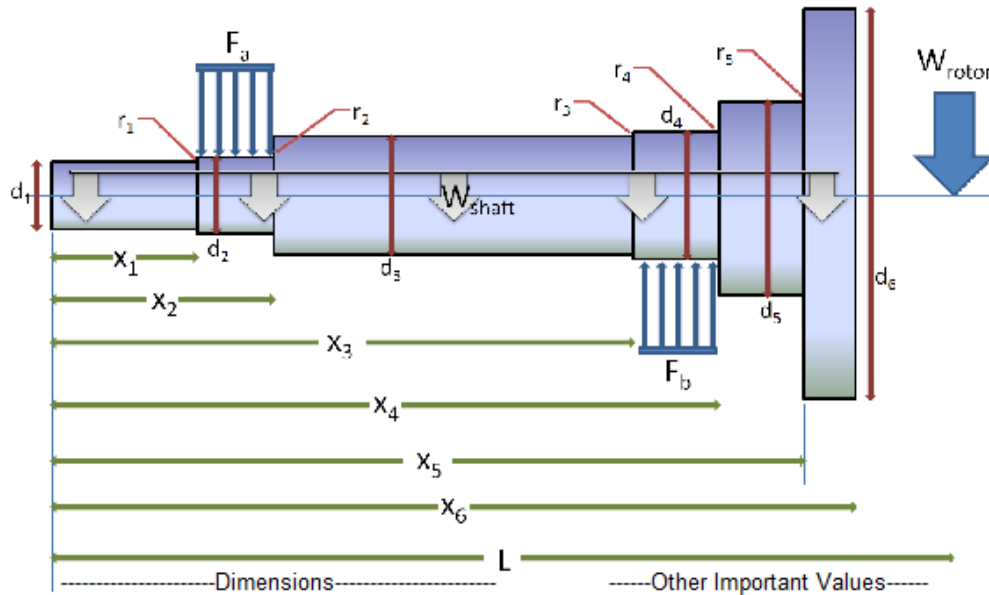
--------------------Dimensions----------------------   ------Other Important Values------

$x_1 := 1.5$ $d_1 := 1.625$ $r_1 := 0.0625$ $rho := 0.284$

$x_2 := 3.625$ $d_2 := 1.77$ $r_2 := 0.039$ $w_{rotor} := 250$

$T_{max} := 9000$

$x_3 := 6.096$ $d_3 := 1.875$ $r_3 := 0.145$ $S_y := 100000$

$x_4 := 9.00$ $d_4 := 2.1654$ $r_4 := 0.059$ $S_{ut} := 115000$

$x_5 := 10.50$ $d_5 := 2.375$ $r_5 := 0.094$ $E := 30000000$

$\nu := 0.28$

$x_6 := 11.00$ $d_6 := 4.90$

$L_{overall} := x_6 + 3.12 = 14.12$

$L_{key} := 1.00$

$L_A := 1.496$

$r_{key} := 0.01$

$L_B := 2.2786$

$b_{key\_width} := 0.375$

$x := 0, 0.01 .. L_{overall}$

$t_{key\_depth} := 0.1875$

Note : $D_{5\_Max} := 3.579 - 1 = 2.579$ $Key_{no} := 3$

$$d_o(x) := \begin{vmatrix} d_1 & \text{if } x < x_1 \\ d_2 & \text{if } x_1 \le x < x_2 \\ d_3 & \text{if } x_2 \le x < x_3 \\ d_4 & \text{if } x_3 \le x < x_4 \\ d_5 & \text{if } x_4 \le x < x_5 \\ d_6 & \text{if } x_5 \le x \le x_6 \\ 0 & \text{otherwise} \end{vmatrix} \qquad D_{large}(x) := \begin{vmatrix} d_2 & \text{if } x < x_1 \\ d_3 & \text{if } x_1 \le x < x_2 \\ d_4 & \text{if } x_2 \le x < x_3 \\ d_5 & \text{if } x_3 \le x < x_4 \\ d_6 & \text{if } x_4 \le x < x_5 \\ 0 & \text{otherwise} \end{vmatrix}$$

$$A_s(x) := \pi \cdot \left(\frac{d_o(x)^2}{4} \right) \qquad x_a := x_2 - \frac{L_A}{2} \qquad x_b := x_4 - \frac{L_B}{2}$$

$$w_1 := \frac{\pi \cdot d_1^2}{4} \cdot rho \cdot x_1 = 0.883 \qquad w_4 := \frac{\pi \cdot d_4^2}{4} \cdot rho \cdot (x_4 - x_3) = 3.037$$

$$w_2 := \frac{\pi \cdot d_2^2}{4} \cdot rho \cdot (x_2 - x_1) = 1.485 \qquad w_5 := \frac{\pi \cdot d_5^2}{4} \cdot rho \cdot (x_5 - x_4) = 1.887$$

$$w_3 := \frac{\pi \cdot d_3^2}{4} \cdot rho \cdot (x_3 - x_2) = 1.938 \qquad w_6 := \frac{\pi \cdot d_6^2}{4} \cdot rho \cdot (x_6 - x_5) = 2.678$$

$$F_a := \frac{-w_1 \left(x_b - \frac{x_1 - 0}{2} \right) - w_2 \left(x_b - \frac{x_2 - x_1}{2} - x_1 \right) - w_3 \left(x_b - \frac{x_3 - x_2}{2} - x_2 \right) - w_4 \left(x_b - \frac{x_4 - x_3}{2} - x_3 \right)}{x_b - x_a} + \dots$$

$$\dots + \frac{w_5 \left(x_4 + \frac{x_5 - x_4}{2} - x_b \right) + w_6 \left(x_5 + \frac{x_6 - x_5}{2} - x_b \right) + w_{rotor} \cdot (L_{overall} - x_b)}{x_b - x_a} = 312.06$$

$$F_b := \frac{-w_1 \left(x_a - \frac{x_1 - 0}{2} \right) - w_2 \left(x_a - \frac{x_2 - x_1}{2} - x_1 \right) + w_3 \left(x_2 + \frac{x_3 - x_2}{2} - x_a \right) + w_4 \left(x_3 + \frac{x_4 - x_3}{2} - x_a \right)}{x_b - x_a} + \dots$$

$$\dots + \frac{w_5 \left(x_4 + \frac{x_5 - x_4}{2} - x_a \right) + w_6 \left(x_5 + \frac{x_6 - x_5}{2} - x_a \right) + w_{rotor} \cdot (L_{overall} - x_a)}{x_b - x_a} = 573.969$$

$$Sum\_F_y := w_1 + w_2 + w_3 + w_4 + w_5 + w_6 + w_{rotor} + F_a - F_b = -1.137 \times 10^{-13}$$

This is zero, there is just a rounding issue with significant figures

$$\text{sing}(x,a,n) := \begin{vmatrix} \text{if } x \geq a \\ \quad \begin{vmatrix} 0 & \text{if } n < 0 \\ (x-a)^n & \text{if } n \geq 0 \end{vmatrix} \\ 0 \quad \text{otherwise} \end{vmatrix}$$

For distributed loads of a discrete length:

$$\text{sing}_d(x,a,b,n) := (\text{sing}(x,a,n) - \text{sing}(x,b,n))$$

$$Q_x(x) := \frac{-w_1}{x_1}\cdot\text{sing}_d(x,0,x_1,0) + \frac{-F_a}{L_A}\cdot\text{sing}_d(x,x_2-L_A,x_2,0) + \frac{-w_2}{x_2-x_1}\cdot\text{sing}_d(x,x_1,x_2,0) + \frac{-w_3}{x_3-x_2}\cdot\text{sing}_d(x,x_2,x_3,0) + \ldots$$

$$\ldots + \frac{-w_4}{x_4-x_3}\cdot\text{sing}_d(x,x_3,x_4,0) + \frac{F_b}{L_B}\cdot\text{sing}_d(x,x_4-L_B,x_4,0) + \frac{-w_5}{x_5-x_4}\cdot\text{sing}_d(x,x_4,x_5,0) + \ldots$$

$$\ldots + \frac{-w_6}{x_6-x_5}\cdot\text{sing}_d(x,x_5,x_6,0) - w_{rotor}\cdot\text{sing}(x,L_{overall},-1)$$

$$V_x(x) := \frac{-w_1}{x_1}\cdot\text{sing}_d(x,0,x_1,1) + \frac{-F_a}{L_A}\cdot\text{sing}_d(x,x_2-L_A,x_2,1) + \frac{-w_2}{x_2-x_1}\cdot\text{sing}_d(x,x_1,x_2,1) + \frac{-w_3}{x_3-x_2}\cdot\text{sing}_d(x,x_2,x_3,1) + \ldots$$

$$\ldots + \frac{-w_4}{x_4-x_3}\cdot\text{sing}_d(x,x_3,x_4,1) + \frac{F_b}{L_B}\cdot\text{sing}_d(x,x_4-L_B,x_4,1) + \frac{-w_5}{x_5-x_4}\cdot\text{sing}_d(x,x_4,x_5,1) + \ldots$$

$$\ldots + \frac{-w_6}{x_6-x_5}\cdot\text{sing}_d(x,x_5,x_6,1) - w_{rotor}\cdot\text{sing}(x,L_{overall},0)$$

$$M_x(x) := \frac{-w_1}{2x_1}\cdot\text{sing}_d(x,0,x_1,2) + \frac{-F_a}{2(L_A)}\cdot\text{sing}_d(x,x_2-L_A,x_2,2) + \frac{-w_2}{2(x_2-x_1)}\cdot\text{sing}_d(x,x_1,x_2,2) + \ldots$$

$$\ldots + \frac{-w_3}{2(x_3-x_2)}\cdot\text{sing}_d(x,x_2,x_3,2) + \frac{-w_4}{2(x_4-x_3)}\cdot\text{sing}_d(x,x_3,x_4,2) + \frac{F_b}{2(L_B)}\cdot\text{sing}_d(x,x_4-L_B,x_4,2) + \ldots$$

$$\ldots + \frac{-w_5}{2(x_5-x_4)}\cdot\text{sing}_d(x,x_4,x_5,2) + \frac{-w_6}{2(x_6-x_5)}\cdot\text{sing}_d(x,x_5,x_6,2) - w_{rotor}\cdot\text{sing}(x,L_{overall},1)$$

$T_a := T_{max} \cdot 0 = 0$
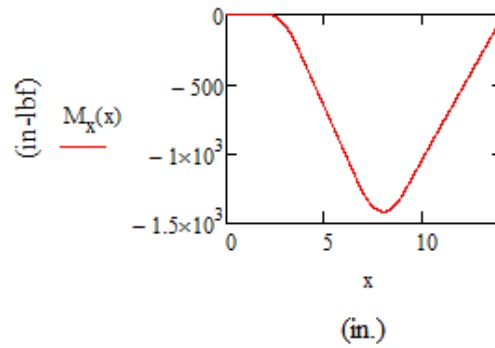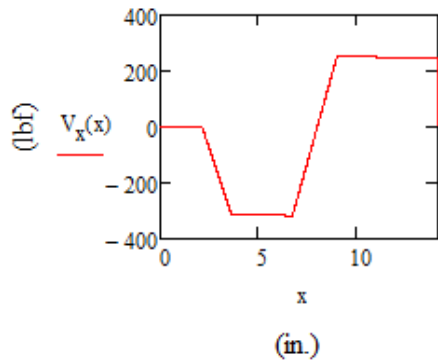
$T_m := T_{max} \cdot 1 = 9 \times 10^3$

$V_a(x) := V_x(x)$

$V_m := 0$

$M_a(x) := M_x(x)$

$M_m := 0$

$I_x(x) := \frac{\pi}{64} \cdot \left(d_o(x)^4\right)$

$J_z(x) := \frac{\pi}{32} \cdot \left(d_o(x)^4\right)$

$I_1 := \frac{\pi \cdot d_1^4}{64} = 0.342$

$I_2 := \frac{\pi \cdot d_2^4}{64} = 0.482$

$I_3 := \frac{\pi \cdot d_3^4}{64} = 0.607$

$I_4 := \frac{\pi \cdot d_4^4}{64} = 1.079$

$I_5 := \frac{\pi \cdot d_5^4}{64} = 1.562$

$I_6 := \frac{\pi \cdot d_6^4}{64} = 28.298$

$M_x(L_{overall}) = -2.236 \times 10^{-12}$

$V_x(L_{overall}) = -2.842 \times 10^{-14}$

▲ Singularity Functions

▼ Stress Concentration Factors

$r_{notch}(x) := \begin{vmatrix} r_1 & \text{if } x_1 - r_1 \le x < x_1 \\ r_2 & \text{if } x_2 - r_2 \le x < x_2 \\ r_3 & \text{if } x_3 - r_3 \le x < x_3 \\ r_4 & \text{if } x_4 - r_4 \le x < x_4 \\ r_5 & \text{if } x_5 - r_5 \le x < x_5 \\ r_{key} & \text{if } 0 \le x < L_{key} + \frac{b_{key\_width}}{2} \\ 0 & \text{otherwise} \end{vmatrix}$

$D\_d(x) := \begin{vmatrix} \dfrac{d_2}{d_1} & \text{if } x_1 - r_1 \le x < x_1 \\ \dfrac{d_3}{d_2} & \text{if } x_2 - r_2 \le x < x_2 \\ \dfrac{d_4}{d_3} & \text{if } x_3 - r_3 \le x < x_3 \\ \dfrac{d_5}{d_4} & \text{if } x_4 - r_4 \le x < x_4 \\ \dfrac{d_6}{d_5} & \text{if } x_5 - r_5 \le x < x_5 \end{vmatrix}$

Neubers constant determined through linear interpolation of Table 6-6 in Machine Desing: An Integrated Approach, Third Edition, by Norton

$$
\text{Neubers}_{bending} := \begin{vmatrix}
\dfrac{S_{ut} - 50000}{55000 - 50000} \cdot (0.118 - 0.130) + 0.130 & \text{if } 50000 < S_{ut} \le 55000 \\[2mm]
\dfrac{S_{ut} - 55000}{60000 - 55000} \cdot (0.108 - 0.118) + 0.118 & \text{if } 55000 < S_{ut} \le 60000 \\[2mm]
\dfrac{S_{ut} - 60000}{70000 - 60000} \cdot (0.093 - 0.108) + 0.108 & \text{if } 60000 < S_{ut} \le 70000 \\[2mm]
\dfrac{S_{ut} - 70000}{80000 - 70000} \cdot (0.080 - 0.093) + 0.093 & \text{if } 70000 < S_{ut} \le 80000 \\[2mm]
\dfrac{S_{ut} - 80000}{90000 - 80000} \cdot (0.070 - 0.080) + 0.080 & \text{if } 80000 < S_{ut} \le 90000 \\[2mm]
\dfrac{S_{ut} - 90000}{100000 - 90000} \cdot (0.062 - 0.070) + 0.070 & \text{if } 90000 < S_{ut} \le 100000 \\[2mm]
\dfrac{S_{ut} - 100000}{110000 - 100000} \cdot (0.055 - 0.062) + 0.062 & \text{if } 100000 < S_{ut} \le 110000 \\[2mm]
\dfrac{S_{ut} - 110000}{120000 - 110000} \cdot (0.049 - 0.055) + 0.055 & \text{if } 110000 < S_{ut} \le 120000 \\[2mm]
\dfrac{S_{ut} - 120000}{130000 - 120000} \cdot (0.044 - 0.049) + 0.049 & \text{if } 120000 < S_{ut} \le 130000 \\[2mm]
\dfrac{S_{ut} - 130000}{140000 - 130000} \cdot (0.039 - 0.044) + 0.044 & \text{if } 130000 < S_{ut} \le 140000 \\[2mm]
\dfrac{S_{ut} - 140000}{160000 - 140000} \cdot (0.031 - 0.039) + 0.039 & \text{if } 140000 < S_{ut} \le 160000 \\[2mm]
\dfrac{S_{ut} - 160000}{180000 - 160000} \cdot (0.024 - 0.031) + 0.031 & \text{if } 160000 < S_{ut} \le 180000 \\[2mm]
\dfrac{S_{ut} - 180000}{200000 - 180000} \cdot (0.018 - 0.024) + 0.024 & \text{if } 180000 < S_{ut} \le 200000 \\[2mm]
\dfrac{S_{ut} - 200000}{220000 - 200000} \cdot (0.013 - 0.018) + 0.018 & \text{if } 200000 < S_{ut} \le 220000 \\[2mm]
\dfrac{S_{ut} - 220000}{240000 - 220000} \cdot (0.009 - 0.013) + 0.013 & \text{if } 220000 < S_{ut} \le 240000
\end{vmatrix}
$$

To determine the Neuber's Constant for torsion, use the Neuber's constant of a steel with an ultimate tensile strength 20 kpsi greater.

$$S_{tor} := S_{ut} + 20000$$

$$Neubers_{torsion} := \begin{vmatrix} \dfrac{S_{tor} - 50000}{55000 - 50000} \cdot (0.118 - 0.130) + 0.130 & \text{if } 50000 < S_{tor} \le 55000 \\[2mm] \dfrac{S_{tor} - 55000}{60000 - 55000} \cdot (0.108 - 0.118) + 0.118 & \text{if } 55000 < S_{tor} \le 60000 \\[2mm] \dfrac{S_{tor} - 60000}{70000 - 60000} \cdot (0.093 - 0.108) + 0.108 & \text{if } 60000 < S_{tor} \le 70000 \\[2mm] \dfrac{S_{tor} - 70000}{80000 - 70000} \cdot (0.080 - 0.093) + 0.093 & \text{if } 70000 < S_{tor} \le 80000 \\[2mm] \dfrac{S_{tor} - 80000}{90000 - 80000} \cdot (0.070 - 0.080) + 0.080 & \text{if } 80000 < S_{tor} \le 90000 \\[2mm] \dfrac{S_{tor} - 90000}{100000 - 90000} \cdot (0.062 - 0.070) + 0.070 & \text{if } 90000 < S_{tor} \le 100000 \\[2mm] \dfrac{S_{tor} - 100000}{110000 - 100000} \cdot (0.055 - 0.062) + 0.062 & \text{if } 100000 < S_{tor} \le 110000 \\[2mm] \dfrac{S_{tor} - 110000}{120000 - 110000} \cdot (0.049 - 0.055) + 0.055 & \text{if } 110000 < S_{tor} \le 120000 \\[2mm] \dfrac{S_{tor} - 120000}{130000 - 120000} \cdot (0.044 - 0.049) + 0.049 & \text{if } 120000 < S_{tor} \le 130000 \\[2mm] \dfrac{S_{tor} - 130000}{140000 - 130000} \cdot (0.039 - 0.044) + 0.044 & \text{if } 130000 < S_{tor} \le 140000 \\[2mm] \dfrac{S_{tor} - 140000}{160000 - 140000} \cdot (0.031 - 0.039) + 0.039 & \text{if } 140000 < S_{tor} \le 160000 \\[2mm] \dfrac{S_{tor} - 160000}{180000 - 160000} \cdot (0.024 - 0.031) + 0.031 & \text{if } 160000 < S_{tor} \le 180000 \\[2mm] \dfrac{S_{tor} - 180000}{200000 - 180000} \cdot (0.018 - 0.024) + 0.024 & \text{if } 180000 < S_{tor} \le 200000 \\[2mm] \dfrac{S_{tor} - 200000}{220000 - 200000} \cdot (0.013 - 0.018) + 0.018 & \text{if } 200000 < S_{tor} \le 220000 \\[2mm] \dfrac{S_{tor} - 220000}{240000 - 220000} \cdot (0.009 - 0.013) + 0.013 & \text{if } 220000 < S_{tor} \le 240000 \end{vmatrix}$$

$$q_{bending}(x) := \begin{cases} \dfrac{1}{1 + \dfrac{Neubers_{bending}}{\sqrt{r_{notch}(x)}}} & \text{if } r_{notch}(x) \neq 0 \\[4mm] 0 & \text{otherwise} \end{cases}$$

$$q_{torsion}(x) := \begin{cases} \dfrac{1}{1 + \dfrac{Neubers_{torsion}}{\sqrt{r_{notch}(x)}}} & \text{if } r_{notch}(x) \neq 0 \\[4mm] 0 & \text{otherwise} \end{cases}$$

$$t_{fillet}(x) := \begin{cases} \dfrac{d_2 - d_1}{2} & \text{if } x_1 - r_1 \leq x < x_1 \\[3mm] \dfrac{d_3 - d_2}{2} & \text{if } x_2 - r_2 \leq x < x_2 \\[3mm] \dfrac{d_4 - d_3}{2} & \text{if } x_3 - r_3 \leq x < x_3 \\[3mm] \dfrac{d_5 - d_4}{2} & \text{if } x_4 - r_4 \leq x < x_4 \\[3mm] \dfrac{d_6 - d_5}{2} & \text{if } x_5 - r_5 \leq x < x_5 \\[3mm] 0 & \text{otherwise} \end{cases}$$

$$C_{1\_tor}(x) := 0.905 + 0.783 \cdot \sqrt{\frac{t_{fillet}(x)}{r_{notch}(x)}} - 0.075 \frac{t_{fillet}(x)}{r_{notch}(x)}$$

$$C_{2\_tor}(x) := -0.437 - 1.969 \cdot \sqrt{\frac{t_{fillet}(x)}{r_{notch}(x)}} + 0.553 \frac{t_{fillet}(x)}{r_{notch}(x)}$$

$$C_{3\_tor}(x) := 1.557 + 1.073 \cdot \sqrt{\frac{t_{fillet}(x)}{r_{notch}(x)}} - 0.578 \frac{t_{fillet}(x)}{r_{notch}(x)}$$

$$C_{4\_tor}(x) := -1.061 + 0.171 \cdot \sqrt{\frac{t_{fillet}(x)}{r_{notch}(x)}} + 0.086 \frac{t_{fillet}(x)}{r_{notch}(x)}$$

Note: This equation for Kt bending only applies when r/d is between 0.002 and 0.3, and when D/d is between 1.01 and 6.0. (Pilkey, page 408)

$$K_{t\_bending}(x) := \left| \begin{array}{l} 0.632 + 0.377 \cdot (D\_d(x))^{-4.4} + \left(\dfrac{r_{notch}(x)}{d_o(x)} \right)^{-0.5} \cdot \sqrt{\dfrac{-0.14 - 0.363(D\_d(x))^2 + 0.503(D\_d(x))^4}{1 - 2.39(D\_d(x))^2 + 3.368(D\_d(x))^4}} \quad \text{if } D\_d \\[2em] \left[1.426 + 0.1643 \left(\dfrac{0.1}{\frac{r_{key}}{d_o(x)}} \right) - 0.0019 \left(\dfrac{0.1}{\frac{r_{key}}{d_o(x)}} \right)^2 \right] \quad \text{if } L_{key} \le x < L_{key} + \dfrac{b_{key\_width}}{2} \\[2em] \left[1.426 + 0.1643 \left(\dfrac{0.1}{\frac{r_{key}}{d_o(x)}} \right) - 0.0019 \left(\dfrac{0.1}{\frac{r_{key}}{d_o(x)}} \right)^2 \right] \quad \text{if } 0 \le x < L_{key} \\[2em] 1 \quad \text{otherwise} \end{array} \right.$$

Note: assumed US and British standard for Kt of key

Note; For torsion to work properly, we must keep the t/r between 0.25 and 4.0. (Pilkey, page 409)

$$K_{t\_torsion}(x) := \left| \begin{array}{l} C_{1\_tor}(x) + C_{2\_tor}(x) \cdot \left(\dfrac{2 \cdot t_{fillet}(x)}{D_{large}(x)} \right) + C_{3\_tor}(x) \cdot \left(\dfrac{2 \cdot t_{fillet}(x)}{D_{large}(x)} \right)^2 + C_{4\_tor}(x) \cdot \left(\dfrac{2 \cdot t_{fillet}(x)}{D_{large}(x)} \right)^3 \quad \text{if } D\_d(x) \\[2em] 3.4 \quad \text{if } L_{key} \le x < L_{key} + \dfrac{b_{key\_width}}{2} \\[2em] \left[1.953 + 0.1434 \left(\dfrac{0.1}{\frac{r_{key}}{d_o(x)}} \right) - 0.0021 \left(\dfrac{0.1}{\frac{r_{key}}{d_o(x)}} \right)^2 \right] \quad \text{if } 0 \le x < L_{key} \\[2em] 1 \quad \text{otherwise} \end{array} \right.$$

$$K_f(x) := 1 + q_{bending}(x) \cdot \left(K_{t\_bending}(x) - 1 \right)$$

$$K_{fs}(x) := 1 + q_{torsion}(x) \cdot \left(K_{t\_torsion}(x) - 1 \right)$$

$$K_{fm}(x) := K_f(x)$$
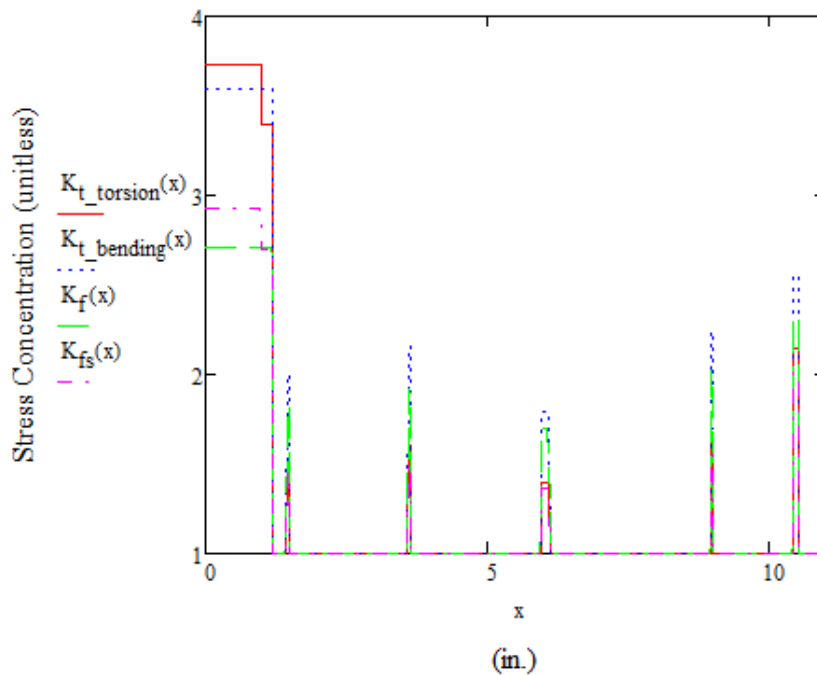
$$K_{fsm}(x) := K_{fs}(x)$$

Stress Concentration Factors

Von Mises Stresses

Torsional Shear Stress at outer fibers (uniform along surface of shaft) (not alternating):

$$\tau_{xz\_a}(x) := \frac{K_{fs}(x) \cdot T_a \cdot \frac{d_o(x)}{2}}{J_z(x)} \qquad \tau_{xz\_m}(x) := \frac{K_{fsm}(x) \cdot T_m \cdot \frac{d_o(x)}{2}}{J_z(x)} \qquad \tau_{xz\_m}(5) = 6.954 \times 10^3$$

Maximum Bending Normal Stress (furthest from neutral axis) (alternating):

$$\sigma_{x\_a}(x) := \frac{K_f(x) \cdot M_a(x) \cdot \frac{d_o(x)}{2}}{I_x(x)} \qquad \sigma_{x\_m}(x) := \frac{K_{fm}(x) \cdot M_m \cdot \frac{d_o(x)}{2}}{I_x(x)} \qquad \sigma_{x\_a}(5) = -1.036 \times 10^3$$

Maximum transverse Shear Stress (at neutral axis):

$$\tau_{transverse\_a}(x) := \frac{K_{fs}(x) \cdot 2 \cdot V_a(x)}{A_s(x)} \qquad \tau_{transverse\_m}(x) := \frac{K_{fsm}(x) \cdot 2 \cdot V_m}{A_s(x)} \qquad \tau_{transverse\_a}(5) = -228.532$$

Alternating and Mean von Mises stresses at the top edge (furthest from the neutral axis):

$$\sigma'_{a\_a}(x) := \sqrt{\sigma_{x\_a}(x)^2 + 0^2 - \sigma_{x\_a}(x) \cdot 0 + 3 \cdot \tau_{xz\_a}(x)^2} \qquad \sigma'_{a\_a}(5) = 1.036 \times 10^3$$

$$\sigma'_{m\_a}(x) := \sqrt{\sigma_{x\_m}(x)^2 + 0^2 - \sigma_{x\_m}(x) \cdot 0 + 3 \cdot \tau_{xz\_m}(x)^2} \qquad \sigma'_{m\_a}(5) = 1.204 \times 10^4$$

Alternating and Mean von Mises stresses at the side edge (at neutral axis) (this point may be on one side or the other, depending on if the shear is in the positive or negative y direction. The results are taken at the point where the shear stresses add):

$$\tau_{a\_total}(x) := \left| \tau_{transverse\_a}(x) \right| + \tau_{xz\_a}(x) \qquad\qquad \tau_{a\_total}(5) = 228.532$$

$$\tau_{m\_total}(x) := \left| \tau_{transverse\_m}(x) \right| + \tau_{xz\_m}(x) \qquad\qquad \tau_{m\_total}(5) = 6.954 \times 10^3$$

$$\sigma'_{a\_b}(x) := \sqrt{0^2 + 0^2 - 0 \cdot 0 + 3 \cdot \tau_{a\_total}(x)^2} \qquad\qquad \sigma'_{a\_b}(5) = 395.828$$

$$\sigma'_{m\_b}(x) := \sqrt{0^2 + 0^2 - 0 \cdot 0 + 3 \cdot \tau_{m\_total}(x)^2} \qquad\qquad \sigma'_{m\_b}(5) = 1.204 \times 10^4$$

Von Mises Stresses
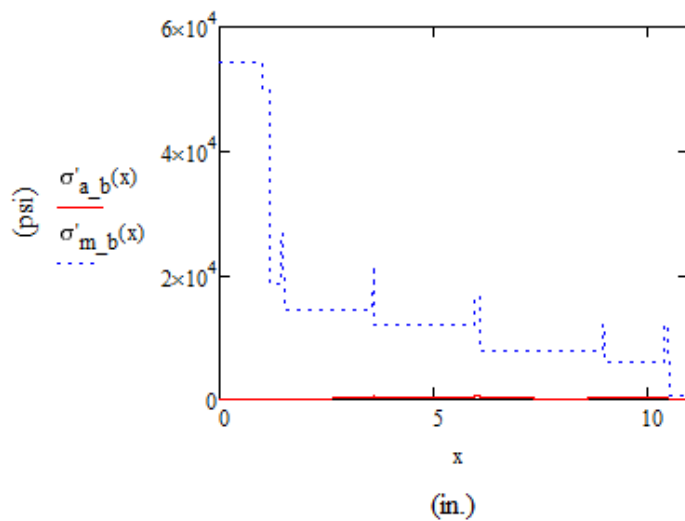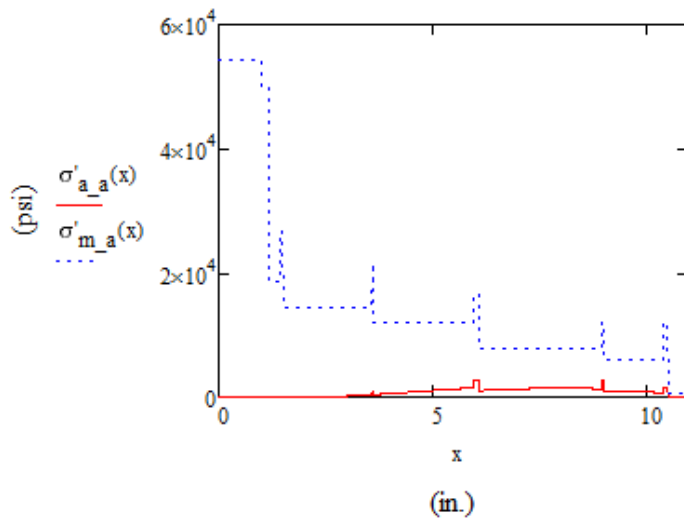
Corrected Fatigue Strength

Bending load, no axial

$C_{load} := 1$ Less than 450 C operational temperature

$C_{temp} := 1$ 99% Reliability

$C_{reliab} := 0.814$

Between 0.3 and 10 inches in diameter

$C_{size}(x) := 0.869 \cdot d_o(x)^{-0.097}$

$C_{surf} := 2.7 \cdot \left(\dfrac{S_{ut}}{1000}\right)^{-0.265} = 0.768$ Machined Surface

$S_{e'} := 0.5 \cdot S_{ut}$

$S_f(x) := S_{e'} \cdot C_{load} \cdot C_{temp} \cdot C_{reliab} \cdot C_{size}(x) \cdot C_{surf}$

Corrected Fatigue Strength

Safety Factor Calculations

Assuming Case 4 Load Scenario for Safety Factor Calculations:
   Both mlternating and mean stresses can increase under service
   conditions over the lifetime of the part.

Safety Factor for point on top surface of shaft:

$$\sigma'_{ms\_a}(x) := \dfrac{S_{ut} \cdot \left(S_f(x)^2 - S_f(x) \cdot \sigma'_{a\_a}(x) + S_{ut} \cdot \sigma'_{m\_a}(x)\right)}{S_f(x)^2 + S_{ut}^2}$$

$$\sigma'_{as\_a}(x) := -\dfrac{S_f(x)}{S_{ut}}\left(\sigma'_{ms\_a}(x)\right) + S_f(x)$$

$$ZS_a(x) := \sqrt{\left(\sigma'_{m\_a}(x) - \sigma'_{ms\_a}(x)\right)^2 + \left(\sigma'_{a\_a}(x) - \sigma'_{as\_a}(x)\right)^2}$$

$$OZ_a(x) := \sqrt{\left(\sigma'_{a\_a}(x)\right)^2 + \left(\sigma'_{m\_a}(x)\right)^2}$$

$$N_{f\_a}(x) := \dfrac{OZ_a(x) + ZS_a(x)}{OZ_a(x)}$$

$N_{f\_a}(0.01) = 1.282$ Minimum Safety Factor

Safety Factor for point at side edge (at neutral axis) (this point may be on one side or the other, depending on if the shear is in the positive or negative y direction. The results are taken at the point where the shear stresses add):

$$\sigma'_{ms\_b}(x) := \frac{S_{ut} \left(S_f(x)^2 - S_f(x) \cdot \sigma'_{a\_b}(x) + S_{ut} \cdot \sigma'_{m\_b}(x) \right)}{S_f(x)^2 + S_{ut}^2}$$

$$\sigma'_{as\_b}(x) := -\frac{S_f(x)}{S_{ut}} \left(\sigma'_{ms\_b}(x) \right) + S_f(x)$$

$$ZS_b(x) := \sqrt{\left(\sigma'_{m\_b}(x) - \sigma'_{ms\_b}(x) \right)^2 + \left(\sigma'_{a\_b}(x) - \sigma'_{as\_b}(x) \right)^2}$$

$$OZ_b(x) := \sqrt{\left(\sigma'_{a\_b}(x) \right)^2 + \left(\sigma'_{m\_b}(x) \right)^2}$$

$$N_{f\_b}(x) := \frac{OZ_b(x) + ZS_b(x)}{OZ_b(x)}$$

$$N_{f\_b}(0.01) = 1.282$$
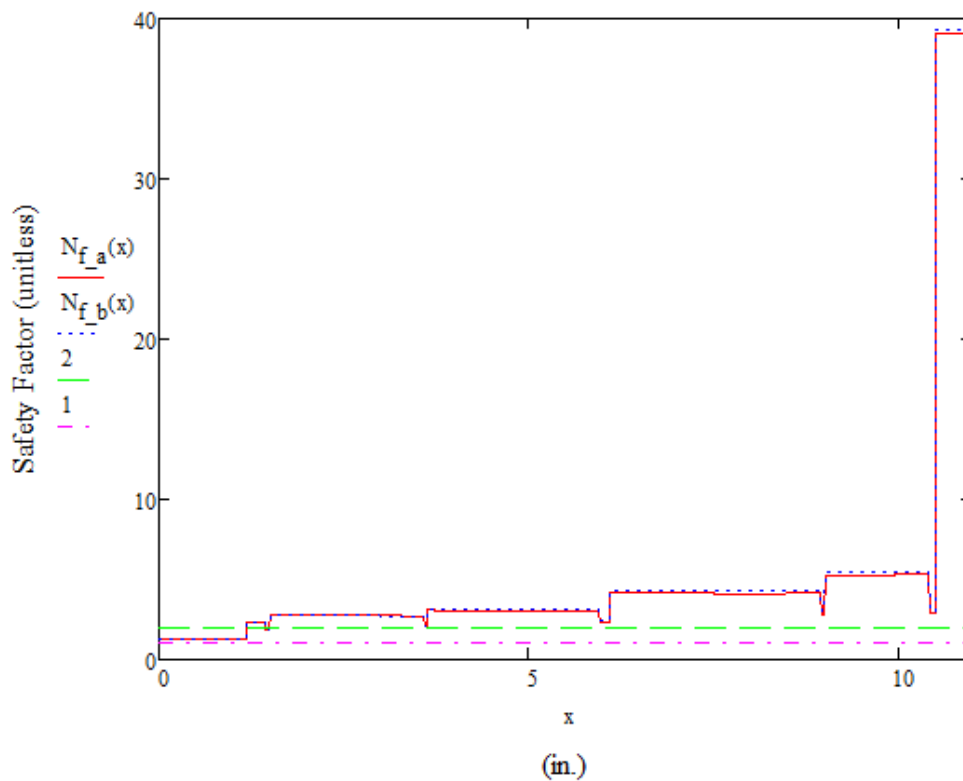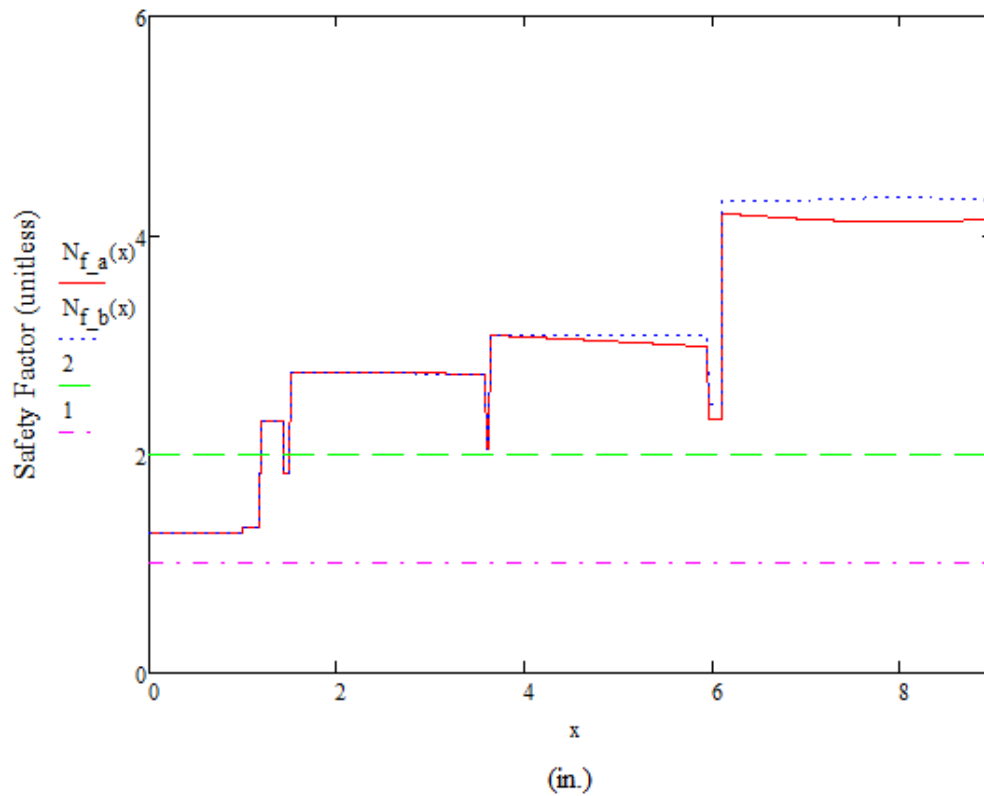
▼ Deflection of Shaft

Torsional
Deflection:

$$J_1 := \frac{\pi \cdot d_1^{\,4}}{32} = 0.685$$

$$J_2 := \frac{\pi \cdot d_2^{\,4}}{32} = 0.964$$

$$J_3 := \frac{\pi \cdot d_3^{\,4}}{32} = 1.213$$

$$J_4 := \frac{\pi \cdot d_4^{\,4}}{32} = 2.159$$

$$J_5 := \frac{\pi \cdot d_5^{\,4}}{32} = 3.124$$

$$\frac{\pi \cdot d_6^{\,4}}{\ldots}$$

$$G_{shaft} := \frac{E}{2(1 + \nu)} = 1.172 \times 10^7$$

$$\theta_{deflection} := \frac{T_{max}}{G_{shaft}}\left(\frac{x_1}{J_1} + \frac{x_2 - x_1}{J_2} + \frac{x_3 - x_2}{J_3} + \frac{x_4 - x_3}{J_4} + \frac{x_5 - x_4}{J_5} + \frac{x_6 - x_5}{J_6}\right) = 6.349 \times 10^{-3} \cdot rad$$

$$\theta_{deflection\_degrees} := \theta_{deflection} \cdot \frac{180}{\pi} = 0.364$$

Bending Deflection:

$$\theta = \int \frac{M}{EI}\, dz + C_3$$

$$\delta = \int \int \frac{M}{EI}\, dz\, dz + C_3 \cdot z + C_4$$

$$I_{x\_}(x) := \begin{cases} I_1 & \text{if } x < x_1 \\ I_2 & \text{if } x_1 \leq x < x_2 \\ I_3 & \text{if } x_2 \leq x < x_3 \\ I_4 & \text{if } x_3 \leq x < x_4 \\ I_5 & \text{if } x_4 \leq x < x_5 \\ I_6 & \text{if } x_5 \leq x \leq x_6 \end{cases}$$

This is posing a problem. Basically, I think I will have to go segment by segment and figure out what the deflection is. This could pose an issue, as I am not sure exactly how to pull it off.

$$Z_1 := 0$$

$$Z_2 := 0$$
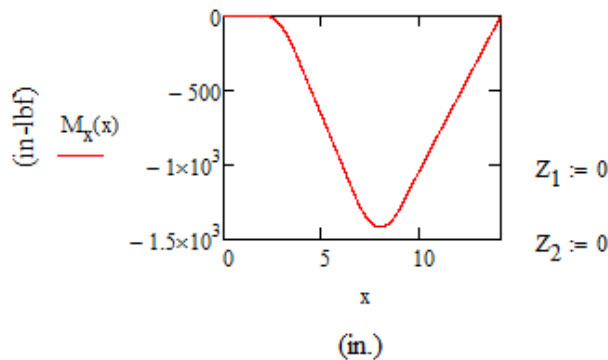
$$V_x(L_{overall}) = -2.842 \times 10^{-14}$$

$$M_x(L_{overall}) = -2.236 \times 10^{-12}$$

$$\theta_x(x) := \frac{-w_1}{6x_1 \cdot E \cdot I_1} \cdot sing_d(x,0,x_1,3) + \frac{-F_a}{6(L_A) \cdot E \cdot I_2} \cdot sing_d(x,x_2 - L_A,x_2,3) + \frac{-w_2}{6(x_2 - x_1) \cdot E \cdot I_2} \cdot sing_d(x,x_1,x_2,3) + \ldots$$

$$\ldots + \frac{-w_3}{6(x_3 - x_2) \cdot E \cdot I_3} \cdot sing_d(x,x_2,x_3,3) + \frac{-w_4}{6(x_4 - x_3) \cdot E \cdot I_4} \cdot sing_d(x,x_3,x_4,3) + \frac{F_b}{6(L_B) \cdot E \cdot I_4} \cdot sing_d(x,x_4 - L_B,x_4,3) + \ldots$$

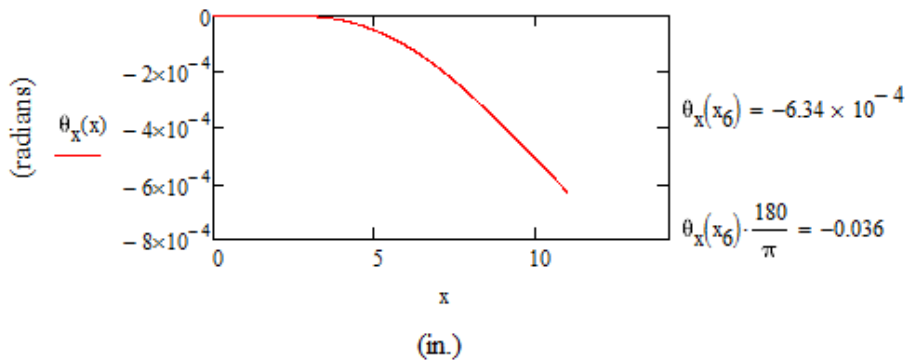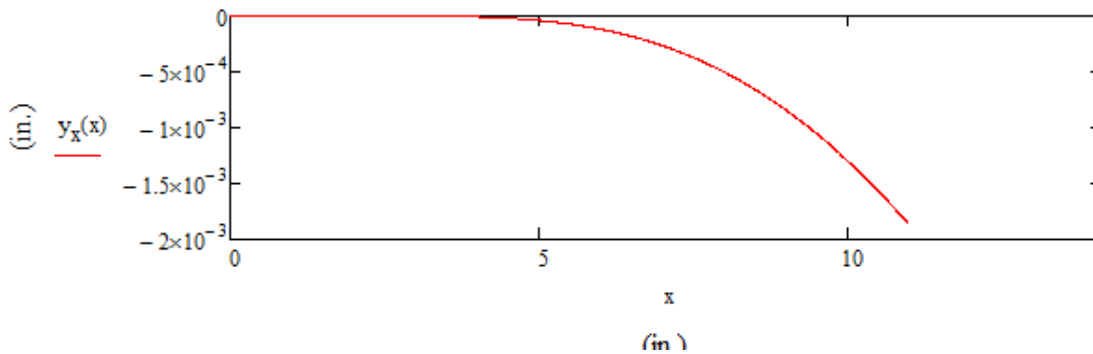$$\ldots + \frac{-w_5}{6(x_5 - x_4) \cdot E \cdot I_5} \cdot sing_d(x,x_4,x_5,3) + \frac{-w_6}{6(x_6 - x_5) \cdot E \cdot I_6} \cdot sing_d(x,x_5,x_6,3) - \frac{w_{rotor}}{2} \cdot sing(x,L_{overall},2) + \frac{Z_1}{E \cdot I_{x\_}(x)}$$

$$\theta_x(x_6) = -6.34 \times 10^{-4}$$

$$\theta_x(x_6) \cdot \frac{180}{\pi} = -0.036$$

$$y_x(x) := \frac{-w_1}{24x_1 \cdot E \cdot I_1} \cdot sing_d(x,0,x_1,4) + \frac{-F_a}{24(L_A) \cdot E \cdot I_2} \cdot sing_d(x,x_2 - L_A,x_2,4) + \frac{-w_2}{24(x_2 - x_1) \cdot E \cdot I_2} \cdot sing_d(x,x_1,x_2,4) + \ldots$$

$$\ldots + \frac{-w_3}{24(x_3 - x_2) \cdot E \cdot I_3} \cdot sing_d(x,x_2,x_3,4) + \frac{-w_4}{24(x_4 - x_3) \cdot E \cdot I_4} \cdot sing_d(x,x_3,x_4,4) + \ldots$$

$$\ldots + \frac{F_b}{24(L_B) \cdot E \cdot I_4} \cdot sing_d(x,x_4 - L_B,x_4,4) + \frac{-w_5}{24(x_5 - x_4) \cdot E \cdot I_5} \cdot sing_d(x,x_4,x_5,4) + \frac{-w_6}{24(x_6 - x_5) \cdot E \cdot I_6} \cdot sing_d(x,x_5,x_6,4) + \ldots$$

$$\ldots + \frac{-w_{rotor}}{6} \cdot sing(x,L_{overall},3) + \frac{Z_1}{E \cdot I_{x\_}(x)} \cdot x + \frac{Z_2}{E \cdot I_{x\_}(x)}$$

$$y_x(0) = 0 \qquad \text{Therefore: Z1=0}$$

$$y_x(x_a) = -3.506 \times 10^{-7}$$

$$y_x(x_b) = -4.633 \times 10^{-4}$$

$$y_x(x_6) = -1.873 \times 10^{-3}$$

$$y_x(L_{overall}) = \blacksquare$$

Note: This equation does not work for x > x6 because the material properties for the rotor itself are unknown and would change from rotor to rotor.

Note: This deflection calculation assumes that there is no correction factor that specifies that the deflection at the bearings is 0. Results are more conservative than actual deflections are likely to be.

▲ Deflection of Shaft

▼ Length of Keyway

Ideal Dimensions Assuming End-Milled Keyway:

$$r_{key\_ideal}(z) := \frac{1}{48} \cdot d_o(z) \qquad\qquad r_{key\_ideal}(0) = 0.034$$

$$b_{key\_width\_ideal}(z) := 0.25 \cdot d_o(z) \qquad\qquad b_{key\_width\_ideal}(0) = 0.406$$

$$t_{key\_depth\_ideal}(z) := \frac{d_o(z)}{8} \qquad\qquad t_{key\_depth\_ideal}(0) = 0.203$$

Current Key Dimensions:

$$r_{key} = 0.01$$

$$b_{key\_width} = 0.375$$

$$t_{key\_depth} = 0.188$$

Ansi Standard Key Size (based on ratios. Actual standard may vary, specified at top):
Parallel Square Key:

$$b_{key\_width\_ansi} := 0.375$$

$$t_{key\_depth\_ansi} := \frac{b_{key\_width\_ansi}}{2} = 0.188$$

McMaster-Carr High Carbon Square Key:

Annealed 1095 Steel: Will require heat treating after cutting to length

Normalized at 900 C, Air cooled (Properties from Matweb)

http://www.matweb.com/search/DataSheet.aspx?MatGUID=2afc640b240
c4fbcabe2b9ecda1336a4

$$S_{y\_key} := 79800$$

Shear Failure (Safety Factor of 2):

$$S_{ys\_key} := 0.577 \cdot S_{y\_key}$$

$$F_{applied} := \frac{T_{max}}{0.5d_1} = 1.108 \times 10^4$$

$$L_{min\_key\_shear} := \frac{2 \cdot F_{applied}}{S_{ys\_key} \cdot b_{key\_width\_ansi}} = 1.283$$

Bearing Failure (Safety Factor of 2):

$$L_{min\_key\_bearing} := \frac{2F_{applied}}{S_{y\_key} \cdot t_{key\_depth\_ansi}} = 1.481$$

Safety Factor 1.5:

$$L_{key\_shear1\_5} := \frac{1.5 \cdot F_{applied}}{S_{ys\_key} \cdot b_{key\_width}} = 0.962$$

$$L_{key\_bearing1\_5} := \frac{1.5F_{applied}}{S_{y\_key} \cdot t_{key\_depth}} = 1.11$$

Safety Factor of Current Key Length:

$$SF_{key\_shear} := \frac{L_{key} \cdot \left(S_{ys\_key} \cdot b_{key\_width}\right)}{F_{applied}} = 1.559$$

$$SF_{key\_bearing} := \frac{L_{key} \cdot \left(S_{y\_key} \cdot t_{key\_depth}\right)}{F_{applied}} = 1.351$$

▲ Length of Keyway

Torsional Vibration:

$$J_{eff} := \frac{L_{overall}}{\dfrac{x_1}{J_1} + \dfrac{x_2 - x_1}{J_2} + \dfrac{x_3 - x_2}{J_3} + \dfrac{x_4 - x_3}{J_4} + \dfrac{x_5 - x_4}{J_5} + \dfrac{x_6 - x_5}{J_6}}$$

$$k_t := \frac{G_{shaft} \cdot J_{eff}}{L_{overall}} = 1.417 \times 10^6$$

$$I_m := \frac{w_1 \cdot \left(\dfrac{d_1}{2}\right)^2}{2 \cdot 386.4} + \frac{w_2 \cdot \left(\dfrac{d_2}{2}\right)^2}{2 \cdot 386.4} + \frac{w_3 \cdot \left(\dfrac{d_3}{2}\right)^2}{2 \cdot 386.4} + \frac{w_4 \cdot \left(\dfrac{d_4}{2}\right)^2}{2 \cdot 386.4} + \frac{w_5 \cdot \left(\dfrac{d_5}{2}\right)^2}{2 \cdot 386.4} + \frac{w_6 \cdot \left(\dfrac{d_6}{2}\right)^2}{2 \cdot 386.4} = 0.033$$

$$\omega_{n\_torsion} := \sqrt{\frac{k_t}{I_m}} = 6.523 \times 10^3 \quad \text{radians per second}$$

$$\omega_{n\_torsion} \cdot \frac{60}{\pi} = 1.246 \times 10^5 \quad \text{RPM}$$

Vibrational Analysis - Rayleigh-Ritz Method:

Mode Sape (Blevins): $\sin\left(\dfrac{i \cdot \pi \cdot x}{L}\right)$

$$\phi_1(x) := \sin\left(\frac{\pi \cdot x}{x_6}\right)$$

$$\phi_2(x) := \sin\left(\frac{2\pi \cdot x}{x_6}\right)$$

$$\phi'_1(x) := \left(\frac{\pi}{x_6}\right) \cdot \cos\left(\frac{\pi \cdot x}{x_6}\right)$$

$$\phi'_2(x) := \left(\frac{2\pi}{x_6}\right) \cdot \cos\left(\frac{2\pi \cdot x}{x_6}\right)$$

$$\phi''_1(x) := -\left(\frac{\pi}{x_6}\right)^2 \cdot \sin\left(\frac{\pi \cdot x}{x_6}\right)$$

$$\phi''_2(x) := -\left(\frac{2\pi}{x_6}\right)^2 \cdot \sin\left(\frac{2\pi \cdot x}{x_6}\right)$$

$$I_{x1} := \frac{\pi \cdot d_1^4}{64} = 0.342$$

$$I_{x2} := \frac{\pi \cdot d_2^4}{64} = 0.482$$

$$I_{x3} := \frac{\pi \cdot d_3^4}{64} = 0.607$$

$$I_{x4} := \frac{\pi \cdot d_4^4}{64} = 1.079$$

$$I_{x5} := \frac{\pi \cdot d_5^4}{64} = 1.562$$

$$I_{x6} := \frac{\pi \cdot d_6^4}{64} = 28.298$$

$$m_{11} := \int_0^{x_1} \frac{w_1}{386.4} \cdot \phi_1(x)^2 \, dx + \int_{x_1}^{x_2} \frac{w_2}{386.4} \cdot \phi_1(x)^2 \, dx + \int_{x_2}^{x_3} \frac{w_3}{386.4} \cdot \phi_1(x)^2 \, dx + \int_{x_3}^{x_4} \frac{w_4}{386.4} \cdot \phi_1(x)^2 \, dx + \dots$$

$$\dots + \int_{x_4}^{x_5} \frac{w_5}{386.4} \cdot \phi_1(x)^2 \, dx + \int_{x_5}^{x_6} \frac{w_6}{386.4} \cdot \phi_1(x)^2 \, dx + \frac{w_{rotor}}{386.4} \cdot \phi_1\left(L_{overall}\right)^2$$

$$m_{12\_test} := \int_0^{x_1} \frac{w_1}{386.4} \cdot \phi_1(x) \cdot \phi_2(x) \, dx + \int_{x_1}^{x_2} \frac{w_2}{386.4} \cdot \left(\phi_1(x) \cdot \phi_2(x)\right) \, dx + \int_{x_2}^{x_3} \frac{w_3}{386.4} \cdot \left(\phi_1(x) \cdot \phi_2(x)\right) \, dx + \dots$$

$$\dots + \int_{x_3}^{x_4} \frac{w_4}{386.4} \cdot \left(\phi_1(x) \cdot \phi_2(x)\right) \, dx + \int_{x_4}^{x_5} \frac{w_5}{386.4} \cdot \left(\phi_1(x) \cdot \phi_2(x)\right) \, dx + \int_{x_5}^{x_6} \frac{w_6}{386.4} \cdot \left(\phi_1(x) \cdot \phi_2(x)\right) \, dx + \dots$$

$$\dots + \frac{w_{rotor}}{386.4} \cdot \left(\phi_1\left(L_{overall}\right) \cdot \phi_2\left(L_{overall}\right)\right)$$

$$m_{12} := \frac{w_{rotor}}{386.4} \cdot \left(\phi_1\left(L_{overall}\right) \cdot \phi_2\left(L_{overall}\right)\right) = -0.492$$

$$m_{21\_test} := \int_0^{x_1} \frac{w_1}{386.4} \cdot \phi_1(x) \cdot \phi_2(x) \, dx + \int_{x_1}^{x_2} \frac{w_2}{386.4} \cdot \left(\phi_1(x) \cdot \phi_2(x)\right) \, dx + \int_{x_2}^{x_3} \frac{w_3}{386.4} \cdot \left(\phi_1(x) \cdot \phi_2(x)\right) \, dx + \dots$$

$$\dots + \int_{x_3}^{x_4} \frac{w_4}{386.4} \cdot \left(\phi_1(x) \cdot \phi_2(x)\right) \, dx + \int_{x_4}^{x_5} \frac{w_5}{386.4} \cdot \left(\phi_1(x) \cdot \phi_2(x)\right) \, dx + \int_{x_5}^{x_6} \frac{w_6}{386.4} \cdot \left(\phi_1(x) \cdot \phi_2(x)\right) \, dx + \dots$$

$$\dots + \frac{w_{rotor}}{386.4} \cdot \left(\phi_1\left(L_{overall}\right) \cdot \phi_2\left(L_{overall}\right)\right)$$

$$m_{21} := \frac{w_{rotor}}{386.4} \cdot \left(\phi_1\left(L_{overall}\right) \cdot \phi_2\left(L_{overall}\right)\right) = -0.492$$

$$m_{22} := \int_0^{x_1} \frac{w_1}{386.4} \cdot \phi_2(x)^2 \, dx + \int_{x_1}^{x_2} \frac{w_2}{386.4} \cdot \phi_2(x)^2 \, dx + \int_{x_2}^{x_3} \frac{w_3}{386.4} \cdot \phi_2(x)^2 \, dx + \int_{x_3}^{x_4} \frac{w_4}{386.4} \cdot \phi_2(x)^2 \, dx + \ldots$$

$$\ldots + \int_{x_4}^{x_5} \frac{w_5}{386.4} \cdot \phi_2(x)^2 \, dx + \int_{x_5}^{x_6} \frac{w_6}{386.4} \cdot \phi_2(x)^2 \, dx + \frac{w_{rotor}}{386.4} \cdot \phi_2(L_{overall})^2$$

$$k_{11} := \int_0^{x_1} E \cdot I_{x1} \cdot \phi"_1(x)^2 \, dx + \int_{x_1}^{x_2} E \cdot I_{x2} \cdot \phi"_1(x)^2 \, dx + \int_{x_2}^{x_3} E \cdot I_{x3} \cdot \phi"_1(x)^2 \, dx + \int_{x_3}^{x_4} E \cdot I_{x4} \cdot \phi"_1(x)^2 \, dx + \ldots$$

$$\ldots + \int_{x_4}^{x_5} E \cdot I_{x5} \cdot \phi"_1(x)^2 \, dx + \int_{x_5}^{x_6} E \cdot I_{x6} \cdot \phi"_1(x)^2 \, dx + E \cdot x_a \cdot \phi"_1(x_a)^2 + E \cdot x_b \cdot \phi"_1(x_b)^2$$

$$k_{12\_test} := \int_0^{x_1} E \cdot I_{x1} \cdot \phi"_1(x) \cdot \phi"_2(x) \, dx + \int_{x_1}^{x_2} E \cdot I_{x2} \cdot \left(\phi"_1(x) \cdot \phi"_2(x) \right) dx + \int_{x_2}^{x_3} E \cdot I_{x3} \cdot \left(\phi"_1(x) \cdot \phi"_2(x) \right) dx + \ldots$$

$$\ldots + \int_{x_3}^{x_4} E \cdot I_{x4} \cdot \left(\phi"_1(x) \cdot \phi"_2(x) \right) dx + \int_{x_4}^{x_5} E \cdot I_{x5} \cdot \left(\phi"_1(x) \cdot \phi"_2(x) \right) dx + \ldots$$

$$\ldots + \int_{x_5}^{x_6} E \cdot I_{x6} \cdot \left(\phi"_1(x) \cdot \phi"_2(x) \right) dx + E \cdot x_a \cdot \left(\phi"_1(x_a) \cdot \phi"_2(x_a) \right) + E \cdot x_b \cdot \left(\phi"_1(x_b) \cdot \phi"_2(x_b) \right)$$

$$k_{12} := E \cdot x_a \cdot \left(\phi"_1(x_a) \cdot \phi"_2(x_a) \right) + E \cdot x_b \cdot \left(\phi"_1(x_b) \cdot \phi"_2(x_b) \right) = -3.104 \times 10^6$$

$$k_{21\_test} := \int_0^{x_1} E \cdot I_{x1} \cdot \phi"_1(x) \cdot \phi"_2(x) \, dx + \int_{x_1}^{x_2} E \cdot I_{x2} \cdot \left(\phi"_1(x) \cdot \phi"_2(x) \right) dx + \int_{x_2}^{x_3} E \cdot I_{x3} \cdot \left(\phi"_1(x) \cdot \phi"_2(x) \right) dx + \ldots$$

$$\ldots + \int_{x_3}^{x_4} E \cdot I_{x4} \cdot \left(\phi"_1(x) \cdot \phi"_2(x) \right) dx + \int_{x_4}^{x_5} E \cdot I_{x5} \cdot \left(\phi"_1(x) \cdot \phi"_2(x) \right) dx + \ldots$$

$$\ldots + \int_{x_5}^{x_6} E \cdot I_{x6} \cdot \left(\phi"_1(x) \cdot \phi"_2(x) \right) dx + E \cdot x_a \cdot \left(\phi"_1(x_a) \cdot \phi"_2(x_a) \right) + E \cdot x_b \cdot \left(\phi"_1(x_b) \cdot \phi"_2(x_b) \right)$$

$$k_{22} := \int_0^{x_1} E \cdot I_{x1} \cdot \phi''_2(x)^2 \, dx + \int_{x_1}^{x_2} E \cdot I_{x2} \cdot \phi''_2(x)^2 \, dx + \int_{x_2}^{x_3} E \cdot I_{x3} \cdot \phi''_2(x)^2 \, dx + \int_{x_3}^{x_4} E \cdot I_{x4} \cdot \phi''_2(x)^2 \, dx + \ldots$$

$$\ldots + \int_{x_4}^{x_5} E \cdot I_{x5} \cdot \phi''_2(x)^2 \, dx + \int_{x_5}^{x_6} E \cdot I_{x6} \cdot \phi''_2(x)^2 \, dx + E \cdot x_a \cdot \phi''_2(x_a)^2 + E \cdot x_b \cdot \phi''_2(x_b)^2$$

$$\begin{bmatrix} \left(k_{11} - \omega^2 \cdot m_{11}\right) & \left(k_{12} - \omega^2 \cdot m_{12}\right) \\ \left(k_{21} - \omega^2 \cdot m_{21}\right) & \left(k_{22} - \omega^2 \cdot m_{22}\right) \end{bmatrix}$$

Then find the determinant to find the characteristic equation:

$$characteristic := \left(k_{22} - \alpha \cdot m_{22}\right) \cdot \left(k_{11} - \alpha \cdot m_{11}\right) - \left(k_{21} - \alpha \cdot m_{21}\right) \cdot \left(k_{12} - \alpha \cdot m_{12}\right)$$

$$\alpha^2 \left(m_{11} \cdot m_{22} - m_{12} \cdot m_{21}\right) + \alpha \left(k_{21} \cdot m_{12} + k_{12} \cdot m_{21} - k_{22} \cdot m_{11} - k_{11} \cdot m_{22}\right) + \left(k_{11} \cdot k_{22} - k_{21} \cdot k_{12}\right)$$

$$a_{char} := \left(m_{11} \cdot m_{22} - m_{12} \cdot m_{21}\right) = 0.032$$

$$b_{char} := \left(k_{21} \cdot m_{12} + k_{12} \cdot m_{21} - k_{22} \cdot m_{11} - k_{11} \cdot m_{22}\right) = -1.905 \times 10^7$$

$$c_{char} := k_{11} \cdot k_{22} - k_{21} \cdot k_{12} = 9.534 \times 10^{13}$$

$$\omega_{nat\_1} := \sqrt{\frac{-b_{char} + \sqrt{b_{char}^2 - 4 \cdot a_{char} \cdot c_{char}}}{2 \cdot a_{char}}} = 2.411 \times 10^4$$

$$\omega_{nat\_2} := \sqrt{\frac{-b_{char} - \sqrt{b_{char}^2 - 4 \cdot a_{char} \cdot c_{char}}}{2 \cdot a_{char}}} = 2.247 \times 10^3 \text{ rad/sec}$$

$$\omega_{nat\_adj} := \omega_{nat\_2} \cdot \frac{60}{2 \cdot \pi} = 2.145 \times 10^4 \qquad \text{RPM}$$

Alternate version (not assuming the off diagonals will cancel):

$$a_{char\_2} := \left(m_{11} \cdot m_{22} - m_{12\_test} \cdot m_{21\_test}\right) = 0.025$$

$$b_{char\_2} := \left(k_{21\_test} \cdot m_{12\_test} + k_{12\_test} \cdot m_{21\_test} - k_{22} \cdot m_{11} - k_{11} \cdot m_{22}\right) = -1.771 \times 10^{7}$$

$$c_{char\_2} := k_{11} \cdot k_{22} - k_{21\_test} \cdot k_{12\_test} = 8.562 \times 10^{13}$$

$$\omega_{nat\_1\_alt} := \sqrt{\frac{-b_{char\_2} + \sqrt{b_{char\_2}^2 - 4 \cdot a_{char\_2} \cdot c_{char\_2}}}{2 \cdot a_{char\_2}}} = 2.638 \times 10^{4}$$

$$\omega_{nat\_2\_alt} := \sqrt{\frac{-b_{char\_2} - \sqrt{b_{char\_2}^2 - 4 \cdot a_{char\_2} \cdot c_{char\_2}}}{2 \cdot a_{char\_2}}} = 2.206 \times 10^{3} \ \text{rad/sec}$$

$$\omega_{nat\_adj\_alt} := \omega_{nat\_2\_alt} \cdot \frac{60}{2 \cdot \pi} = 2.107 \times 10^{4} \quad \text{RPM}$$

▲ Vibration Analysis

Appendix B- Thermal Expansion Mathcad Analysis

Thermal Expansion Calculations

Knowns:

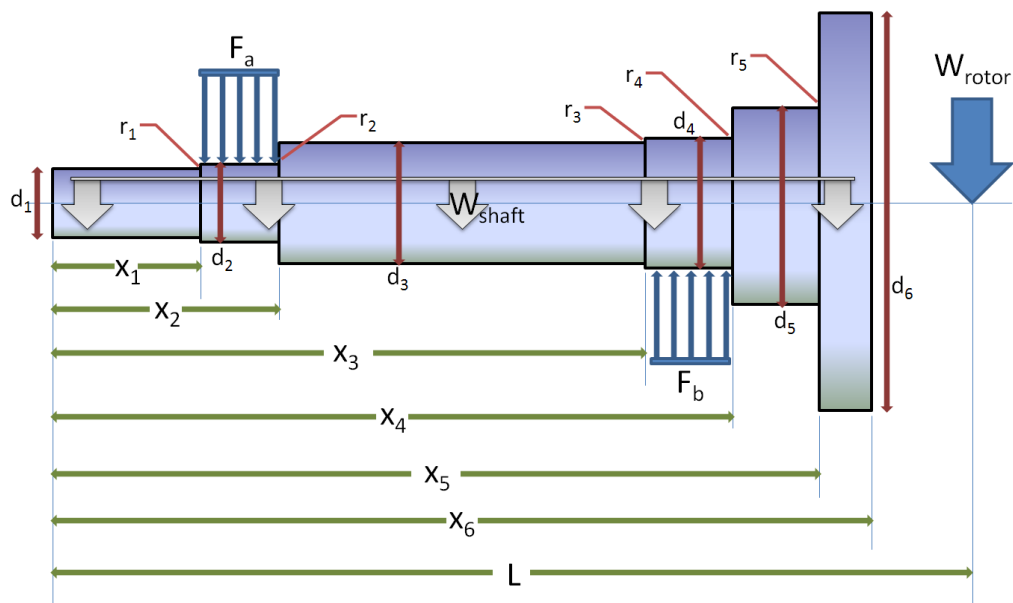$$\alpha := 6.78 \cdot 10^{-6} \qquad L := 11 \qquad \Delta T := 100$$
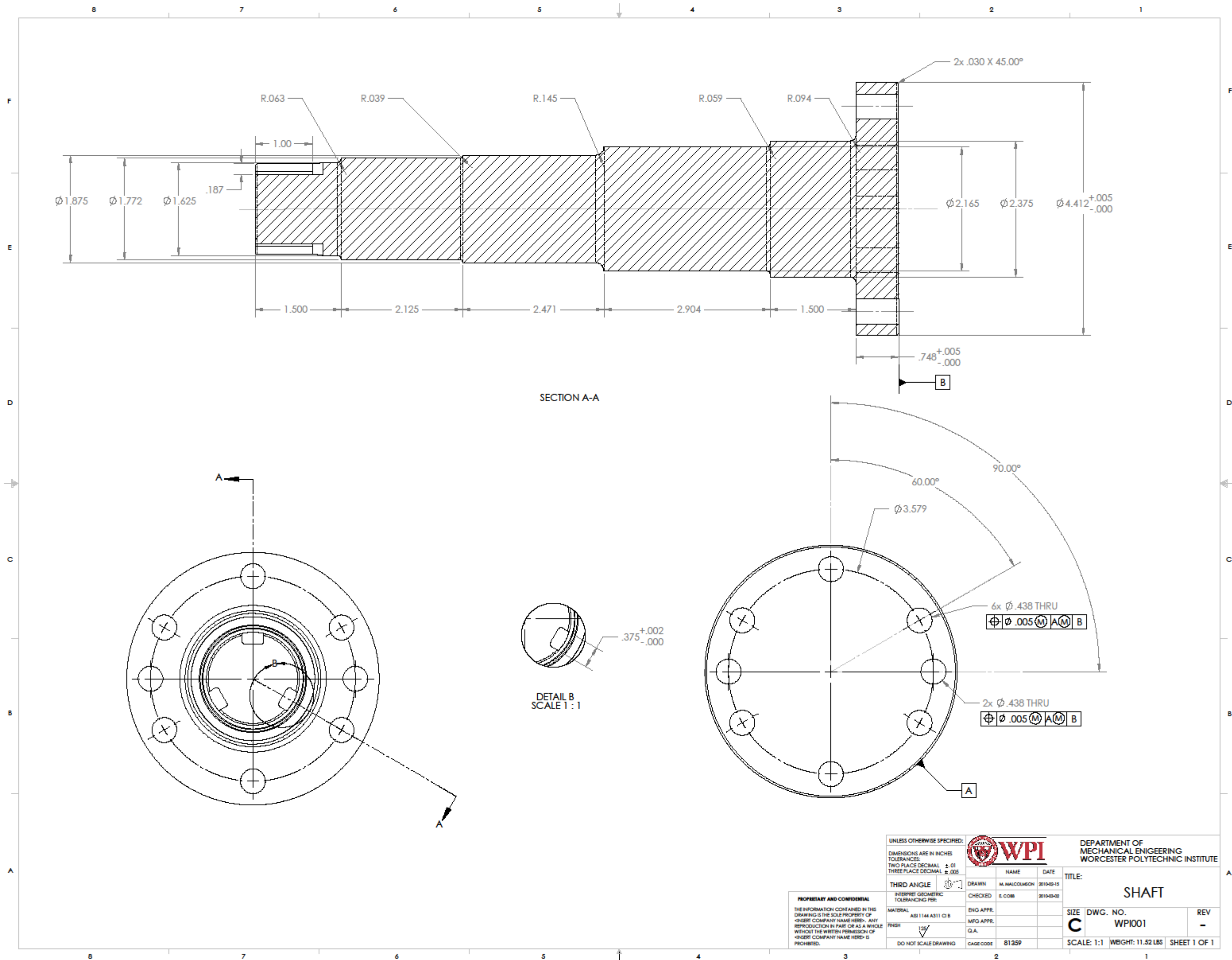
Equation:

$$\Delta L := \alpha \cdot L \cdot \Delta T$$

Soltuion:

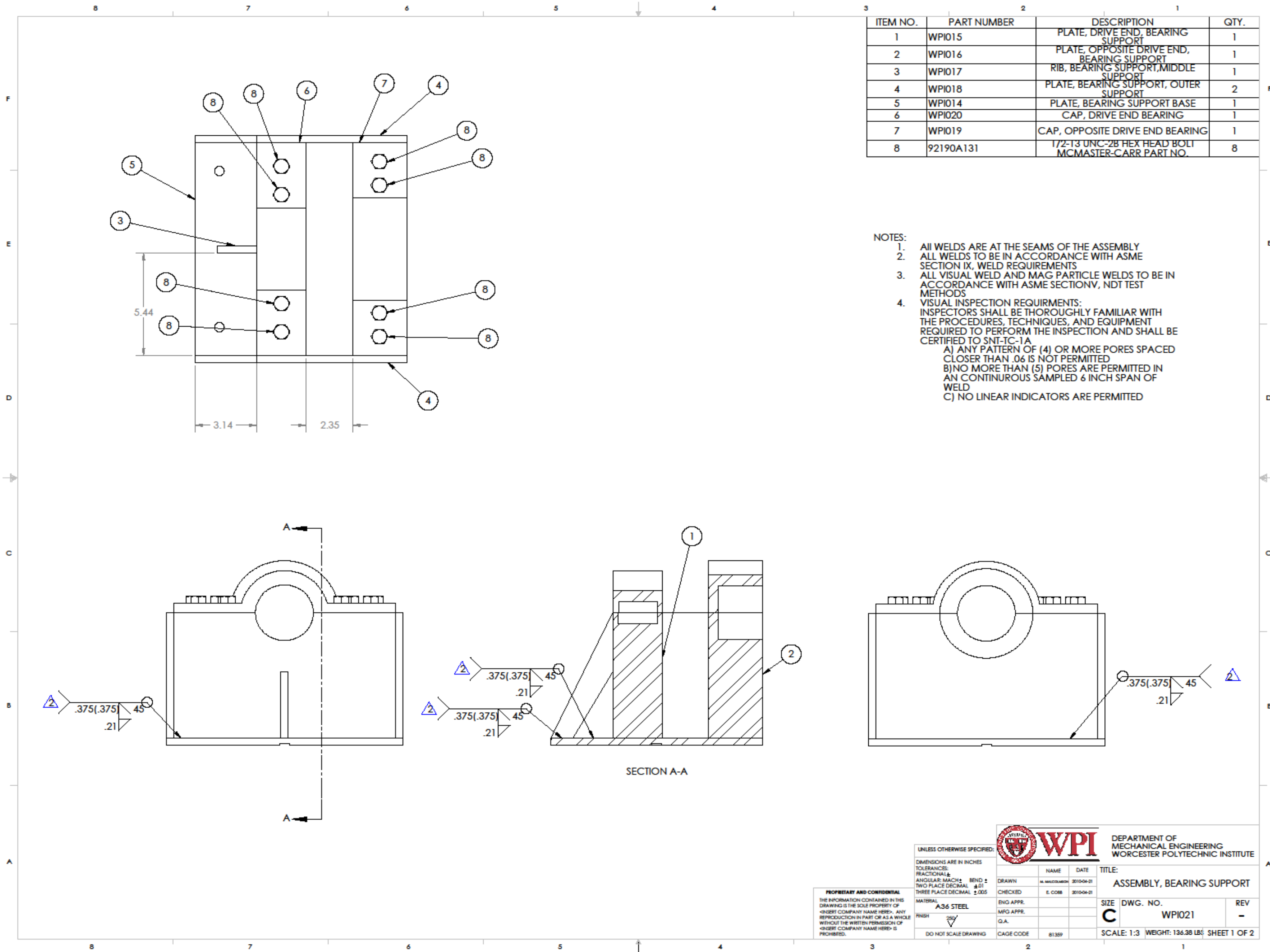$$\Delta L := \alpha \cdot L \cdot \Delta T = 7.458 \times 10^{-3} \qquad\qquad \Delta L := .036 \, in$$
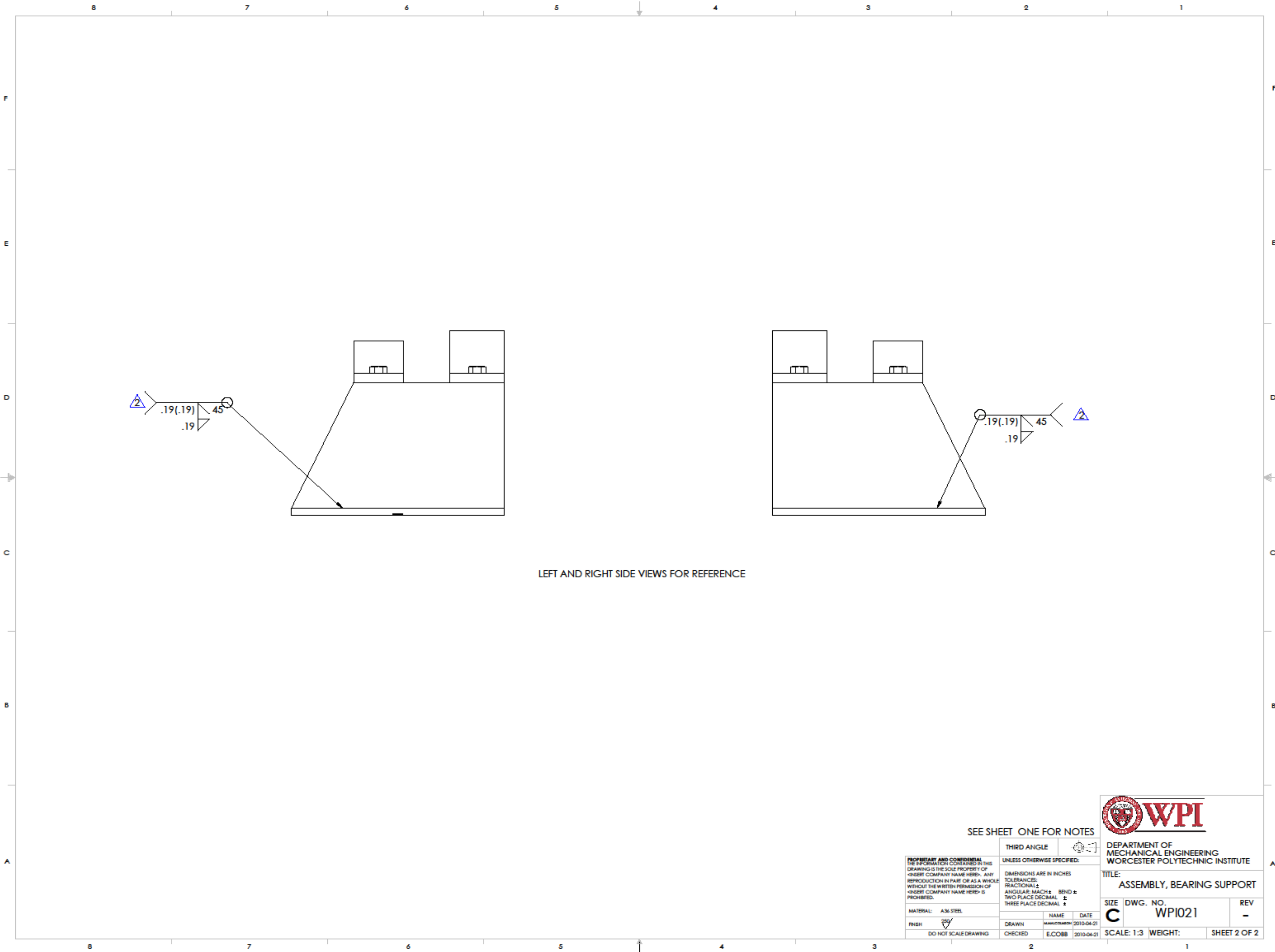
ITEM NO.	PART NUMBER	DESCRIPTION	QTY.
1	WPI015	PLATE, DRIVE END, BEARING SUPPORT	1
2	WPI016	PLATE, OPPOSITE DRIVE END, BEARING SUPPORT	1
3	WPI017	RIB, BEARING SUPPORT, MIDDLE SUPPORT	1
4	WPI018	PLATE, BEARING SUPPORT, OUTER SUPPORT	2
5	WPI014	PLATE, BEARING SUPPORT BASE	1
6	WPI020	CAP, DRIVE END BEARING	1
7	WPI019	CAP, OPPOSITE DRIVE END BEARING	1
8	92190A131	1/2-13 UNC-2B HEX HEAD BOLT MCMASTER-CARR PART NO.	8

NOTES:
1. All WELDS ARE AT THE SEAMS OF THE ASSEMBLY
2. ALL WELDS TO BE IN ACCORDANCE WITH ASME SECTION IX, WELD REQUIREMENTS
3. ALL VISUAL WELD AND MAG PARTICLE WELDS TO BE IN ACCORDANCE WITH ASME SECTIONV, NDT TEST METHODS
4. VISUAL INSPECTION REQUIRMENTS:
   INSPECTORS SHALL BE THOROUGHLY FAMILIAR WITH THE PROCEDURES, TECHNIQUES, AND EQUIPMENT REQUIRED TO PERFORM THE INSPECTION AND SHALL BE CERTIFIED TO SNT-TC-1A
   A) ANY PATTERN OF (4) OR MORE PORES SPACED CLOSER THAN .06 IS NOT PERMITTED
   B) NO MORE THAN (5) PORES ARE PERMITTED IN AN CONTINUROUS SAMPLED 6 INCH SPAN OF WELD
   C) NO LINEAR INDICATORS ARE PERMITTED

SECTION A-A

ASSEMBLY, BEARING SUPPORT

DEPARTMENT OF MECHANICAL ENGINEERING WORCESTER POLYTECHNIC INSTITUTE

SIZE **C** | DWG. NO. WPI021 | REV –

SCALE: 1:3 | WEIGHT: 136.38 LBS | SHEET 1 OF 2

MATERIAL: A36 STEEL

LEFT AND RIGHT SIDE VIEWS FOR REFERENCE

.19(.19)   45
.19

.19(.19)   45
.19

SEE SHEET ONE FOR NOTES

THIRD ANGLE

UNLESS OTHERWISE SPECIFIED:

DIMENSIONS ARE IN INCHES
TOLERANCES:
FRACTIONAL±
ANGULAR: MACH±   BEND ±
TWO PLACE DECIMAL   ±
THREE PLACE DECIMAL   ±

MATERIAL: A36 STEEL

FINISH   250√

DO NOT SCALE DRAWING

	NAME	DATE
DRAWN	HUMAICOLBSON	2010-04-21
CHECKED	E.COBB	2010-04-21

DEPARTMENT OF
MECHANICAL ENGINEERING
WORCESTER POLYTECHNIC INSTITUTE

TITLE:
ASSEMBLY, BEARING SUPPORT

SIZE	DWG. NO.	REV
C	WPI021	–

SCALE: 1:3   WEIGHT: SHEET 2 OF 2

C

.375

10.75

.50

2x R.03

DETAIL A
SCALE 1 : 2

A

2x 8.25

2x 1.25

4x Ø .53 THRU

⊕ Ø .020 Ⓜ A Ⓜ B Ⓜ C

2x 1.88

2x R.13

12.00

B

NOTE:
1.   STOCK FINISH ACCEPTABLE

WPI

DEPARTMENT OF
MECHANICAL ENGINEERING
WORCESTER POLYTECHNIC INSTITUTE

TITLE:
PLATE, BEARING SUPPORT BASE

SIZE A   DWG. NO.   WPI014   REV –

SCALE: 1:4   WEIGHT: 13.40 LBS   SHEET 1 OF 1

.27

4x Ø 1/2 - 13 UNC-2B
▽ 1.50

⊕ | Ø .020 Ⓜ | AⓂ | BⓂ | C

2.50   1.97

4x 1.25

A

2x 1.50   2x 1.25

R1.970 +.002 / -.000

R1.47

C

B

6.625

11.25

NOTE:
1.   STOCK FINISH ACCEPTABLE

UNLESS OTHERWISE SPECIFIED:
DIMENSIONS ARE IN INCHES
TOLERANCES:
TWO PLACE DECIMAL   ± .01
THREE PLACE DECIMAL ± .005

THIRD ANGLE

MATERIAL
A36 STEEL

FINISH
250

DO NOT SCALE DRAWING

	NAME	DATE
DRAWN	M.MALCOLMSON	2010-04-18
CHECKED	E.COBB	2010-04-18
ENG APPR.		
MFG APPR.		
Q.A.		
Cage Code	81359	

DEPARTMENT OF
MECHANICAL ENGINEERING
WORCESTER POLYTECHNIC INSTITUTE

TITLE:
PLATE, DRIVE END, BEARING SUPPORT

SIZE **A**   DWG. NO. **WPI015**   REV –

SCALE: 1:3   WEIGHT: 48.65 LBS   SHEET 1 OF 1

2x 1.08
2x 1.25
2.75
.47
4x 1.38
4x ∅ 1/2-13 UNC-2B
▽ 1.50
⌖ ∅ .020 Ⓜ A Ⓜ B Ⓜ D

A

R2.365 +.002/-.000
R1.47
D

6.63

B

11.25
C

7.50
2x 1.25
1.88
2x ∅ 1/2-13 UNC-2B
▽ .875
⌖ ∅ .020 Ⓜ A Ⓜ B Ⓜ C

NOTE:
1.   STOCK FINISH ACCEPTABLE

UNLESS OTHERWISE SPECIFIED:
DIMENSIONS ARE IN INCHES
TOLERANCES:
TWO PLACE DECIMAL ± .01
THREE PLACE DECIMAL ± .005

THIRD ANGLE

PROPRIETARY AND CONFIDENTIAL
THE INFORMATION CONTAINED IN THIS
DRAWING IS THE SOLE PROPERTY OF
<INSERT COMPANY NAME HERE>. ANY
REPRODUCTION IN PART OR AS A WHOLE
WITHOUT THE WRITTEN PERMISSION OF
<INSERT COMPANY NAME HERE> IS
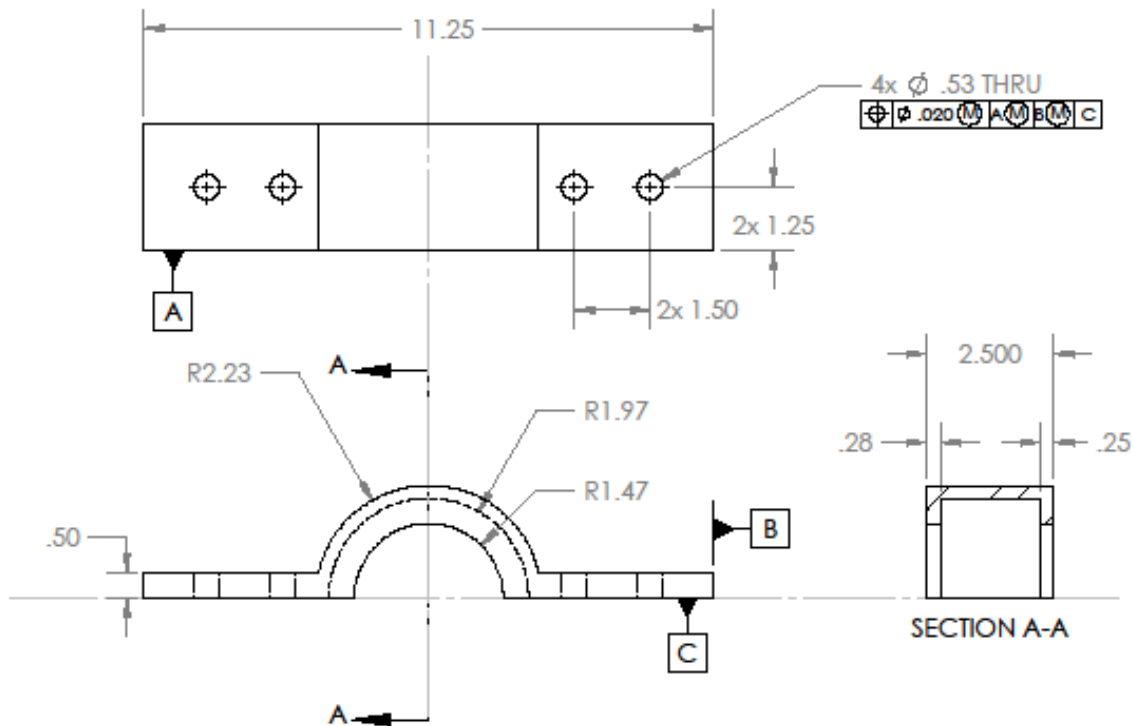PROHIBITED.

MATERIAL
A36 STEEL
FINISH

DO NOT SCALE DRAWING

	NAME	DATE
DRAWN	M.M.M.COLMSON	2010-04-18
CHECKED	E.COBB	2010-04-18
ENG APPR.		
MFG APPR.		
Q.A.		
Cage Code	81359	

DEPARTMENT OF
MECHANICAL ENGINEERING
WORCESTER POLYTECHNIC INSTITUTE

TITLE:
PLATE, OPPOSITE DRIVE END, BEARING SUPPORT

SIZE DWG. NO.   REV
A   WPI016   -

SCALE: 1:4   WEIGHT: 51.74 LBS   SHEET 1 OF 1

.375

3.50

60.0°

2.02

NOTE:
1. STOCK FINISH ACCEPTABLE

UNLESS OTHERWISE SPECIFIED:
DIMENSIONS ARE IN INCHES
TOLERANCES:
TWO PLACE DECIMAL ± .01
THREE PLACE DECIMAL ± .005

THIRD ANGLE

MATERIAL
A36 STEEL

FINISH
250

DO NOT SCALE DRAWING

	NAME	DATE
DRAWN	M.MALCOLMSON	2010-04-18
CHECKED	E.COBB	2010-04-18
ENG APPR.		
MFG APPR.		
Q.A.		
Cage Code	81359	

WPI
DEPARTMENT OF
MECHANICAL ENGINEERING
WORCESTER POLYTECHNIC INSTITUTE

TITLE:
RIB, BEARING SUPPORT MIIDDLE SUPPORT

SIZE: A
DWG. NO.: WPI017
REV: -

SCALE: 1:1   WEIGHT: 0.38   SHEET 1 OF 1

5   4   3   2   1

.375

7.608

A

∥ .01 A B

6.625

64.64°

B

10.748

NOTE:
1.   STOCK FINISH ACCEPTABLE

UNLESS OTHERWISE SPECIFIED:					
DIMENSIONS ARE IN INCHES					
TOLERANCES:					
TWO PLACE DECIMAL ± .01					
THREE PLACE DECIMAL ± .005		NAME	DATE		
THIRD ANGLE	DRAWN	ALINA COLUMBIA	2010-04-18		
	CHECKED	E.COBB	2010-04-18		
MATERIAL	ENG APPR.				
A36 STEEL	MFG APPR.				
FINISH 250	Q.A.				
DO NOT SCALE DRAWING	Cage Code	81369			

WPI

DEPARTMENT OF
MECHANICAL ENGINEERING
WORCESTER POLYTECHNIC INSTITUTE

TITLE:
PLATE, BEARING SUPPORT OUTER SUPPORT

SIZE **A** DWG. NO. WPI018   REV −

SCALE: 1:2   WEIGHT: 6.47 LBS   SHEET 1 OF 1

5   4   3   2   1

4x ⌀.53 THRU
⌖ | ⌀ .020 Ⓜ | AⓂ | BⓂ | C

NOTE:
1.   STOCK FINISH ACCEPTABLE

2x 1.38

2x 1.25

A

R2.75
R2.36
R1.47

B

2.75
.47

SECTION A-A

A

C

.50

A

11.25

UNLESS OTHERWISE SPECIFIED:
DIMENSIONS ARE IN INCHES
TOLERANCES:
FRACTIONAL±
ANGULAR: MACH±   BEND ±
TWO PLACE DECIMAL   ±.01
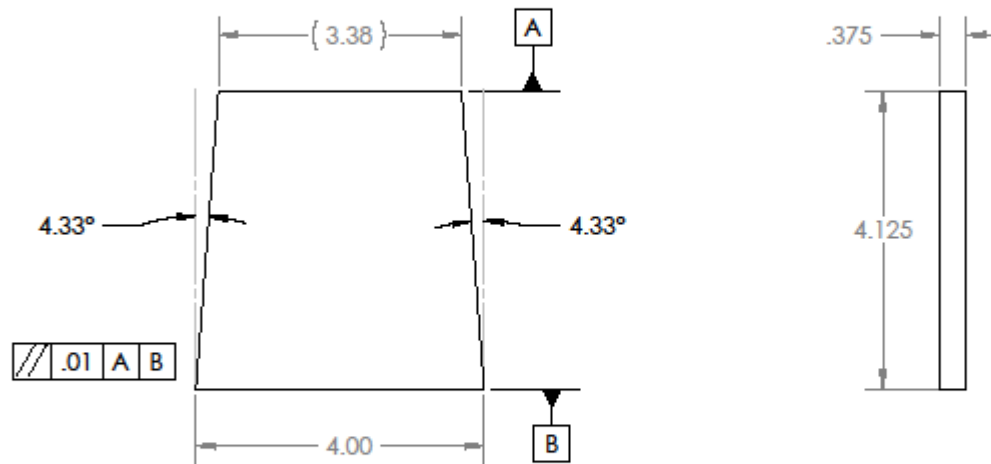THREE PLACE DECIMAL ±.005

MATERIAL
A36 STEEL

FINISH
250√

DO NOT SCALE DRAWING

	NAME	DATE
DRAWN	MAMALCOLMRON	2010-04-20
CHECKED	E. COBB	2010-04-20
ENG APPR.		
MFG APPR.		
Q.A.		
Cage Code	81359	

WPI
DEPARTMENT OF
MECHANICAL ENGINEERING
WORCESTER POLYTECHNIC INSTITUTE

TITLE:
CAP, OPPOSITE DRIVE END, BEARING

SIZE: A   DWG. NO. WPI019   REV: -

SCALE: 1:3   WEIGHT: 5.29 LBS   SHEET 1 OF 1

11.25

4x Ø .53 THRU

Ø .020 M A M B M C

2x 1.25

2x 1.50

A

R2.23

R1.97

R1.47

.50

A

B

C

A

2.500

.28   .25

SECTION A-A

NOTE:
1.   STOCK FINISH ACCEPTABLE

UNLESS OTHERWISE SPECIFIED:
DIMENSIONS ARE IN INCHES
TOLERANCES:
FRACTIONAL±
ANGULAR: MACH±   BEND ±
TWO PLACE DECIMAL   ± .01
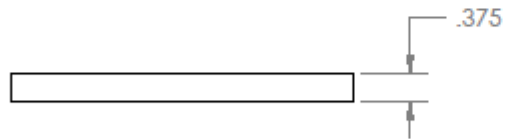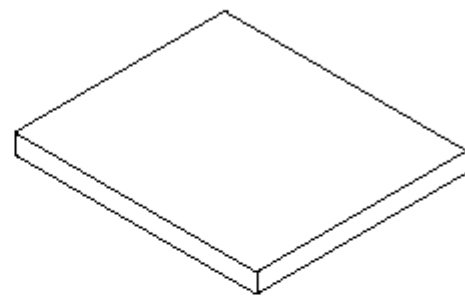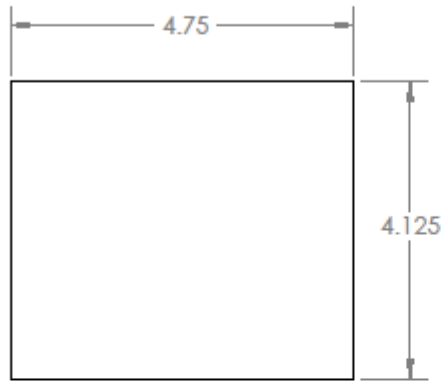THREE PLACE DECIMAL ± .005

MATERIAL
A36 STEEL

FINISH
250/

DO NOT SCALE DRAWING

	NAME	DATE
DRAWN	M.MALCOLMSON	2010-04-21
CHECKED	E. COBB	2010-04-21
ENG APPR.		
MFG APPR.		
Q.A.		
Cage Code	81359	

DEPARTMENT OF
MECHANICAL ENGINEERING
WORCESTER POLYTECHNIC INSTITUTE

WPI

TITLE:
CAP, DRIVE END BEARING

SIZE DWG. NO.   REV
A   WPI020   -

SCALE: 1:3   WEIGHT: 3.91 LBS   SHEET 1 OF 1

5   4   3   2   1

ITEM NO.	PART NUMBER	DESCRIPTION	QTY.
1	WPI 004	PLATE, TORQUE METER SUPPORT, TOP	1
2	WPI 006	RIB, TORQUE METER SUPPORT, CENTER	1
3	WPI 005	PLATE, TORQUE METER SUPPORT, SIDE	2
4	WPI 003	PLATE, TORQUE METER SUPPORT BOTTOM	1

SECTION A-A
SCALE 1 : 1.5

1 ▷ 4 SIZE F HOLES DRILLED AFTER ASSEMBLY IS WELDED LOCATIONS AS PER DIMENSIONED

2 ▷ STOCK FINISH ACCEPTABLE

DEPARTMENT OF
MECHANICAL ENGINEERING
WORCESTER POLYTECHNIC INSTITUTE

TITLE: TORQUE METER SUPPORT

MATERIAL A36 STRUCTURAL STEEL

SIZE C   DWG. NO. WPI 002   REV —

SCALE: 2:3   WEIGHT: 10.32 LB   SHEET 1 OF 1

4X Ø .386 THRU
⊕ | Ø .010 (M) A(M) B(M) | C

2.75

.63
.50
6.50

A

R.025 TYP
.100

DETAIL A
SCALE 1 : 1

.375

B

C

R.125 TYP
.500 +.001/-.000 TYP

4.00

1.75

3.50

7.50

NOTES:
1. MILL CHANNEL IN BOTTOM FACE
2. REFERENCE SIDES FROM CHANNEL
3. STOCK FINISH ACCEPTABLE

THIRD ANGLE

UNLESS OTHERWISE SPECIFIED:
DIMENSIONS ARE IN INCHES
TOLERANCES:
FRACTIONAL±
ANGULAR: MACH± BEND ±
TWO PLACE DECIMAL ± .01
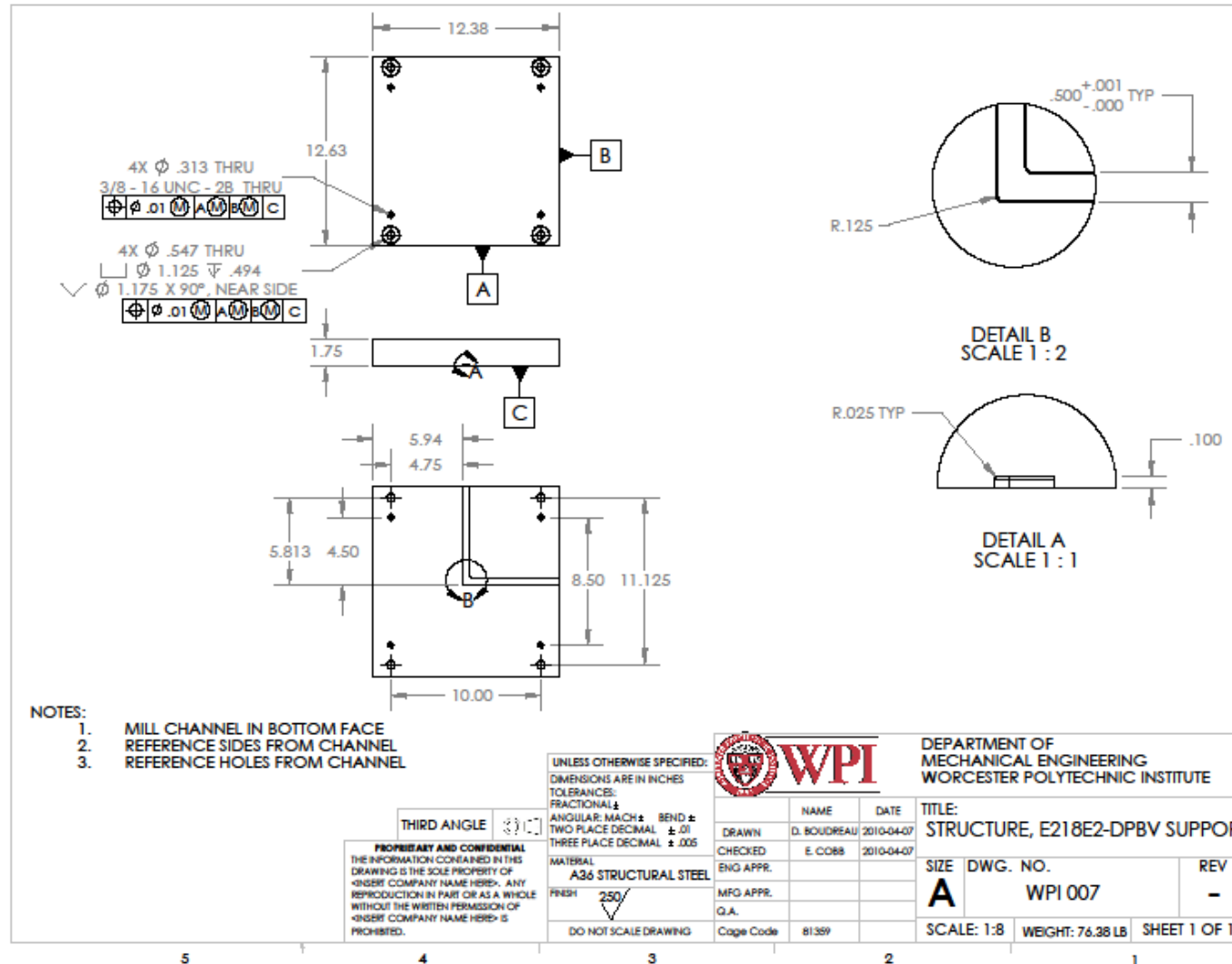THREE PLACE DECIMAL ± .005

MATERIAL
A36 STRUCTURAL STEEL

FINISH
250/

DO NOT SCALE DRAWING

	NAME	DATE
DRAWN	D. BOUDREAU	2010-04-07
CHECKED	E. COBB	2010-04-07
ENG APPR.		
MFG APPR.		
Q.A.		
Cage Code	81359	

WPI
DEPARTMENT OF
MECHANICAL ENGINEERING
WORCESTER POLYTECHNIC INSTITUTE

TITLE:
PLATE, TORQUE METER SUPPORT, BOTTOM

SIZE A DWG. NO. WPI 003 REV –

SCALE: 1:3 WEIGHT: 3.03 LB SHEET 1 OF 1

5.50

3.375

.375

NOTE:
1. STOCK FINISH ACCEPTABLE

THIRD ANGLE

UNLESS OTHERWISE SPECIFIED:
DIMENSIONS ARE IN INCHES
TOLERANCES:
FRACTIONAL±
ANGULAR: MACH±   BEND ±
TWO PLACE DECIMAL   ±.01
THREE PLACE DECIMAL ±.005

MATERIAL
A36 STRUCTURAL STEEL

FINISH
250/

DO NOT SCALE DRAWING

	NAME	DATE
DRAWN	D. BOUDREAU	2010-04-07
CHECKED	E. COBB	2010-04-07
ENG APPR.		
MFG APPR.		
Q.A.		
Cage Code	81359	

WPI

DEPARTMENT OF
MECHANICAL ENGINEERING
WORCESTER POLYTECHNIC INSTITUTE

TITLE:
PLATE, TORQUE METER SUPPORT,
TOP

SIZE: A   DWG. NO. WPI 004   REV –

SCALE: 1:8   WEIGHT: 1.97 LB   SHEET 1 OF 1

NOTE:
1.   STOCK FINISH ACCEPTABLE

{ 3.38 }

A

4.33°   4.33°

.375

4.125

// | .01 | A | B

4.00

B

UNLESS OTHERWISE SPECIFIED:
DIMENSIONS ARE IN INCHES
TOLERANCES:
FRACTIONAL±
ANGULAR: MACH±   BEND ±
TWO PLACE DECIMAL   ±.01
THREE PLACE DECIMAL ±.005

THIRD ANGLE

MATERIAL
A36 STRUCTURAL STEEL

FINISH
250

DO NOT SCALE DRAWING

	NAME	DATE
DRAWN	D. BOUDREAU	2010-04-07
CHECKED	E. COBB	2010-04-07
ENG APPR.		
MFG APPR.		
Q.A.		
Cage Code	81359	

WPI

DEPARTMENT OF
MECHANICAL ENGINEERING
WORCESTER POLYTECHNIC INSTITUTE

TITLE:
PLATE, TORQUE METER SUPPORT
SIDE

SIZE A

DWG. NO.
WPI 005

REV
–

SCALE: 1:2   WEIGHT: 1.62 LB   SHEET 1 OF 1

5   4   3   2   1

4.75

4.125

.375

NOTE:
1.   STOCK FINISH ACCEPTABLE

UNLESS OTHERWISE SPECIFIED:

DIMENSIONS ARE IN INCHES
TOLERANCES:
FRACTIONAL±
ANGULAR: MACH±   BEND ±
TWO PLACE DECIMAL   ±.01
THREE PLACE DECIMAL ±.005

THIRD ANGLE

MATERIAL
A36 STRUCTURAL STEEL

FINISH 250

DO NOT SCALE DRAWING

	NAME	DATE
DRAWN	D. BOUDREAU	2010-04-07
CHECKED	E. COBB	2010-04-07
ENG APPR.		
MFG APPR.		
Q.A.		
Cage Code	81359	

DEPARTMENT OF
MECHANICAL ENGINEERING
WORCESTER POLYTECHNIC INSTITUTE

WPI

TITLE:
PLATE, TORQUE METER SUPPORT,
CENTER

SIZE A

DWG. NO.
WPI 006

REV
–

SCALE: 1:2   WEIGHT: 2.08 LB   SHEET 1 OF 1

Appendix F- Prime Mover Support Drawings

12.38

12.63

4X Ø .313 THRU
3/8 - 16 UNC - 2B THRU
⊕ | ⌀ .01 Ⓜ A Ⓜ BⓂ C

4X Ø .547 THRU
⌴ Ø 1.125 ▽ .494
∨ Ø 1.175 X 90° , NEAR SIDE
⊕ | ⌀ .01 Ⓜ A Ⓜ BⓂ C

B

A

C

1.75

5.94
4.75

5.813   4.50

8.50   11.125

B

10.00

.500 +.001 -.000 TYP

R.125

DETAIL B
SCALE 1 : 2

R.025 TYP

.100

DETAIL A
SCALE 1 : 1

NOTES:
1.   MILL CHANNEL IN BOTTOM FACE
2.   REFERENCE SIDES FROM CHANNEL
3.   REFERENCE HOLES FROM CHANNEL

UNLESS OTHERWISE SPECIFIED:
DIMENSIONS ARE IN INCHES
TOLERANCES:
FRACTIONAL ±
ANGULAR: MACH ±   BEND ±
TWO PLACE DECIMAL   ± .01
THREE PLACE DECIMAL ± .005
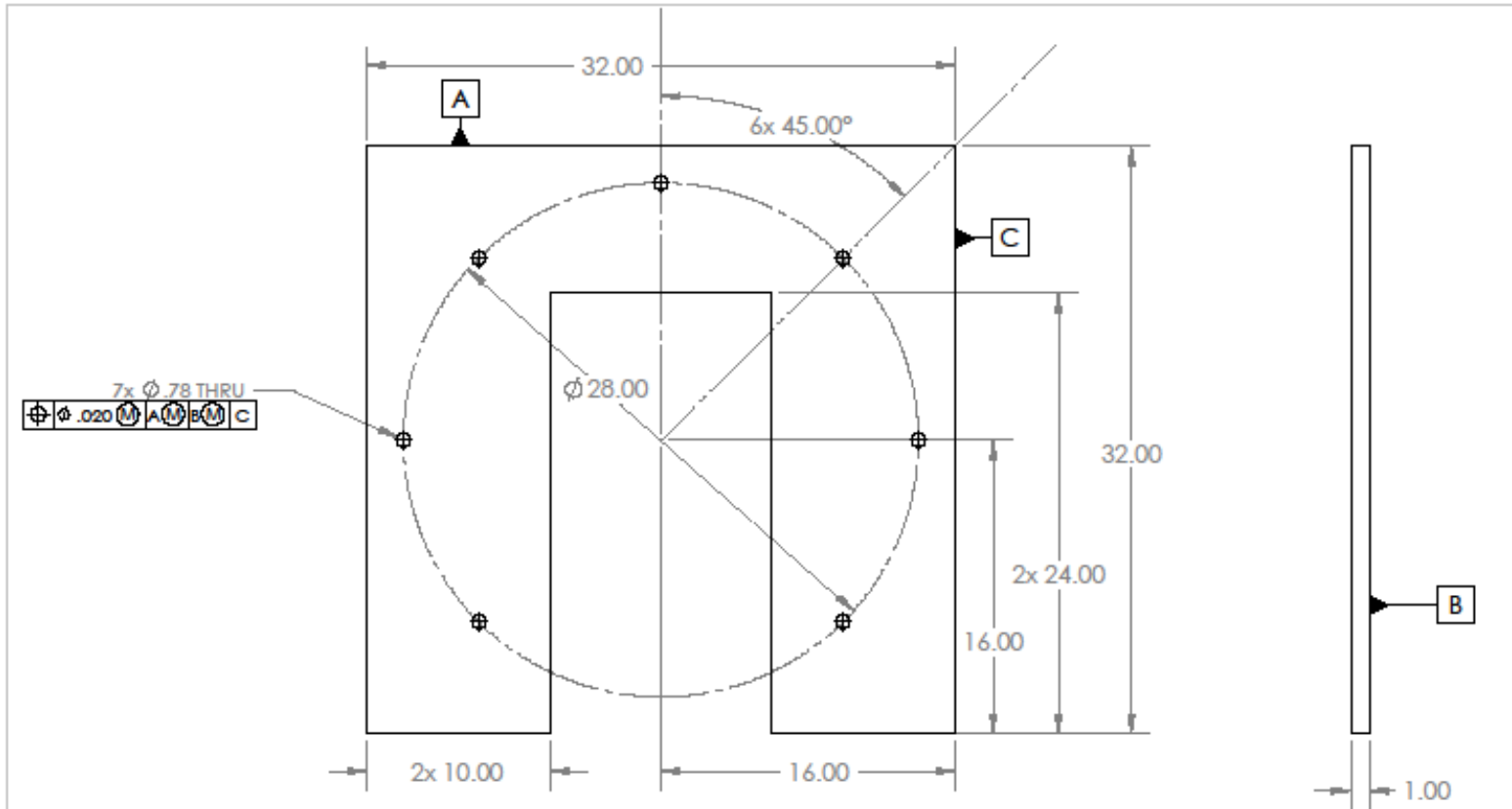
THIRD ANGLE

PROPRIETARY AND CONFIDENTIAL
THE INFORMATION CONTAINED IN THIS
DRAWING IS THE SOLE PROPERTY OF
<INSERT COMPANY NAME HERE>. ANY
REPRODUCTION IN PART OR AS A WHOLE
WITHOUT THE WRITTEN PERMISSION OF
<INSERT COMPANY NAME HERE> IS
PROHIBITED.

MATERIAL
A36 STRUCTURAL STEEL
FINISH
250

DO NOT SCALE DRAWING

	NAME	DATE
DRAWN	D. BOUDREAU	2010-04-07
CHECKED	E. COBB	2010-04-07
ENG APPR.		
MFG APPR.		
Q.A.		
Cage Code	81359	

WPI
DEPARTMENT OF
MECHANICAL ENGINEERING
WORCESTER POLYTECHNIC INSTITUTE

TITLE:
STRUCTURE, E218E2-DPBV SUPPORT

SIZE DWG. NO.   REV
A   WPI 007   -

SCALE: 1:8   WEIGHT: 76.38 LB   SHEET 1 OF 1

ITEM NO.	PART NUMBER	DESCRIPTION	QTY.
1	WPI022	PLATE, STATOR SUPPORT BASE	2
2	WPI023	PLATE, STATOR SUPPORT BOLT	1
3	WPI024	PLATE, STATOR SUPPORT SIDE	2
4	WPI025	RIB, STATOR SUPPORT	4
5	WPI026	PLATE, STATOR SUPPORT TOP	1

NOTES:
1. All WELDS ARE AT THE SEAMS OF THE ASSEMBLY

2. ALL WELDS TO BE IN ACCORDANCE WITH ASME SECTION IX, WELD REQUIREMENTS

3. ALL VISUAL WELD AND MAG PARTICLE WELDS TO BE IN ACCORDANCE WITH ASME SECTIONV, NDT TEST METHODS

4. VISUAL INSPECTION REQUIRMENTS: INSPECTORS SHALL BE THOROUGHLY FAMILIAR WITH THE PROCEDURES, TECHNIQUES, AND EQUIPMENT REQUIRED TO PERFORM THE INSPECTION AND SHALL BE CERTIFIED TO SNT-TC-1A
   A) ANY PATTERN OF (4) OR MORE PORES SPACED CLOSER THAN .06 IS NOT PERMITTED
   B)NO MORE THAN (5) PORES ARE PERMITTED IN AN CONTINUROUS SAMPLED 6 INCH SPAN OF WELD
   C) NO LINEAR INDICATORS ARE PERMITTED

SECTION A-A

DEPARTMENT OF
MECHANICAL ENGINEERING
WORCESTER POLYTECHNIC INSTITUTE

TITLE: ASSEMBLY, STATOR SUPPORT

MATERIAL: A36 STEEL

SIZE: C   DWG. NO. WPI027   REV: -

SCALE: 1:5   WEIGHT: SHEET 1 OF 2

LEFT SIDE VIEW

.375(.375) 45
.21 △2

RIGHT SIDE VIEW

△2 .375(.375) 45
.21

SEE SHEET ONE FOR NOTES

UNLESS OTHERWISE SPECIFIED:

DIMENSIONS ARE IN INCHES
TOLERANCES:
FRACTIONAL±
ANGULAR: MACH±   BEND ±
TWO PLACE DECIMAL   ±
THREE PLACE DECIMAL ±

MATERIAL: A36 STEEL

FINISH

	NAME	DATE
DRAWN	M.MALCOMSON	2010-04-21
CHECKED	E.COBB	2010-04-21

DO NOT SCALE DRAWING

WPI
DEPARTMENT OF
MECHANICAL ENGINEERING
WORCESTER POLYTECHNIC INSTITUTE

TITLE:
ASSEMBLY, BEARING SUPPORT

SIZE **C** DWG. NO. WPI027   REV **–**

SCALE: 1:5   WEIGHT: SHEET 2 OF 2

16.00

16.00

.375

NOTE:
1. STOCK FINISH ACCEPTABLE

UNLESS OTHERWISE SPECIFIED:
DIMENSIONS ARE IN INCHES
TOLERANCES:
FRACTIONAL±
ANGULAR: MACH±   BEND ±
TWO PLACE DECIMAL   ± .01
THREE PLACE DECIMAL ± .005

MATERIAL
A36 STEEL

FINISH
250

DO NOT SCALE DRAWING

	NAME	DATE
DRAWN	H.MALCOLMSON	2010-04-21
CHECKED	E.COBB	2010-04-21
ENG APPR.		
MFG APPR.		
Q.A.		
Cage Code	81359	

DEPARTMENT OF
MECHANICAL ENGINEERING
WORCESTER POLYTECHNIC INSTITUTE

TITLE:
PLATE, STATOR SUPPORT BASE

SIZE A   DWG. NO.   WPI022   REV −

SCALE: 1:4   WEIGHT: 27.23 LBS   SHEET 1 OF 1

NOTE:
1. STOCK FINISH ACCEPTABLE

32.00

A

6x 45.00°

C

7x ∅.78 THRU

⊕ | ⌀ .020 Ⓜ | A Ⓜ | B Ⓜ | C

∅ 28.00

32.00

2x 24.00

16.00

B

2x 10.00

16.00

1.00

UNLESS OTHERWISE SPECIFIED:
DIMENSIONS ARE IN INCHES
TOLERANCES:
FRACTIONAL±
ANGULAR: MACH±   BEND ±
TWO PLACE DECIMAL   ±.01
THREE PLACE DECIMAL ±.005

	NAME	DATE
DRAWN	M. MALCOLMSON	2010-04-21
CHECKED	E. COBB	2010-04-21
ENG APPR.		
MFG APPR.		
Q.A.		

MATERIAL
A36 STEEL

FINISH
250

DO NOT SCALE DRAWING

Cage Code   81369

DEPARTMENT OF
MECHANICAL ENGINEERING
WORCESTER POLYTECHNIC INSTITUTE

WPI

TITLE:
PLATE, STATOR SUPPORT BOLT

SIZE A   DWG. NO.   WPI023   REV −

SCALE: 1:8   WEIGHT: 207.85 LBS   SHEET 1 OF 1

16.00

.375

32.00

NOTE:
1.   STOCK FINISH ACCEPTABLE

UNLESS OTHERWISE SPECIFIED:
DIMENSIONS ARE IN INCHES
TOLERANCES:
FRACTIONAL±
ANGULAR: MACH±   BEND ±
TWO PLACE DECIMAL   ± .01
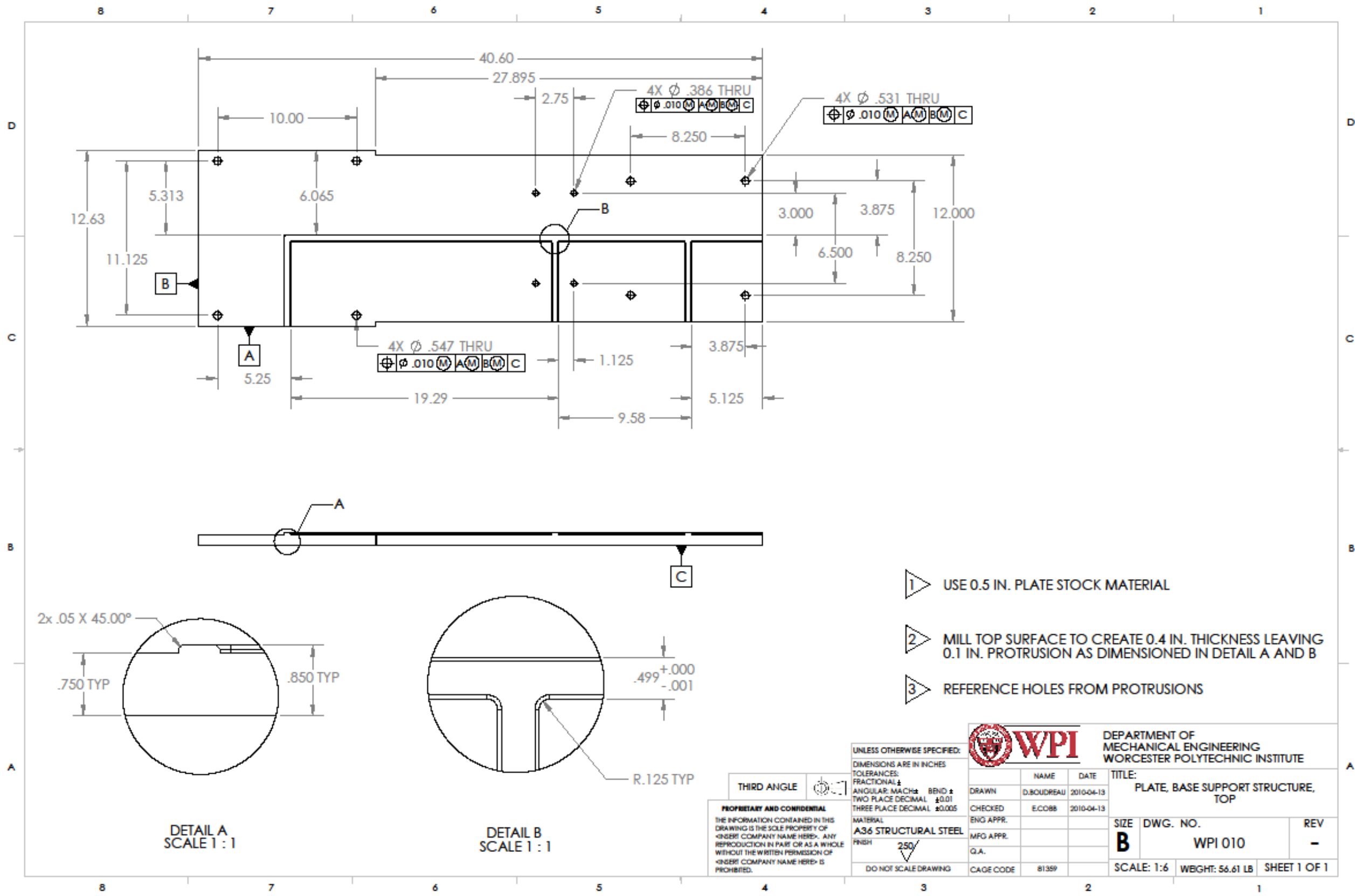THREE PLACE DECIMAL ± .005

MATERIAL
A36 STEEL

FINISH
250

DO NOT SCALE DRAWING

	NAME	DATE
DRAWN	H.MALCOLMSON	2010-04-21
CHECKED	E.COBB	2010-04-21
ENG APPR.		
MFG APPR.		
Q.A.		
Cage Code	81359	

DEPARTMENT OF
MECHANICAL ENGINEERING
WORCESTER POLYTECHNIC INSTITUTE

WPI

TITLE:
PLATE, STATOR SUPPORT SIDE

SIZE	DWG. NO.	REV
A	WPI024	–

SCALE: 1:8   WEIGHT: 54.45 LBS   SHEET 1 OF 1

5   4   3   2   1

NOTE:
1. STOCK FINISH ACCEPTABLE
2. SHARP EDGES NOT REQUIRED

30.00

79.37°

5.63

.375

UNLESS OTHERWISE SPECIFIED:			DEPARTMENT OF MECHANICAL ENGINEERING WORCESTER POLYTECHNIC INSTITUTE		
DIMENSIONS ARE IN INCHES TOLERANCES: FRACTIONAL± ANGULAR: MACH± BEND ± TWO PLACE DECIMAL ± .01 THREE PLACE DECIMAL ± .005					
	NAME	DATE	TITLE: RIB, STATOR SUPPORT		
DRAWN	M.MALCOLMSON	2010-04-21			
CHECKED	E.COBB	2010-04-21			
MATERIAL A36 STEEL	ENG APPR.		SIZE A	DWG. NO. WPI025	REV –
FINISH 250	MFG APPR.				
	Q.A.				
DO NOT SCALE DRAWING	Cage Code	81359	SCALE: 1:6	WEIGHT: 9.57 LBS	SHEET 1 OF 1

16.00

32.75

.375

NOTE:
1.   STOCK FINISH ACCEPTABLE

UNLESS OTHERWISE SPECIFIED:
DIMENSIONS ARE IN INCHES
TOLERANCES:
FRACTIONAL±
ANGULAR: MACH±   BEND ±
TWO PLACE DECIMAL   ± .01
THREE PLACE DECIMAL ± .005

MATERIAL
A36 STEEL

FINISH

DO NOT SCALE DRAWING

	NAME	DATE
DRAWN	HUMACOLMBOH	2010-04-21
CHECKED	E.COBB	2010-04-21
ENG APPR.		
MFG APPR.		
Q.A.		
Cage Code	81359	

DEPARTMENT OF
MECHANICAL ENGINEERING
WORCESTER POLYTECHNIC INSTITUTE

WPI

TITLE:
PLATE, STATOR SUPPORT TOP

SIZE **A**   DWG. NO.   WPI026   REV **-**

SCALE: 1:8   WEIGHT:196.50 LBS   SHEET 1 OF 1

ITEM NO.	PART NUMBER	DESCRIPTION	QTY.
1	WPI 009	PLATE, BASE SUPPORT STRUCTURE, BOTTOM	1
2	WPI 011	RIB, BASE SUPPORT STRUCTURE, AXIAL	1
3	WPI 012	RIB, BASE SUPPORT STRUCTURE, SHORT	8
4	WPI 013	RIB, BASE SUPPORT STRUCTURE, LONG	10
5	WPI 010	PLATE, BASE SUPPORT STRUCTURE, TOP	1

12.70

27.895

16.00

12.00

R.125 TYP

A

.500

DETAIL A
SCALE 1 : 1

1 ▷ RADIUS OF FILLET NOT CRITICAL
ADJUST FOR MANUFACTURING AS NECESSARY

DEPARTMENT OF
MECHANICAL ENGINEERING
WORCESTER POLYTECHNIC INSTITUTE

WPI

UNLESS OTHERWISE SPECIFIED:
DIMENSIONS ARE IN INCHES
TOLERANCES:
FRACTIONAL±
ANGULAR: MACH±   BEND ±
TWO PLACE DECIMAL   ±.01
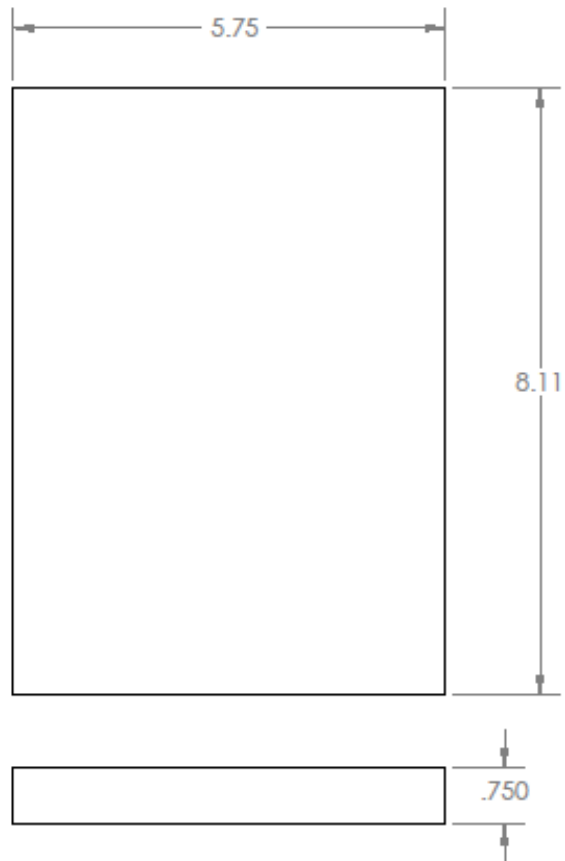THREE PLACE DECIMAL ±.005

THIRD ANGLE

MATERIAL
A36 STRUCTURAL STEEL

FINISH
250

DO NOT SCALE DRAWING

	NAME	DATE
DRAWN	D. BOUDREAU	2010-04-07
CHECKED	E. COBB	2010-04-07
ENG APPR.		
MFG APPR.		
Q.A.		
Cage Code	81359	

TITLE:
PLATE, BASE SUPPORT STRUCTURE, BOTTOM

SIZE DWG. NO.   REV
A   WPI 009   –

SCALE: 1:8   WEIGHT: 76.28 LB   SHEET 1 OF 1

40.60
27.895
2.75
4X Ø .386 THRU
⊕ Ø .010 M A M B M C
4X Ø .531 THRU
⊕ Ø .010 M A M B M C
10.00
8.250
12.63
5.313
6.065
11.125
3.000
3.875
12.000
6.500
8.250
B
4X Ø .547 THRU
⊕ Ø .010 M A M B M C
3.875
5.25
1.125
19.29
5.125
9.58

A

DETAIL A
SCALE 1 : 1

2x .05 X 45.00°
.750 TYP
.850 TYP

DETAIL B
SCALE 1 : 1

.499 +.000 / -.001
R.125 TYP

1 ▷ USE 0.5 IN. PLATE STOCK MATERIAL

2 ▷ MILL TOP SURFACE TO CREATE 0.4 IN. THICKNESS LEAVING 0.1 IN. PROTRUSION AS DIMENSIONED IN DETAIL A AND B

3 ▷ REFERENCE HOLES FROM PROTRUSIONS

THIRD ANGLE

UNLESS OTHERWISE SPECIFIED:
DIMENSIONS ARE IN INCHES
TOLERANCES:
FRACTIONAL ±
ANGULAR: MACH± BEND ±
TWO PLACE DECIMAL ±0.01
THREE PLACE DECIMAL ±0.005

	NAME	DATE
DRAWN	D.BOUDREAU	2010-04-13
CHECKED	E.COBB	2010-04-13
ENG APPR.		
MFG APPR.		
Q.A.		

MATERIAL: A36 STRUCTURAL STEEL
FINISH: 250

DO NOT SCALE DRAWING

CAGE CODE: 81359

WPI
DEPARTMENT OF
MECHANICAL ENGINEERING
WORCESTER POLYTECHNIC INSTITUTE

TITLE:
PLATE, BASE SUPPORT STRUCTURE, TOP

SIZE: B
DWG. NO.: WPI 010
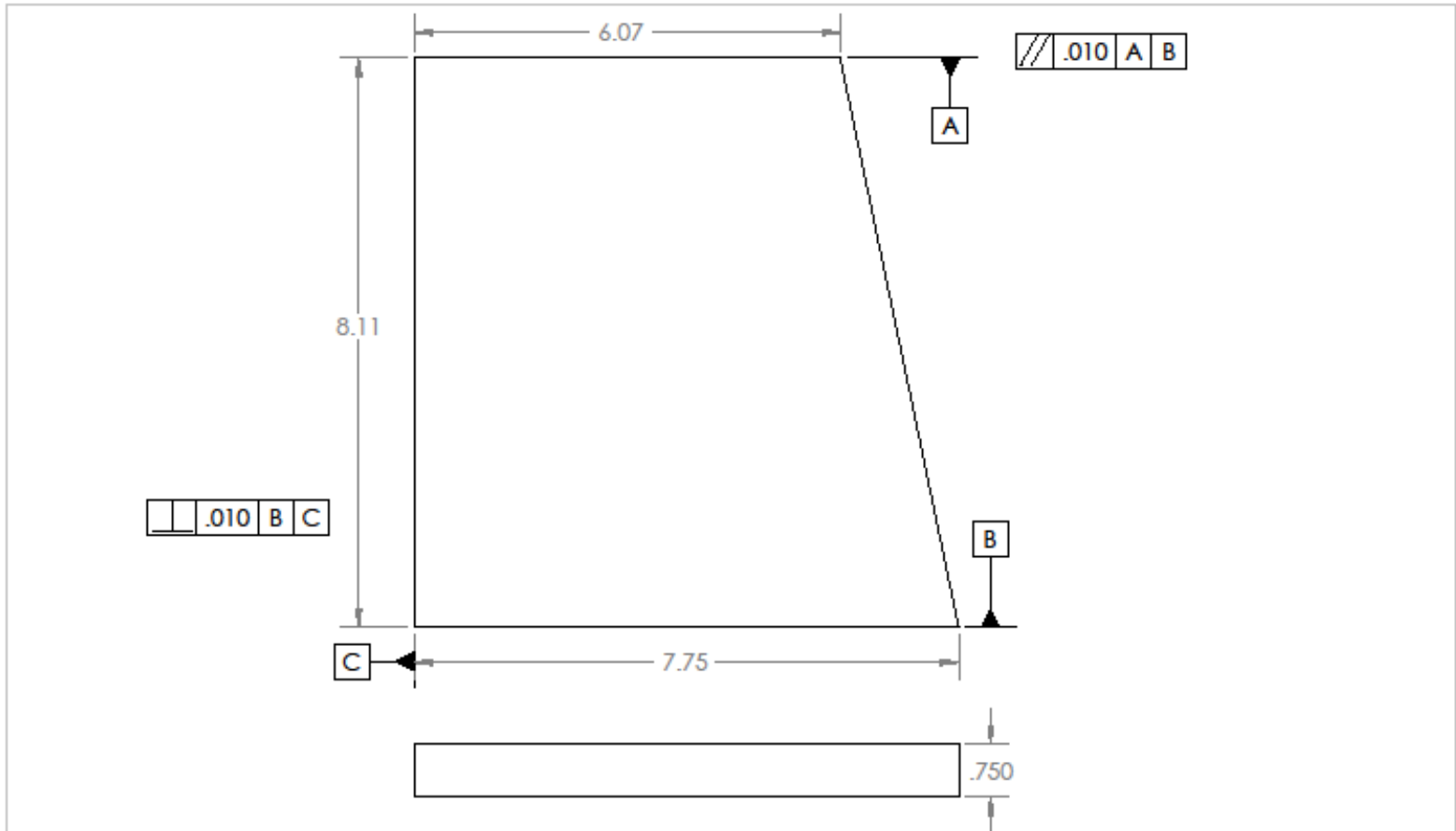REV: –

SCALE: 1:6 WEIGHT: 56.61 LB SHEET 1 OF 1

40.47

8.11

.50

DEPARTMENT OF
MECHANICAL ENGINEERING
WORCESTER POLYTECHNIC INSTITUTE

WPI

	NAME	DATE
DRAWN	D. BOUDREAU	2010-04-07
CHECKED	E. COBB	2010-04-07
ENG APPR.		
MFG APPR.		
Q.A.		
Cage Code	81359	

TITLE:

RIB, BASE SUPPORT STRUCTURE, AXIAL

SIZE	DWG. NO.	REV
A	WPI 011	–

SCALE: 1:8   WEIGHT: 48.66 LB   SHEET 1 OF 1

5   4   3   2   1

5.75

8.11

.750

THIRD ANGLE

UNLESS OTHERWISE SPECIFIED:

DIMENSIONS ARE IN INCHES
TOLERANCES:
FRACTIONAL±
ANGULAR: MACH±   BEND ±
TWO PLACE DECIMAL   ± .01
THREE PLACE DECIMAL ± .005

MATERIAL
A36 STRUCTURAL STEEL

FINISH
250

DO NOT SCALE DRAWING

	NAME	DATE
DRAWN	D. BOUDREAU	2010-04-07
CHECKED	E. COBB	2010-04-07
ENG APPR.		
MFG APPR.		
Q.A.		
Cage Code	81359	

WPI
DEPARTMENT OF
MECHANICAL ENGINEERING
WORCESTER POLYTECHNIC INSTITUTE

TITLE:
RIB, BASE SUPPORT STRUCTURE
SHORT

SIZE **A** DWG. NO. WPI 012 REV **–**

SCALE: 1:2   WEIGHT: 5.19 LB   SHEET 1 OF 1

6.07

// .010 A B

A

8.11

⊥ .010 B C

B

C ◄ 7.75

.750

THIRD ANGLE ⊕⊟⊡

UNLESS OTHERWISE SPECIFIED:

DIMENSIONS ARE IN INCHES
TOLERANCES:
FRACTIONAL±
ANGULAR: MACH±   BEND ±
TWO PLACE DECIMAL   ± .01
THREE PLACE DECIMAL ± .005

MATERIAL
A36 STRUCTURAL STEEL

FINISH
250/

DO NOT SCALE DRAWING

	NAME	DATE
DRAWN	D. BOUDREAU	2010-04-07
CHECKED	E. COBB	2010-04-07
ENG APPR.		
MFG APPR.		
Q.A.		
Cage Code	81359	

WPI
DEPARTMENT OF
MECHANICAL ENGINEERING
WORCESTER POLYTECHNIC INSTITUTE

TITLE:
RIB, BASE SUPPORT STRUCTURE,
LONG

SIZE	DWG. NO.	REV
A	WPI 013	–

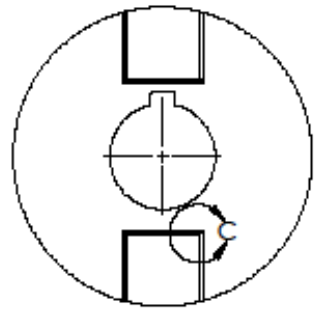SCALE: 1:2   WEIGHT: 6.23 LB   SHEET 1 OF 1

5   4   3   2   1

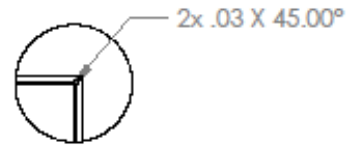## Appendix I- Prime Mover to Torque Meter Coupling Drawings

ITEM NO.	PART NUMBER	DESCRIPTION	QTY.
1	WPI028	COUPLING, PRIME MOVER TO TORQUE METER	1
2	WPI029	CONNECTOR, PRIME MOVER TO TORQUE METER	1
3	WPI030	COUPLING, TORQUE METER TO PRIME MOVER	1

SECTION A-A

UNLESS OTHERWISE SPECIFIED:

DIMENSIONS ARE IN INCHES
TOLERANCES:
FRACTIONAL±
ANGULAR: MACH±   BEND ±
TWO PLACE DECIMAL   ±.01
THREE PLACE DECIMAL ±.005

MATERIAL
A36 STEEL

FINISH   125

DO NOT SCALE DRAWING

	NAME	DATE
DRAWN	M. MALCOLMSON	2010-04-22
CHECKED	E. COBB	2010-04-22
ENG APPR.		
MFG APPR.		
Q.A.		
CAGE CODE	81359	

DEPARTMENT OF
MECHANICAL ENGINEERING
WORCESTER POLYTECHNIC INSTITUE

TITLE:

ASSEMBLY, PRIME MOVER TO
TORQUE METER COUPLING

SIZE **A** DWG. NO. **WPI031** REV **-**

SCALE: 1:4   WEIGHT: 26.60 LBS   SHEET 1 OF 1

.50

Ø6.00

.25

Ø2.13

Ø3.00

2x R.03

DETAIL A
SCALE 2 : 3

1.47

.50

.50

1.00

5.00

2x R.06

DETAIL B
SCALE 2 : 3

2x .03 X 45.00°

DETAIL C
SCALE 2 : 3

UNLESS OTHERWISE SPECIFIED:

DIMENSIONS ARE IN INCHES
TOLERANCES:
FRACTIONAL±
ANGULAR: MACH±   BEND ±
TWO PLACE DECIMAL   ± .01
THREE PLACE DECIMAL   ± .005

MATERIAL
A36 STEEL

FINISH
125

DO NOT SCALE DRAWING

	NAME	DATE
DRAWN	M.MALCOLMSON	2010-04-21
CHECKED	R.COBB	2010-04-21
ENG APPR.		
MFG APPR.		
Q.A.		
Cage Code	81359	

WPI

DEPARTMENT OF
MECHANICAL ENGINEERING
WORCESTER POLYTECHNIC INSTITUTE

TITLE:
COUPLING, PRIME MOVER TO
TORQUE METER

SIZE **A**   DWG. NO.
WPI028

REV
–

SCALE: 1:3   WEIGHT: 7.96 LBS   SHEET 1 OF 1

2x 2.25   Ø6.00

2x 1.00

B   B

SECTION B-B

2x .03 X 45.00°

2x R.06

DETAIL C
SCALE 2 : 3

1.500

2x .03 X 45.00°

2x R.06

SECTION A-A

A

2x 2.20

2x 1.50

A

UNLESS OTHERWISE SPECIFIED:

DIMENSIONS ARE IN INCHES
TOLERANCES:
FRACTIONAL±
ANGULAR: MACH±   BEND ±
TWO PLACE DECIMAL   ±.01
THREE PLACE DECIMAL ±.005

MATERIAL
A36 STEEL

FINISH
125

DO NOT SCALE DRAWING

	NAME	DATE
DRAWN	M.MALCOLMSON	2010-04-22
CHECKED	E. COBB	2010-04-22
ENG APPR.		
MFG APPR.		
Q.A.		
CAGE CODE	81359	

WPI

DEPARTMENT OF
MECHANICAL ENGINEERING
WORCESTER POLYTECHNIC INSTITUE

TITLE:
CONNECTOR, PRIME MOVER TO
TORQUE METERR COUPLING

SIZE A   DWG. NO. WPI029   REV -
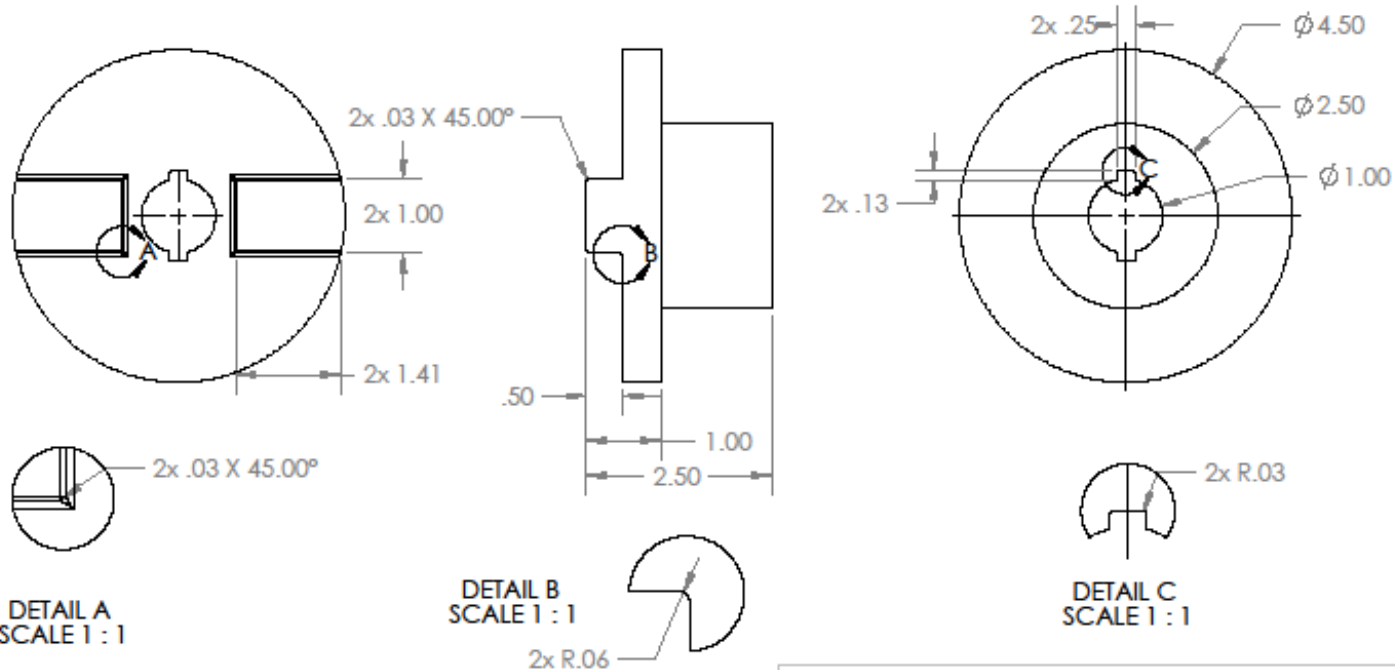
SCALE: 1:3   WEIGHT: 10.45 LBS   SHEET 1 OF 1

5   4   3   2   1

Ø6.00
4x R.03
Ø3.50
Ø1.00
2x .25
2x .13

2x R.06
2.50
.50

2x .03 X 45.00°

DETAIL A
SCALE 2 : 3

UNLESS OTHERWISE SPECIFIED:

DIMENSIONS ARE IN INCHES
TOLERANCES:
FRACTIONAL±
ANGULAR: MACH±   BEND ±
TWO PLACE DECIMAL   ± .01
THREE PLACE DECIMAL ± .005

MATERIAL
A36 STEEL

FINISH
125

DO NOT SCALE DRAWING

	NAME	DATE
DRAWN	N.MALCOLMSON	2010-04-22
CHECKED	E. COBB	2010-04-22
ENG APPR.		
MFG APPR.		
Q.A.		
CAGE CODE	81359	

DEPARTMENT OF
MECHANICAL ENGINEERING
WORCESTER POLYTECHNIC INSTITUE

TITLE:

COUPLING, TORQUE METER
TO PRIME MOVER

SIZE A

DWG. NO. WPI030

REV —

SCALE: 1:3   WEIGHT: 8.19 LBS   SHEET 1 OF 1

Appendix J- Torque Meter to Shaft Coupling Drawings

ITEM NO.	PART NUMBER	DESCRIPTION	QTY.
1	WPI033	CONNECTOR, TORQUE METER TO SHAFT	1
2	WPI032	COUPLING, TORQUE METER TO SHAFT	1
3	WPI034	COUPLING, SHAFT TO TORQUE METER	1

SECTION A-A

UNLESS OTHERWISE SPECIFIED:

DIMENSIONS ARE IN INCHES
TOLERANCES:
FRACTIONAL±
ANGULAR: MACH±   BEND ±
TWO PLACE DECIMAL   ± .01
THREE PLACE DECIMAL   ± .005

MATERIAL
A 36 STEEL

FINISH
125

DO NOT SCALE DRAWING

	NAME	DATE
DRAWN	M. MALCOLMSON	2010-04-22
CHECKED	E. COBB	2010-04-22
ENG APPR.		
MFG APPR.		
Q.A.		
CAGE CODE	81359	

WPI

DEPARTMENT OF
MECHANICAL ENGINEERING
WORCESTER POLYTECHNIC INSTITUE

TITLE:

ASSEMBLY, TORQUE METER TO SHAFT COUPLING

SIZE	DWG. NO.	REV
A	WPI035	-

SCALE: 1:3   WEIGHT: 13.04 LBS   SHEET 1 OF 1

2x .03 X 45.00°

2x 1.00

2x 1.41

2x .03 X 45.00°

DETAIL A
SCALE 1 : 1

.50

1.00

2.50

2x R.06

DETAIL B
SCALE 1 : 1

2x .25

Ø 4.50

Ø 2.50

Ø 1.00

2x .13

2x R.03

DETAIL C
SCALE 1 : 1

UNLESS OTHERWISE SPECIFIED:			

DIMENSIONS ARE IN INCHES
TOLERANCES:
FRACTIONAL±
ANGULAR: MACH±   BEND ±
TWO PLACE DECIMAL   ± .01
THREE PLACE DECIMAL ± .005

	NAME	DATE
DRAWN	M. MALCOLMSON	2010-04-22
CHECKED	E. COBB	2010-04-22
ENG APPR.		
MFG APPR.		
Q.A.		

MATERIAL
A36 STEEL

FINISH
125

DO NOT SCALE DRAWING

CAGE CODE   81359

WPI
DEPARTMENT OF
MECHANICAL ENGINEERING
WORCESTER POLYTECHNIC INSTITUE

TITLE:
COUPLING, TORQUE METER TO SHAFT

SIZE A

DWG. NO.   WPI032

REV   –

SCALE: 1:2   WEIGHT: 4.29 LBS   SHEET 1 OF 1

A

2x .88

2x 1.06

Ø 4.50

D

A

1.50

SECTION A-A

2x .03 X 45.00°

2x 1.47

C

2x 1.01

B   B

2x R.06
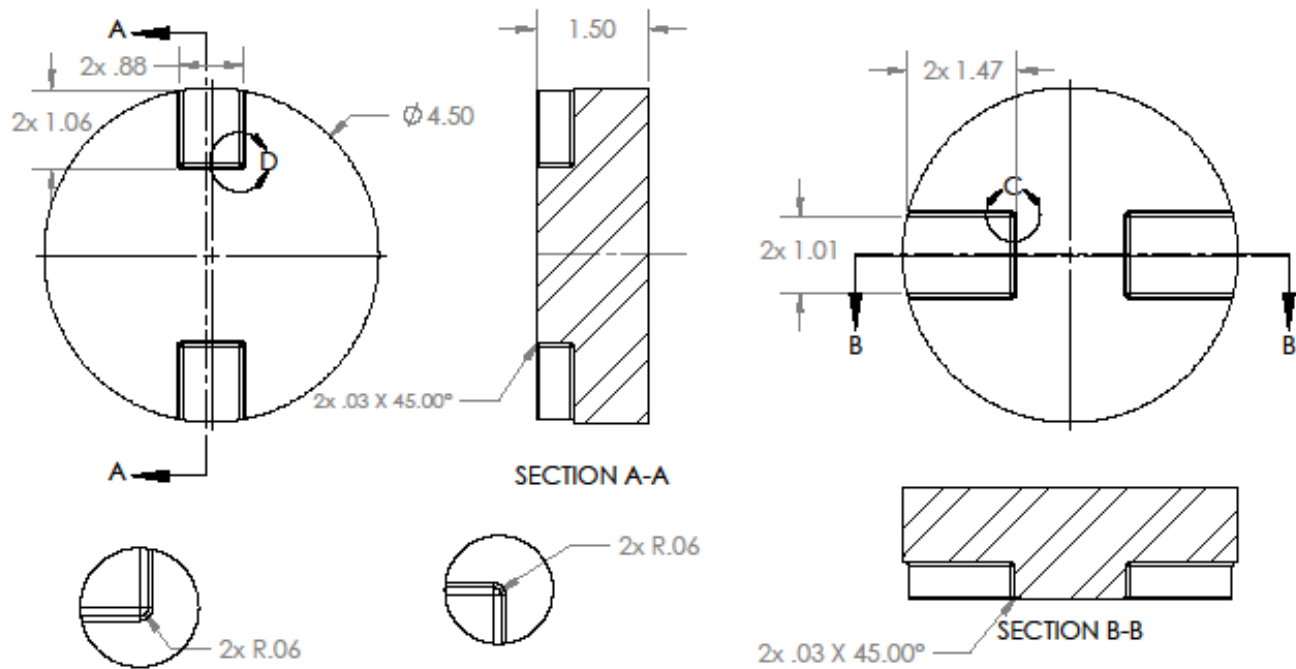
DETAIL D
SCALE 1 : 1

DETAIL C
SCALE 1 : 1

2x R.06

SECTION B-B

2x .03 X 45.00°

UNLESS OTHERWISE SPECIFIED:			
DIMENSIONS ARE IN INCHES TOLERANCES: FRACTIONAL± ANGULAR: MACH± BEND ± TWO PLACE DECIMAL ±.01 THREE PLACE DECIMAL ±.005		NAME	DATE
	DRAWN	M.MALCOLMSON	2010-04-22
	CHECKED	E. COBB	2010-04-22
MATERIAL A36 STEEL	ENG APPR.		
	MFG APPR.		
FINISH	Q.A.		
DO NOT SCALE DRAWING	CAGE CODE 81359		

DEPARTMENT OF
MECHANICAL ENGINEERING
WORCESTER POLYTECHNIC INSTITUE

TITLE:

CONNECTOR, TORQUE METER TO SHAFT

SIZE **A** DWG. NO. WPI033 REV

SCALE: 1:2 WEIGHT: 6.12 LBS SHEET 1 OF 1

2x .75

2x 1.00

A

DETAIL A
SCALE 1 : 1

2x .03 X 45.00°

Ø 4.50

3x .38

Ø 2.50

3x .19

C

Ø 1.63

DETAIL C
SCALE 1 : 1

6x R.03

.50

1.00

1.75

B

DETAIL B
SCALE 1 : 1

2x R.06

WPI

DEPARTMENT OF
MECHANICAL ENGINEERING
WORCESTER POLYTECHNIC INSTITUE

UNLESS OTHERWISE SPECIFIED:

DIMENSIONS ARE IN INCHES
TOLERANCES:
FRACTIONAL±
ANGULAR: MACH±   BEND ±
TWO PLACE DECIMAL   ± .01
THREE PLACE DECIMAL ± .005

	NAME	DATE
DRAWN	H.MALCOLMSON	2010-04-22
CHECKED	E. COBB	2010-04-22
ENG APPR.		
MFG APPR.		
Q.A.		

MATERIAL
A36 STEEL

FINISH
125

DO NOT SCALE DRAWING

CAGE CODE 81359

TITLE:
COUPLING, SHAFT TO TORQUE METER

SIZE A DWG. NO. WPI034 REV –

SCALE: 1:2   WEIGHT: 9.58 LBS   SHEET 1 OF 1

5   4   3   2   1